



TECHNISCHE
UNIVERSITÄT
WIEN

Vienna University of Technology Univ. Prof. Dr. Friedrich Franek

Diese Dissertation

haben begutachtet:

Univ. Prof. Dr. Günter Allmaier

Univ. Prof. Dr. Friedrich Franek

DISSERTATION

Condition monitoring of ionic liquids as novel industrial lubricants by means of artificial alteration and selected analytical techniques: LDI-TOF-MS and tandem MS, HPLC-ESI-MS, GC-EI-MS

Ausgeführt zum Zwecke der Erlangung des akademischen Grades eines

Doktors der Naturwissenschaften

unter der Leitung von

Univ. Prof. Dr. Günter Allmaier

E164

Institut für Chemische Technologien und Analytik

Eingereicht an der Technischen Universität Wien

Fakultät für Technische Chemie

von

Ing. Lucia Pisárová

0928439

Viktor-Kaplan-Straße 11

2700 Wiener Neustadt, Österreich

Wiener Neustadt, Mai 2013

Acknowledgements

I wish to express many thanks to the people who accompanied me on my way throughout my PhD studies.

The story of my dissertation started with the chance to join the exceptional European project MINILUBES, which enabled collaboration not just of many great minds, but also connected many hearts from almost every corner of Europe into tight friendships. This remarkable experience would not be possible without the scientific devotion of Dr. Nicole Doerr, who made it happen. I would also like to thank her for her guidance throughout the years, indispensable remarks and insights given, which helped me to grow as a scientist.

My gratitude also goes to Prof. Guenter Allmaier, who as my supervisor was always helpful with every matter to be solved, has given me a solid theoretical background as my lecturer and provided me with the possibility to get practical training under the guidance of recognized MS specialist, Dr. Ernst Pittenauer. I am grateful to have had the supervision of Dr. Pittenauer, for his availability and joy to discuss any topic of mass spectrometry, for his patience to clarify any open questions and for his valuable research suggestions and practical tips.

I am also very thankful to Prof. Friedrich Franek for giving me the first insights into the scientific discipline of tribology and for having the chance to attend several of his lectures. I am grateful for his time and efforts invested to provide invaluable inputs to the thesis revision.

Many thanks for the support, understanding and discussions go to my PhD co-fellows with which I shared the highs and the lows and all the other experiences of my post-graduate life. I especially address this to Charlotte Besser and Christoph Gabler who were there for me from the beginning; to the already experienced fellows at the time of my start: Enrico Corniani, Davide Bianchi, Stefan Eder and Agnieszka Tomala; to the Minilubers sharing the same path with me; Adina Neacsu, Nicholas Shore, Francesco Pagano, Catarina Mendonca, Vladimir Pejakovic, just to mention the few.

I have learned a lot from my senior researcher colleagues and advisors, among other Prof. Ichiro Minami, Dr. Stefan Stolte, Dr. Vladimir Totolin and Dr. Andjelka Ristic.

This thesis would not have materialized without the funding provided by the European Commission within the framework of the FP7 programme – Marie Curie Initial Training Network MINILUBES (No. 216011-2); "Austrian COMET Programme" (Project K2

XTribology, No. 824187) mainly carried out within the ‘Excellence Centre of Tribology’ – AC²T research GmbH; ERDF funding and support by the province of Lower Austria within the project "Onlab"; the grant available from the Austrian Science Foundation (Grant No. P15008 to G.A.); the Vienna University of Technology (to G.A.); the Polish Ministry of Research and Higher Education grants (No. NN204527139) and (No. DS 8200-4-0085-1), and partial support by KAKENHI (No. 23246030).

My biggest and warmest thanks belong to my beloved husband Mirko Pisar for his ever-present love, support and understanding in every step of my life.

Summary

The degradation of conventional lubricants has been extensively studied and it is known to be promoted by thermo-oxidative stress. On the other hand, the long-term stability of ionic liquids (ILs) as potential novel lubricants is scarcely investigated. Thus, the main aim of the thesis was to investigate how the IL stability is affected by common effects that can be expected in a tribosystem, such as temperature, air, water and presence of metals. Additionally, performance of selected ILs connected with surface interactions was evaluated by obtaining the information on their tribological behavior in the system concerned – such as friction coefficient, wear volume, surface tribo-film – and on corrosion. Within the scope of the presented work, IL environmental acceptability was assessed by means of selected ILs toxicity and biodegradability studies as ILs attempted to be used as lubricants have to fulfill REACH legislative requirements.

The studied IL representatives were based on quaternary ammonium cations with and without side chain functionalization by incorporating polar oxygen containing groups. The IL counter anions were based on non-halogenated hydrophilic and halogenated hydrophobic moieties. In order to gain information about IL long-term stability under selected conditions, short-term laboratory experiments utilizing subsequent temperature increase to the same IL bulk, in order to accelerate the degradation processes were performed. Frequent sampling enabled to follow IL chemical changes on molecular level by use of several mass spectrometric techniques, namely, LDI, MALDI, ESI and EI mass spectrometry with different types of analyzer and tandem MS. Hence, degradation product formation in the IL liquid phase and evolution of volatile species into the gas phase was assessed. SRV tribometer with ball-on-disc contact was used to determine selected IL tribological performance. Toxicity tests of different biological complexity were performed together with ready biodegradability assay in order to determine IL environmental impact.

The IL stability investigation using mass spectrometry as the main tool revealed that the IL cation and anion stability cannot be considered separately, as with particular cation moiety the IL could perform stable or be prone to degradation depending on IL anion. The proposed degradation mechanism requires presence of nucleophilic species, e.g., nucleophilic anions, and is based on thermally induced cross-methylation by anion-originating intermediates. Polar functional groups, such as ether also lead to decreased IL stability regardless of IL anion moiety. Following the IL degradation process by frequent sampling and quantification, it can be stated that the degradation reaction kinetics are slow and that no catalytic effect of metal or water was observed. Additionally, the abundant volatiles in the gas phase indicates that

caution should be taken once the ILs are used as lubricants in closed systems due to possibility of significant pressure build-up. It was also observed that evolved degradation product can negatively influence the intact IL tribological properties especially at higher temperatures, in terms of increased friction and wear. Care has to be taken when assessing environmental impact of only intact ILs as these can undergo chemical modification in the course of their use as lubricants due to degradation mechanisms taking place. Indeed, the most environmentally benign IL among the investigated ILs is transformed into a degradation product toxic to aquatic organisms and is not readily biodegradable. Hence, the joint interdisciplinary assessment is needed in order to develop truly high-performance and sustainable IL lubricants.

Zusammenfassung

Die Schädigung konventioneller Schmierstoffe wurde extensiv untersucht und es ist bekannt, dass diese durch thermisch-oxidative Belastungen gefördert wird. Die Langzeitstabilität ionischer Flüssigkeiten (IF) als potenzielle neue Schmierstoffe wurde jedoch bisher kaum erforscht. Deshalb war die Hauptzielsetzung dieser Arbeit, die Einflüsse üblicher Bedingungen, die in einem Tribosystem zu erwarten sind, wie z. B. Temperatur, Luft (Sauerstoff), Wasser und Metalle auf die Langzeitstabilität ionischer Flüssigkeiten zu untersuchen. Außerdem wurde die Leistungsfähigkeit ausgewählter ionischer Flüssigkeiten bezüglich ihrer Oberflächenwechselwirkungen bewertet – durch Messung der tribologischen Eigenschaften wie z. B. Reibkoeffizient, Verschleißvolumen, Tribofilmbildung und Korrosivität. Im Rahmen dieser Arbeit wurde die Umweltverträglichkeit ausgewählter ionischer Flüssigkeiten durch Studien zu Toxizität und biologischer Abbaubarkeit untersucht, da potenzielle Schmierstoffe die Anforderungen der gesetzlichen REACH-Kriterien erfüllen müssen.

Die untersuchten Vertreter ionischer Flüssigkeiten basierten auf quartären Ammoniumkationen mit und ohne Funktionalisierung der Seitenkette durch polare sauerstoffhaltige Gruppen. Die Anionen basierten auf nicht-halogenierten hydrophilen und halogenierten hydrophoben Gruppen. Um Informationen über die Langzeitstabilität unter verschiedenen Bedingungen zu erhalten, wurden Kurzzeit-Laborexperimente unter sequentieller Erhöhung der Temperatur an IF-Proben durchgeführt, um die Abbauprozesse zu beschleunigen. Häufige Probennahme ermöglichte die Verfolgung der chemischen Veränderungen auf molekularer Ebene durch massenspektroskopische Methoden, im Einzelnen LDI, MALDI, ESI und EI Massenspektroskopie mit verschiedenen Detektoren und Tandem-MS. Auf diese Weise wurden Abbauprodukte in der Flüssigkeit und gasförmige Produkte erfasst. Die tribologischen Eigenschaften ausgewählter IF wurden mittels SRV-Tribometer mit Kugel-Scheibe-Kontakt untersucht. Verschiedene Untersuchungen zur Toxizität mit variabler biologischer Komplexität gaben zusammen mit Standardverfahren zur biologischen Abbaubarkeit Aufschlüsse über die Umweltverträglichkeit.

Die Stabilitätsuntersuchungen mittels massenspektroskopischer Methoden als Hauptwerkzeug zeigten, dass die Stabilitäten von Kation und Anion nicht einzeln betrachtet werden können, da sich ein bestimmtes Kation mit unterschiedlichen Anionen stabil oder mit ausgeprägter Abbauneigung verhalten kann. Der vorgeschlagene Abbaumechanismus erfordert die Verfügbarkeit von nukleophilen Spezies, z. B. nukleophilen Anionen, und basiert auf der thermisch induzierten Kreuzmethylierung durch Intermediate des Anions. Polare funktionelle

Gruppen wie Ether führten ebenfalls zu einer Erniedrigung der Stabilität, unabhängig vom Anion. Aus der Betrachtung des Abbauprozesses mit häufiger Probennahme und quantitativer Analytik konnte geschlossen werden, dass die Reaktionsgeschwindigkeit des Abbaus langsam ist und kein katalytischer Effekt vorhandener Metalle beobachtet werden konnte. Außerdem gaben die zahlreichen flüchtigen Abbauprodukte in der Gasphase Hinweise darauf, dass Vorsicht geboten ist bei der Verwendung ionischer Flüssigkeiten als Schmierstoffe in geschlossenen Systemen, da ein signifikanter Druckanstieg möglich ist. Es wurde ebenfalls festgestellt, dass das Entstehen von Abbauprodukten die tribologischen Eigenschaften auch intakter IF negativ beeinflussen kann, speziell bei höheren Temperaturen, was sich durch erhöhte Reibung und Verschleiß äußert. Werden zur Bewertung der Umweltverträglichkeit ausschließlich intakte IF herangezogen, kann dies zu Fehleinschätzungen führen, da die IF im Laufe der Verwendung als Schmierstoffe chemischen Modifizierungen unterworfen sein können. Insbesondere die umweltverträglichste IF unter den betrachteten wird zu einem für Wasserorganismen toxischen und nicht biologisch abbaubaren Produkt transformiert. Aus diesem Grund ist eine interdisziplinäre Betrachtung und Bewertung erforderlich, um tatsächlich hochleistungsfähige und umweltverträgliche Schmierstoffe auf Basis ionischer Flüssigkeiten zu entwickeln.

Table of content

1. Ionic liquids (ILs)	11
1.1. IL origins and definition.....	11
1.2. IL classification and physico-chemical properties	11
1.2.1. IL liquid range and melting point.....	12
1.2.2. IL viscosity.....	13
1.2.3. IL density.....	13
1.3. References	14
2. Ionic liquids in tribology	15
2.1. Applied methods for investigation of IL tribological performance	15
2.1.1. White light confocal microscopy	15
2.1.2. Wear volume calculation.....	15
2.1.3. Scanning electron microscopy – energy dispersive X-ray spectrometry (SEM-EDX)	16
2.1.4. X-ray photoelectron spectroscopy (XPS).....	16
2.2. ILs as neat lubricants.....	16
2.2.1. IL lubrication mechanism.....	17
2.2.1.1. Tribological effects of IL alkyl chains	17
2.2.1.2. Tribological effects of IL tribochemical reactions	18
2.2.2. Topics related to the application of ILs as lubricant	19
2.2.2.1. Tribocorrosion	19
2.2.2.2. Additive availability for IL lubricants.....	19
2.2.2.3. IL stability	20
2.3. ILs as additives.....	20
2.3.1. ILs as additives in water.....	20
2.3.2. ILs as additives in mineral and synthetic oils	21
2.4. References	21
3. Stability of lubricants and methods employed in lubricant analysis	24
3.1. Stability of hydrocarbon based lubricants	24
3.1.1. Oxidation stability	24
3.1.2. Thermal stability	25
3.1.3. Hydrolytic stability.....	25
3.2. Stability of IL lubricants.....	26
3.2.1. IL cation derived stability	26
3.2.2. Alkyl chain effects on IL stability.....	27
3.2.3. IL anion derived stability	27
3.3. Methods employed in lubricant stability evaluation	27
3.3.1. Standard test methods for investigation of conventional lubricants stability.....	28

3.3.2. Commonly employed experiments for investigation of IL lubricants stability	29
3.3.3. Routine analysis for condition monitoring of conventional lubricants	29
3.4. References	30
4. Applied analytical techniques for IL degradation studies.....	35
4.1. Time-of-flight mass spectrometry (TOF-MS).....	35
4.1.1. Laser desorption/ionization (LDI).....	35
4.1.2. Matrix-assisted laser desorption/ionization (MALDI).....	36
4.1.3. Time-of-flight mass spectrometer (TOF) and applied analyzing modes	38
4.1.3.1 Linear time-of-flight (LTOF) mass analyzer	38
4.1.3.2 Delayed (or pulsed) extraction	39
4.1.3.3 Reflectron time-of-flight (RTOF) mass analyzer.....	39
4.1.3.4 Post-source decay (PSD)	40
4.1.3.5 High-energy collision induced dissociation (HE-CID).....	41
4.2. High performance liquid chromatography coupled to electrospray ionization linear ion trap orbitrap mass spectrometry (HPLC-ESI-LIT-orbitrap-MS)	41
4.2.1. High performance liquid chromatography (HPLC)	41
4.2.1.1. Normal and reverse phase chromatography	43
4.2.1.2. Isocratic and gradient separation mode	43
4.2.2. Electrospray ionization (ESI)	44
4.2.2.1. Proposed models of gas phase ion formations	45
4.2.2.2. HPLC-ESI-MS on-line coupling	45
4.2.3. Linear ion trap orbitrap mass spectrometry (LIT-orbitrap-MS).....	46
4.2.3.1. Linear ion trap (LIT) mass analyzer.....	47
4.2.3.2. Orbitrap mass analyzer and integrated detection	48
4.3. Headspace cold trap gas chromatography electron ionization mass spectrometry (HS-CT-GC-EI-MS)	50
4.3.1. Headspace and cold trap techniques.....	50
4.3.2. Capillary gas chromatography (GC)	50
4.3.2.1. Split and splitless injection techniques.....	51
4.3.2.2. Gas-solid and gas-liquid chromatography.....	52
4.3.2.3. Isothermal and gradient temperature program	53
4.3.3. Electron ionization (EI)	54
4.3.3.1. Open split and direct GC-EI-MS coupling.....	54
4.3.4. Quadrupole mass analyzer	55
4.4. References	57
5. Applied methods for IL (eco)toxicity and biodegradability assessment	61
5.1. Acetylcholinesterase inhibition assay	61
5.2. Cell viability assay with IPC-81 cells	61
5.3. Luminescence inhibition assay with the marine bacterium <i>Vibrio fischeri</i>	62
5.4. Acute immobilization assay with <i>Daphnia magna</i>	62
5.5. Ready biodegradability according to OECD 301F manometric respirometry	63

5.6. References	64
6. Publications within the thesis topic.....	68
6.1. Thermo-oxidative stability and corrosion properties of ammonium based ionic liquids	68
6.2. Ionic liquid long-term stability assessment and its contribution to toxicity and biodegradation study of untreated and altered ionic liquids.....	80
6.3. Insight into degradation of ammonium-based ionic liquids and comparison of tribological performance between selected intact and altered ionic liquid	101

1. Ionic liquids (ILs)

1.1. IL origins and definition

First deliberately prepared ionic liquids (ILs) emerged at the beginning of the 20th century in the work of P. Walden describing alkylammonium nitrate salts with melting points approximately up to 100 °C [1.1]. This temperature limitation in IL definition persisted until today although it is only arbitrarily chosen with no chemical or physical significance [1.2]. The IL development continued in the middle of 20th century with chloroaluminate systems (mixtures of alkali halides and aluminium chloride) towards more air and water stable ILs, firstly designed by J. Wilkes and M. Zaworotko and followed by so called functionalized “task-specific” ILs which are designed for particular applications, such as: solvents in organic synthesis and biomass processing, catalysts, engineering fluids, etc. [1.2-1.5].

Ionic liquids are a diverse group of salts composed of organic and usually asymmetric bulky cations combined with inorganic or organic anions where at least one of the ions features delocalized charge. In fact, ionic liquids differ from molten salts only by several means: (1) their wide liquid range lying at much lower temperatures; (2) their cations being of organic nature.

1.2. IL classification and physico-chemical properties

Due to vast IL structural variability, straight-forward classification of ILs is a difficult task. The most convenient IL division can be into protic and aprotic IL classes depending on presence of proton donor and acceptor site. Aprotic ILs are formed from cations based on organic molecular-ions and represent the majority of synthesized ILs. Protic ILs are formed by proton transfer between equimolar mixture of pure Bronsted acid and pure Bronsted base and hence can be more conductive than aprotic ILs [1.5]. Room-temperature ionic liquids (RTILs) represent separate sub-group defined solely on their melting point lying at or below room temperature. In Table 1 are summarized the most common cation and anion moieties used for IL structural design.

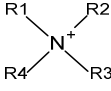
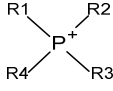
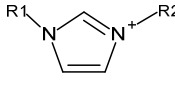
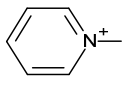
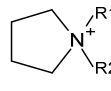
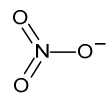
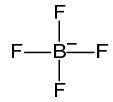
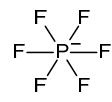
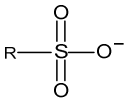
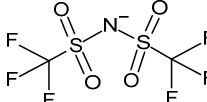
Cations					
	ammonium	phosphonium	imidazolium	pyridinium	pyrrolidinium
Anions					
	nitrate	tetrafluoroborate	hexafluorophosphate	sulphonate	bis(trifluoromethylsulfonyl)imide

Table 1. Summarized common IL cation and anion moieties.

R_n (n = 1 to 4) – organic group

As ILs structural possibilities are enormous, there is almost no uniform property describing ILs as a class of compounds, apart from their ion conductivity. In fact the broadness of their physico-chemical properties covers often both extremes, as they can be: (1) negligible volatile, but also distillable, (2) non-toxic and even edible, but also poisonous, (3) non-flammable however also combustible, etc. [1.6]. The particular IL physico-chemical properties depend strongly on the selected IL cation and anion combination, whereas anions affect chemical properties and cations mainly determine physical properties, and on the nature and strength of their interactions mostly based on the Coulomb and van der Waals forces.

1.2.1. IL liquid range and melting point

IL liquid range lies between IL solidification (crystallization, glassification) and decomposition temperature, as ILs are practically non-volatile. It can be considerably wide, in some cases up to 200 °C or 300 °C, in contrast to narrow liquid range of molecular solvents [1.6, 1.7].

As ILs are composed of organic cations, they can exhibit melting points deep below zero temperatures. However, many ILs tend to glass formations or exhibit supercooling by cooling and hence obtained solidification (glass) temperatures do not correspond to their melting points. In order to obtain reproducible thermodynamic data, the small cooled IL sample amounts have to be slowly heated allowing for long equilibration times [1.8].

IL melting points are determined by both IL moieties, but the main reduction in melting point is due to bulky asymmetric cations as increasing ion symmetry increases melting points due to more efficient ion-ion packing. Additionally, increase in anion size causes melting point to decrease due to weaker Coulombic interactions. The effect of the alkyl chain length on IL melting points is more complex. Linear alkyl substituents have many rotational degrees of

freedom and hence are capable of conformational changes. Thus, cations with short alkyl chains ($C_n \leq 3$) tend to form crystalline phases, while the intermediate chain lengths ($4 \leq C_n < 12$) exhibit broad liquid range and tendency to supercool and the long alkyl chain lengths ($C_n > 12$) result in liquid-crystalline phases. Additionally, alkyl chain branching leads to higher melting points [1.5, 1.6, 1.8, 1.9].

The dominant force that influences the melting points in ILs is Coulombic attraction between ions in addition to hydrogen bonding ability and van der Waals interactions. To summarize, IL melting point is a result of cation and anion symmetry, alkyl chain flexibility and charge accessibility and can be strongly affected by presence of impurities [1.6-1.10].

1.2.2. IL viscosity

ILs are generally viscous liquids with viscosities comparable to oils, and are 2 to 3 orders of magnitude more viscous than conventional organic solvents. For ILs with fixed anion and similar alkyl chain length, viscosity increases with cations following the order imidazolium < pyridinium < pyrrolidinium [1.6, 1.9, 1.11]. In general, ILs with symmetric or almost spherical anions are more viscous than those with asymmetric anions. Additionally, increase in alkyl side chain length causes viscosity increase. ILs viscosity is also strongly dependent on the temperature and decreases significantly with temperature increase. Presence of small amounts of impurities can also have remarkable impact on ILs viscosities as, e.g., chloride impurities can increase IL viscosity dramatically. The IL viscosity is mainly controlled by the factors related to hydrogen bonding, van der Waals interactions, molecular weight and bulkiness of their moieties [1.6, 1.11, 1.12].

1.2.3. IL density

Majority of ILs is denser than water with values ranging from $1 \text{ g}\cdot\text{cm}^{-3}$ to $1.6 \text{ g}\cdot\text{cm}^{-3}$ at 293 °K [1.9]. As with organic solvents, their densities are closely related to the IL molar mass, so ILs containing heavy atoms are found to be more dense. Additionally, increase in alkyl chain lengths causes density decrease [1.6, 1.9]. On the other hand, impurities in ILs have far less pronounced effect on IL densities. However, water saturated ILs have lower densities than dried ones. Similarly, increasing contents of halide contaminations lead to decrease of ILs density. The IL densities appear to be the least sensitive to variations in temperature among IL physical properties [1.6, 1.12, 1.13].

1.3. References

- [1.1] Walden P. Über die Molekulargröße und elektrische Leitfähigkeit einiger geschmolzener Salze. *Bull Acad Impér Sci St Pétersbourg* 1914; 8:405-422.
- [1.2] Plechkova NV, Seddon KR. Applications of ionic liquids in the chemical industry. *Chem Soc Rev* 2008; 37:123-150.
- [1.3] Kirchner B. Preface. In: Kirchner B, editor. *Ionic liquids*. 1st ed. Heidelberg: Springer; 2010, xi-xiii.
- [1.4] Wilkes JS. Introduction. In: Wasserscheid P, Welton T, editors. *Ionic liquids in synthesis*. 1st ed. Weinheim: Wiley-VCH; 2003, 1-6.
- [1.5] Angell CA, Ansari Y, Zhao Z. Ionic liquids: past, present and future. *Faraday Discuss* 2012; 154:9-27.
- [1.6] Rooney D, Jacquemin J, Gardas R. Thermophysical properties of ionic liquids. In: Kirchner B, editor. *Ionic liquids*. 1st ed. Heidelberg: Springer; 2010, 185-212.
- [1.7] Aparicio S, Atilhan M, Karadas F. Thermophysical properties of pure ionic liquids: review of present situation. *Ind Eng Chem Res* 2010; 49:9580-9595.
- [1.8] Holbrey JD, Rogers RD. Melting points and phase diagrams. In: Wasserscheid P, Welton T, editors. *Ionic liquids in synthesis*. 1st ed. Weinheim: Wiley-VCH; 2003, 41-55.
- [1.9] Marsh KN, Boxall JA, Lichtenthaler R. Room temperature ionic liquids and their mixtures – a review. *Fluid Phase Equilib* 2004; 219:93-98.
- [1.10] Weingärtner H. Understanding ionic liquids at the molecular level: facts, problems, and controversies. *Angew Chem Int Ed* 2008; 47:654-670.
- [1.11] Endres F, Zein El Abedin S. Air and water stable ionic liquids in physical chemistry. *Phys Chem Chem Phys* 2006; 8:2101-2116.
- [1.12] Seddon KR, Stark A, Torres MJ. Influence of chloride, water and organic solvents on the physical properties of ionic liquids. *Pure Appl Chem* 2000; 72:2275-2287.
- [1.13] Mantz RA, Trulove PC. Viscosity and density of ionic liquids. In: Wasserscheid P, Welton T, editors. *Ionic liquids in synthesis*. 1st ed. Weinheim: Wiley-VCH; 2003, 56-67.

2. Ionic liquids in tribology

2.1. Applied methods for investigation of IL tribological performance

Friction, wear, and lubrication phenomena are principal objectives of tribological investigations carried out within interdisciplinary science of tribology studying interacting surfaces in relative motion. Friction can be defined as a resistance to motion; wear represents a surface damage or removal of material from the moving contact, whereas lubrication serves the purpose of reducing the first two phenomena. Tribometry – the metrological system of tribology – enables evaluation of friction, wear and lubricant performance parameters (e.g., coefficient of friction, wear volume) using tribometer instruments. A tribometer simulates the contact conditions by utilizing material pairings of several geometries, such as pin-on-disk, ball-on-disk, disk-on-disk, etc. [2.1, 2.2].

It is of crucial importance to understand lubricant performance, lubricant-surface interactions and the tribofilm formations, thus several methods described below are commonly employed to investigate these research topics.

2.1.1. White light confocal microscopy

White light confocal microscopy is an optical imaging technique which applies a focused light beam from a point light source, such as Xe lamp, illuminating the studied specimen surface point. The object is imaged in a microscope objective focal plane and formed at the confocal pinhole located in front of the detector, e.g., photomultiplier. Thus, scattered background light from defocused surface locations is eliminated and optical resolution of the image is improved. By scanning the sequence of surface points a topography image of specimen is constructed [2.3-2.5].

2.1.2. Wear volume calculation

The surface topographic data of tribocontact bodies can be obtained by white light confocal microscopy and used to determine wear volumes of specimens by MATLAB® based program developed at AC²T research GmbH. The wear volume calculation of ball on disc tribocontact uses the data from worn surface analysis of tribocontact bodies and from approximated ideal spherical ball and ideal plane as reference surfaces. The wear volume represents the difference between the measured surface after the triboexperiment and the corresponding reference surface [2.6].

2.1.3. Scanning electron microscopy – energy dispersive X-ray spectrometry (SEM-EDX)

A scanning electron microscope is used to produce an image of surface topography providing information about the surface structure and spatial distribution of present microstructures, i.e. morphology. The surface image is obtained by applying focused electron beam on the examined conductive surface placed under vacuum. The primary electrons interact with the sample and lead to production of different signals out of which secondary and back-scattered electrons are detected and serve for sample imaging. Secondary electrons carry information about the surface morphology while back-scattered electrons provide composition contrast, as heavy elements appear brighter in the image [2.7-2.9].

Conjunction of SEM with energy dispersive X-ray detector enables determination of surface elemental composition. After surface bombardment by a focused electron beam, vacancies from ejected electrons become occupied by electrons from higher orbitals and the energy difference is compensated by X-ray emission. As the X-ray energy is element specific, the information about the surface elemental composition can be obtained [2.9].

2.1.4. X-ray photoelectron spectroscopy (XPS)

XPS is a surface analysis technique investigating surface chemical composition with an information depth of maximum 10 nm and enabling lateral resolution down to a few micrometers. The analyzed surface is irradiated under ultra-high vacuum by X-ray photons which leads to emission of core shell photoelectrons. The kinetic energy of photoelectrons corresponds to particular element characteristic electronic binding energies enabling qualitative elemental analysis. Even though the core electrons are not directly involved in chemical bindings, they are affected by bonding environment around the atom which is reflected in their binding energy shifts, called chemical shifts, hence the binding state of atoms can be determined [2.10, 2.11].

2.2. ILs as neat lubricants

IL lubricants represent attractive alternative to conventional lubricants due to several of their unique properties: (1) negligible vapor pressure reducing air pollution, (2) non-flammability as an aspect of safety considerations, (3) higher thermal stability enabling long-term durability or application at elevated temperatures, (4) high thermal conductivity leading to longer machine maintenance intervals and (5) wide liquid range hence expanded operating temperature range. As many IL lubricants proved to be efficient in lowering friction and wear,

this leads to additional reductions of energy and material losses. Furthermore, they can be tailor-made, designed for particular application with desired viscosity-temperature behavior, viscosity index, liquid range, etc.

First research on room temperature IL lubricants started in 2001 with imidazolium tetrafluoroborate ILs exhibiting remarkable friction and anti-wear properties together with high loading capacity which raised awareness of tribological community [2.12]. Since then imidazolium ILs with fluorine-containing anions, such as tetrafluoroborate $[\text{BF}_4]^-$ and hexafluorophosphate $[\text{PF}_6]^-$ have been mainly studied for various tribological contacts as they are easily synthesized, available at reasonable costs and easily structurally modified. Apart from imidazolium cations, ammonium and phosphonium based ILs were investigated as lubricants with promising tribological performance [2.13-2.15].

2.2.1. IL lubrication mechanism

Tribological performance of conventional oils dependent among other on their interaction with surfaces and hence formation of films. IL lubrication mechanism follows the same principle, so adsorption on the sliding surfaces and creation of effective boundary films are crucial effects. As worn metallic surface exhibits positive charge, mostly the IL anions are adsorbed on the friction pairs and their counter cations assemble successively due to IL dipolar nature leading to friction and wear reduction under high loads. It has been also observed that irregular structure of the IL moieties leads to low shear stress, as the measurements of the IL film shear stress revealed significantly lower friction coefficients compared to hydrocarbon lubricants [2.16].

2.2.1.1. Tribological effects of IL alkyl chains

Apart from IL anion role in adsorption processes, also cation alkyl chain lengths have significant effect on the IL tribological properties [2.17]. Alkyl chain length contributes to IL viscosity and due to this fact longer alkyl chains enable formation of densely packed structures leading to better tribological performance, e.g., to friction coefficient decrease [2.13, 2.14, 2.18, 2.19].

Even more impact on IL lubricant performance has functionalization of these alkyl chains, e.g., by ether, ester or carboxyl groups. These polar groups enable stronger interactions of ILs with the tribological surfaces leading to less friction and wear [2.17, 2.18].

Formation of compact chemisorbed film with good anti-wear ability on the metallic surface has been ascribed to IL with ester functional groups due to their hydrolyzation under contact

with atmospheric moisture [2.17]. Corrosion inhibiting property of vinyl functionalized ILs at elevated temperatures has been reported with proposed interaction of vinyl groups with iron surface leading to formation of protective layer [2.20]. ILs with phosphonyl groups on imidazolium ring proved to have superior tribological performance over their non-functionalized derivatives and led to formation of FePO_4 as the tribochemical reaction product [2.15]. Also molecular modeling studies contribute to understanding of IL functional groups effects on the friction coefficient. While using hydroxylated silicon surface, the friction decreases in the following order $-\text{CH}_2\text{OH} > -\text{CN} > -\text{COOH}$ group [2.21]. Therefore, the structurally flexible IL cations which are able to carry multi-functional groups in high number are of great interest.

2.2.1.2. Tribological effects of IL tribochemical reactions

Tribochemical reactions represent chemical reactions of lubricant at the rubbing surface interfaces. For IL lubricants these tribochemical reactions are ascribed mainly to reactions of IL anionic moieties [2.13, 2.18]. In order to investigate these processes X-ray photoelectron spectroscopy (XPS) is mainly applied to the rubbed surfaces together with time-of-flight secondary ion mass spectrometry (TOF-SIMS) to identify the formed compounds [2.22-2.24]. Beneficially, ILs contain tribologically interesting elements, such as B, F, S and P which can be found in present oil lubricant additives, too. Under severe sliding conditions, the IL anions can decompose and in dependency of material in contact they lead to; (1) $[\text{BF}_4]^-$ forming FeB, BN and B_2O_3 , (2) $[\text{PF}_6]^-$ forming FePO_4 and (3) $[\text{NTF}_2]^-$ forming FeS; these formed species can prevent seizures and thus have efficient anti-wear properties [2.14]. TOF-SIMS analysis revealed the presence of FeF^+ in case of $[\text{BF}_4]^-$ and $[\text{NTF}_2]^-$ anions in the inner area of the wear scar, suggesting the potential formation of FeF_2 as protective film [2.13]. The FeF_2 formation has also been observed for imidazolium tetrafluoroborate IL lubricating steel-steel contact where the precipitated wear particles were analyzed by XPS after occurrence of sharp friction peak corresponding to formation of FeF_2 [2.25]. Phosphate boundary films have been reported for IL containing phosphate, thiophosphate anion or phosphonium cation and exhibited better tribological performance over fluoride boundary films [2.26].

To summarize, IL lubricants are able to perform better in terms of friction and wear in comparison to conventional additivated oils. This is due to their dipole character enabling formation of boundary films, enhanced stability and their possibility to create protective surface tribo-layers [2.20, 2.27]. The IL surface tribochemistry, in particular between metal

and the reactive anion is of crucial importance [2.28]. The IL anions decomposition and their tribochemical reactions can lead to the formation of scratch resistant protective surface films such as B_2O_3 , BN, FeF_2 , FeF_3 , $FePO_4$ and FeS reducing the coefficient of friction and wear [2.19]. It turned out that some ILs could be used as high temperature lubricants even at the temperatures close to their thermal decomposition [2.29]. In general, tribochemical processes in ILs represent: dissociation of the anions, oxidation, and formation of metallic phosphates, oxides and fluorides as well as precipitation of ceramic phases such as boron and phosphorus fluorides, boron oxide, boron carbide and boron nitride [2.15]. Due to ILs specific characteristics, such as formation of stable surface adsorbed layers, they have also been effective in break-in period reductions leading to friction decrease [2.28].

2.2.2. Topics related to the application of ILs as lubricant

2.2.2.1. Tribocorrosion

IL tribochemical reactions can also lead to undesired effects, such as severe corrosion causing enhanced wear. For example, $[BF_4]^-$ and $[PF_6]^-$ anions can cause corrosion of steel under humid conditions due to HF generation during their decomposition [2.13, 2.14]. Hence, iron fluoride can be found on steel and can act as catalyst of lubricant degradation possibly causing further substrate corrosion [2.19]. In detail, this effect is ascribed to iron fluoride hydrolysis yielding iron hydroxides and iron oxides and hence resulting in iron rusting [2.26]. As high polarity of ILs enhances their humidity uptake, these anions should be replaced by more hydrophobic ones and preferably halogen-free anions [2.13, 2.14]. Additionally, longer alkyl side chains can contribute to increase of IL hydrophobicity.

2.2.2.2. Additive availability for IL lubricants

Developments in additive technology have been oriented towards conventional lubricants, e.g., mineral oils, hence are hardly soluble in polar IL lubricants. Benzotriazole, successfully applied anticorrosion additive showed good miscibility with imidazolium ILs and protective film formation consisting of $Cu(C_6H_5N_3)$ and Cu_2O at copper alloy surfaces [2.13-2.15, 2.19]. However, benzotriazole usage is limited due to its sublimation point at about 100 °C, so the IL cannot benefit from it at elevated temperatures and under vacuum [2.14]. Among anti-wear additives, tricresylphosphate in ILs was found to reduce wear significantly due to tribo-film formation in comparison to neat IL or neat tricresylphosphate [2.15].

Also specially designed anti-wear additives for ILs based on tetraalkylammonium and tetraalkylphosphonium salts of N-protected aspartic acid dissolved in imidazolium NTF₂

reduced wear and friction significantly [2.30]. More advanced solution is to design ILs with build-in additive functional groups. Lower corrosion has been observed in case of triazole-ILs as triazole ring chemically absorbs at the metallic surface and eliminates locally generated acid formed due to anion decomposition [2.14].

2.2.2.3. IL stability

Even though ILs have generally superior thermo-oxidative stability than conventional oils, at severe conditions they undergo decomposition due to some of these effects; (1) heat generated during friction, (2) extreme pressure at the tribological contact, (3) emission of exo-electrons due to mechanical stress. Hence, chemical reactions, high-pressure reactions and electrochemical reactions can take place during IL lubrication [2.13].

During sliding of tribological contacts, nascent metallic surface is generated which can lead to metal and IL reactions, such as formation of FeF_2 on the rubbed surface which as a Lewis acid can provoke degradation of IL lubricant and, as a consequence, friction and wear rapidly increase [2.13, 2.15]. Hence, halogen-free anions could eliminate IL decomposition risk due to tribochemical reactions and hydrophobic anions can improve their thermo-oxidative stability but longer alkyl chains, even though improving tribological properties can cause decline of IL stability [2.13].

To conclude, knowledge of potential decomposition mechanisms in IL lubricants is of crucial importance for the IL applicability in tribological systems in order to minimize their degradation during service life.

2.3. ILs as additives

Promising results showed even better friction and wear improvement for ILs applied as additives than for ILs as neat lubricants. The effect is ascribed to the fact that small amounts of IL are enough to effectively adsorb on the surfaces while avoiding severe tribo-corrosion [2.15]. However, the price of IL additives should be at least competitive or lower as the traditionally used additives. Due to IL self-organization creating polar and non-polar domains, they are able to be designed for polar and non-polar lubricants.

2.3.1. ILs as additives in water

In the first work of ILs applied as lubricants, it was noted that ILs in presence of water lead to improvement of the anti-wear behavior for some metal-metal contacts. This behavior was

ascribed to the surface smoothening due to mechanical wear and creation of IL electric double layer [2.12, 2.15].

ILs were also used as boundary lubricant additives in water for silicon nitride ceramic surface and lead among other to significantly shortened running-in periods, hence minimizing friction, wear and improving the load carrying capability. The mechanisms taking place were attributed to formation of transfer films on the surface and to the presence of an electric double layer due to negatively charged silicon nitride surface attracting IL cations [2.31].

Nevertheless, care has to be taken for application of IL additives in water in case of anions prone to hydrolysis.

2.3.2. ILs as additives in mineral and synthetic oils

In order to apply ILs as additives in conventional oils, their molecular design has to be taken into account for improvements of their mutual miscibility. In polyethylene glycol it was possible to reach 40 % solubility of NTF₂ based IL with 3 wt.% optimal concentration leading to significant improvement of anti-wear performance with respect to the base oil [2.14]. Also imidazolium ILs at 1 wt.% in synthetic ester propylene glycol dioleate although exhibiting similar friction as neat ILs, have led to more pronounced wear reduction compared to the base oil and neat IL [2.15]. Another type of IL based additives is represented by ammonium and pyridinium cations with attached phosphazene ring group leading to enhanced solubility in conventional lubricants and improved organic oils miscibility in aqueous environments [2.19]. Controversially, long alkyl chains are more effective in case of neat ILs whereas shorter alkyl chains in ILs used as additives were more effective for wear reduction [2.15].

2.4. References

[2.1] Bhushan B. Preface. In: Bhushan B. Introduction to tribology. 1st ed. New York: Wiley; 2002, xvii-xix.

[2.2] Czichos H, Habig KH. Tribologische Mess- und Prueftechnik. In: Czichos H, Habig KH. Tribologie-Handbuch: Tribometrie, Tribomaterialien, Tribotechnik. 3rd ed. Wiesbaden; 2010, 193-252.

[2.3] Semwogerere D, Weeks ER. Confocal microscopy. In: Wnek GE, Bowlin GL, editors. Encyclopedia of biomaterials and biomedical engineering. 1st ed. Marcel Dekker; 2004, 1-10.

[2.4] Jordan HJ, Brodmann R, Valentin J, Grigat M. Confocal white light microscopy. NanoFocus Messtechnik GmbH.

www.zimmerman.com.tw/uploads/ConfocalWhiteLightMicroscopy_Technicalarticle.pdf

- [2.5] Webb RH. Theoretical basis of confocal microscopy. In: Conn PM, editor. *Techniques in confocal microscopy*. 1st ed. San Diego, California, USA: Elsevier; 2010, 3-21.
- [2.6] Hunger H, Litzow U, Genze S, Doerr N, Karner D, Eisenmenger-Sittner C. Tribological characterisation and surface analysis of diesel lubricated sliding contacts. *Tribol Schmierungstech* 2010; 57:6-13.
- [2.7] Khurshheed A. *Scanning electron microscope optics and spectrometers*. 1st ed. Singapore: World scientific publishing; 2011.
- [2.8] Kolasinski KW. *Surface science: foundation of catalysis and nanoscience*. 2nd ed. Chichester, UK: Willey; 2008.
- [2.9] Turner PS, Nockolds CE, Bulcock S. *Electron microscope techniques for surface characterization*. In: O'Connor DJ, Sexton BA, Smart RSC, editors. *Surface analysis methods in materials science*. 2nd ed. Berlin, Germany: Springer; 2003, 85-106.
- [2.10] Bubert H, Riviere JC, Werner WSM. X-ray photoelectron spectroscopy (XPS). In: Friedbacher G, Bubert H, editors. *Surface and thin film analysis: a compendium of principles, instrumentation, and applications*. 2nd ed. Weinheim, Germany: Wiley-VCH; 2011, 7-41.
- [2.11] Christie AB. X-ray photoelectron spectroscopy. In: Walls JM, editor. *Methods of surface analysis*. 1st ed. Cambridge, UK: Cambridge university press; 1989, 127-168.
- [2.12] Ye Ch, Liu W, Chen Y, Yu L. Room temperature ionic liquids: a novel versatile lubricant. *Chem Commun* 2001; 2244-2245.
- [2.13] Minami I. Ionic liquids in tribology. *Molecules* 2009; 14:2286-2305.
- [2.14] Zhou F, Liang Y, Liu W. Ionic liquid lubricants: designed chemistry for engineering applications. *Chem Soc Rev* 2009; 38:2590-2599.
- [2.15] Bermudez MD, Jimenez AE, Sanes J, Carrion FJ. Ionic liquids as advanced lubricant fluids. *Molecules* 2009; 14:2888-2908.
- [2.16] Perkin S, Albrecht T, Klein J. Layering and shear properties of an ionic liquid, 1-ethyl-3-methyl-imidazolium ethylsulfate confined to nano-films between mica surfaces. *Phys Chem Chem Phys* 2010; 12:1243-1247.
- [2.17] Zhu LY, Chen LG, Yang X, Song HB. Functionalized ionic liquids as lubricants for steel-steel contact. *Appl Mech Mater* 2012; 138-139:630-634.
- [2.18] Perkin S. Ionic liquids in confined geometries. *Phys Chem Chem Phys* 2012; 14:5052-5062.
- [2.19] Palacio M, Bhushan B. A review of ionic liquids for green molecular lubrication in nanotechnology. *Tribol Lett* 2010; 40:247-268.

- [2.20] Li D, Cai M, Feng D, Zhou F, Liu W. Excellent lubrication performance and superior corrosion resistance of vinyl functionalized ionic liquid lubricants at elevated temperature. *Tribol Int* 2011; 44:1111-1117.
- [2.21] Nooruddin NS, Wahlbeck PG, Carper WR. Semi-empirical molecular modeling of ionic liquid tribology: ionic liquid-hydroxylated silicon surface interactions. *Tribol Lett* 2009; 36:147-156.
- [2.22] Kamimura H, Kubo T, Minami I, Mori S. Effects and mechanism of additives for ionic liquids as new lubricants. *Tribol Int* 2007; 40:620-625.
- [2.23] Minami I, Kita M, Kubo T, Nanao H, Mori S. The tribological properties of ionic liquids composed of trifluorotris(pentafluoroethyl)phosphate as a hydrophobic anion. *Tribol Lett* 2008; 30:215-223.
- [2.24] Somers AE, Howlett PC, MacFarlane DR, Forsyth M. A review of ionic liquid lubricants. *Lubricants* 2013; 1:3-21
- [2.25] Sanes J, Carrion FJ, Bermudez MD, Martinez-Nicholas G. Ionic liquids as lubricants of polystyrene and polyamide 6-steel contacts. Preparation and properties of new polymeric ionic liquid dispersions. *Tribol Lett* 2006; 21:121-133.
- [2.26] Minami I, Inada T, Sasaki R, Nanao H. Tribo-chemistry of phosphonium-derived ionic liquids. *Tribol Lett* 2010; 40:225-235.
- [2.27] Jimenez AE, Bermudez MD. Ionic liquids as lubricants for steel-aluminum contacts at low and elevated temperatures. *Tribol Lett* 2007; 26:53-60.
- [2.28] Jimenez AE, Bermudez MD. Ionic liquids as lubricants of titanium-steel contact. *Tribol Lett* 2009; 33:111-126.
- [2.29] Jimenez AE, Bermudez MD. Ionic liquids as lubricants of titanium-steel contact. Part 2: friction, wear and surface interactions at high temperature. *Tribol Lett* 2010; 37:431-443.
- [2.30] Minami I, Watanabe N, Nanao H, Mori S, Kukumoto K, Ohno H. Aspartic acid-derived wear preventing and friction reducing agents for ionic liquids. *Chem Lett* 2008; 37:300-301.
- [2.31] Philips BS, Mantz RA, Trulove PC, Zabinski JS. Surface chemistry and tribological behavior of ionic liquid boundary lubrication additives in water. In: Rogers RD, Seddon KR, editors. *Ionic liquids III A: fundamentals, progress, challenges, and opportunities*. ACS Symposium series, 2005; 901:244-253.

3. Stability of lubricants and methods employed in lubricant analysis

3.1. Stability of hydrocarbon based lubricants

Hydrocarbon based lubricants are divided into five categories according to American Petroleum Institute (API). Group I to group III are mineral base oils and group IV are synthetic hydrocarbon base oils, such as polyalphaolefins (PAOs). These groups are classified by certain characteristics, such as viscosity index, amount of saturated hydrocarbons and amount of sulfur compounds. Group V base oils include every other oil type, such as polyol ester, polyglycol and phosphate ester and due to its diversity this group does not possess any specific classification characteristics [3.1].

Variety of service operating conditions can affect lubricant stability, such as temperature, air, moisture and contamination. Temperature represents the most significant factor, hence it is vital to know maximum operating lubricant temperature, as elevated temperatures increase the oxidation rate, additive consumption and cause irreversible viscosity changes. Deterioration of lubricating fluid can lead to equipment failure, as lubricant can no longer efficiently separate surfaces. The primary mechanisms of lubricant deterioration are oxidation and thermal breakdown of the base oil leading to changes in oil chemistry. As stability of a lubricant is mostly determined by its chemical composition, it is important to understand the oil degradation processes.

Additionally, contaminations can have significant effect on lubricant stability, as they can alter degradation mechanisms taking place, by e.g., catalyzing diverse chemical reactions due to presence of metal wear debris, hydrolysis due to water (see 3.1.3.), accelerating additive and base oil degradation due acidic compounds originating from the lower quality fuels, polymer degradation due to shear stress.

3.1.1. Oxidation stability

Oxidation is the predominant process of oil degradation due to presence of dissolved or entrained air, thus antioxidants represent vital additives in oil formulations. Oxidation processes will vary with the base oil quality and the type of antioxidant additives used. Lubricant antioxidants, such as phenolic ones and aromatic amines are sacrificial. They deplete over the time by eliminating free radicals in order to protect the base oil from oxidation. Eventually, the antioxidants are consumed and the base oil oxidation is initiated and propagated by presence of free radicals. Synthetic hydrocarbon oils have better oxidation

stability than conventional mineral oils as they contain less reactive impurities, such as unsaturated hydrocarbons which react more readily with oxygen [3.2].

Common oxidation products formed are carboxylic acids causing depletion of oils basic reserve, followed by oil acidity increase, which leads to rust and surface corrosion. Other formed oxidation by-products are ketones, aldehydes, and esters. Products of oxidation reactions lead to formation of high molecular weight species such as polymers, which are precursors to sludge and varnish. This leads to viscosity rise due to increase in average molecular weight of compounds present in the used oil.

Temperature greatly influences the rate of oxidation, as according to Arrhenius law, reaction rate increases exponentially with increasing temperature. So, as a rule of thumb, the oil oxidative life is reduced by half for every 10 °C temperature rise. The rate of oxidation is further accelerated by presence of water, acids and catalysts, such as copper and iron, which result from wear of tribological material [3.3].

3.1.2. Thermal stability

Thermal stability of oil is its resistance towards degradation processes occurring in the absence of oxygen and is mainly dependent on the chemical structure of the base oil. Hydrocarbon based lubricants have generally higher thermal than oxidative stability. Undesired heat generation in tribosystems is mainly due to conversion of mechanical energy that can be accompanied by temperature increase due to insufficient heat dissipation. Excessive heat causes additive depletion or volatilization and base oil decomposition by providing activation energy for the degradation reactions. The most significant change caused by thermal decomposition is an increase in oils vapor pressure as volatile oil fractions vaporize. Lubricant thermal breakdown can also initiate side reactions, induce polymerization and generate insoluble by-products in the form of sludge and deposits resulting in distinct oil color change. However, effects of thermal decomposition are much less understood than oxidation [3.1, 3.2].

3.1.3. Hydrolytic stability

Mineral base oils and polyalphaolefins (PAOs) have good hydrolytic stability but ester type base oils, such as polyol esters, diesters and phosphate esters are prone to hydrolysis decomposition. When exposed to water, these esters readily hydrolyze into alcohol and acid via de-esterification mechanism, increasing the oils acidity, hence causing corrosion or catalyzing further reactions [3.1, 3.3].

3.2. Stability of IL lubricants

Lubricant thermo-oxidative stability is one of the most important properties for practical applicability of lubricating fluid. In contrast to well understood degradation of conventional hydrocarbon based lubricants, ILs stability is scarcely investigated in depth. Due to vast IL structural variability, it is difficult to generalize IL properties, such as thermo-oxidative stability, hence tremendous research efforts are needed to understand their structure-property relationships. In general, ILs are considered to be more stable than conventional lubricants which often fail at temperatures above 150 °C, hence ILs are especially suitable for high temperature applications [3.4, 3.5].

3.2.1. IL cation derived stability

The most reported degradation products of imidazolium based ILs are alkyimidazoles [3.6, 3.7]. Imidazolium ILs with halide anions decompose by nucleophilic attack of the halide ion to the cation alkyl groups generating haloalkanes in addition to alkyimidazoles [3.8, 3.9]. Thermal decomposition takes place mainly due to C-N bond cleavage at the cation side [3.10]. Thermo-oxidative decomposition of 1,3-dialkylimidazolium ILs is also described to proceed via carbon radical intermediates, originating from C-H bond thermal cleavage which leads to formation of 1-alkene and alkyimidazole [3.11]. Also IL cations with scrambled alkyl chains were detected due to suggested direct exchange of the alkyl chains between two cations [3.7, 3.12]. Additionally, thermal degradation of 1-alkyl-3-methylimidazolium ILs with acetate and chloride anions produced dimeric compounds of two imidazole moieties linked by a methylene group [3.13]. Another imidazolium decomposition pathway is due to deprotonation of its C2-atom by strong nucleophiles, resulting in reactive carbenes [3.12]. The replacement of the acidic C2 hydrogen by linear alkyl groups increases IL stability [3.14].

It was reported that also 1-alkylpyridinium, dialkylpyrrolidinium and tetraalkylammonium based ILs can be decomposed via the same S_N2 mechanism as imidazolium ILs [3.6]. Degradation mechanism of ammonium based ILs is mostly based on Hoffmann elimination induced by heating and producing tertiary amines and alkenes [3.15-3.17]. Another described thermal decomposition mechanism of ammonium ILs is reverse Menshutkin reaction generating amines [3.6, 3.18]. Dicationic ILs have reported higher thermal stability when compared to the monocationic ILs [3.19].

3.2.2. Alkyl chain effects on IL stability

Alkyl chain length does not have large impact on the IL thermal stability [3.6, 3.14]. In case of longer alkyl groups, some C-C bond cleavage can occur [3.10]. Generally, shorter alkyl chains lead to higher IL stability [3.6, 3.11]. Ether functional groups and branched cation side chains decrease IL stability in comparison to non-functionalized cation side chains [3.6, 3.20]. In contrast, fluorinated alkyl chains and allyl side chains on dialkylimidazolium cation seem to enhance IL stability [3.9, 3.21].

3.2.3. IL anion derived stability

Choice of the IL anion has more pronounced effect on IL stability in comparison to cation and alkyl chain contribution [3.4, 3.6, 3.18]. At elevated temperatures, more stable are anions with poor proton abstracting properties, such as bis(trifluoromethylsulfonyl)imide in contrast to nucleophilic anions, such as halides [3.7, 3.14-3.16, 3.22]. In fact, halides, as highly coordinating anions, are the least thermally stable anions used in IL design [3.6, 3.21]. Inorganic anions represented by $[\text{PF}_6]^-$, $[\text{BF}_4]^-$, or organic anions like $[\text{NTF}_2]^-$ improve IL stability at elevated temperatures due to their lower coordinating nature [3.6]. However, $[\text{PF}_6]^-$ and $[\text{BF}_4]^-$ anions are sensitive to moisture and decompose by release of HF [3.12]. Thermal stability of IL decreases in case of more hydrophilic anions especially in the case of fluorinated anions [3.23, 3.24]. Anions containing CN groups in presence of N-based cations, such as pyrrolidinium, lead to decomposition via polymerization under high temperature conditions [3.22].

3.3. Methods employed in lubricant stability evaluation

Established laboratory test methods are used to study lubricant performance under application-oriented conditions. However, it is difficult to predict lubricant stability from laboratory investigation as under the field conditions many complex effects determine lubricant life time, such as high temperature and pressure, wear particles, gases, etc. Lubricant degradation is accelerated by presence of metals which can act as catalysts and enhance reaction rates, especially in the case of oxidation. International standard tests such as ASTM (American Society for Testing and Materials) and DIN (Deutsches Institut für Normung) serve for relative comparisons of lubricants under the same conditions.

3.3.1. Standard test methods for investigation of conventional lubricants stability

Universal oxidation test for hydraulic and turbine oils using the universal oxidation test apparatus described in ASTM D5846 [3.25] utilizes equipment which is defined in ASTM D4871 [3.26]. The oil sample is subjected to 135 °C in presence of air, copper and iron metal catalysts during this test. The test is based on evaluation of acid build-up or formation of insoluble solids resulting from oil's thermo-oxidative degradation. The obtained test result is reported as time required for acid number to increase by 0.5 mg KOH/g in comparison to the new oil sample or time required until insoluble solids begin to form.

Rotating pressure vessel oxidation test (RPVOT) described in ASTM D2272 [3.27] belongs to one of the most known tests for determination of oil oxidation stability. It is a controlled oxidation test performed at 150 °C under oxygen atmosphere, in presence of water and copper catalyst in order to accelerate oil's degradation. Sample of oil is placed into a pressured vessel rotating at 100 min⁻¹. Oil's resistance to oxidation corresponds to the time needed for an oxygen pressure to drop from 620 kPa to at least 175k Pa lower. The remaining useful life (RUL) of lubricant, evaluated as a time, is determined by comparing the test results of oil in service and of a new oil sample. The decreasing RPVOT value indicates the oil's additive package depletion and continuous oil's oxidation. This test is not performed routinely as it is expensive, time consuming and does not take into account sludge or varnish formation which does not necessarily lead to pressure decrease.

A standard test method for oxidation characteristics of inhibited mineral oils known as turbine oil stability test (TOST) is defined by ASTM D943- [3.28] and can be also applied to hydraulic and circulating oils, which are under risk of water contamination. This test is performed in the presence of oxygen, water, copper and iron metal catalysts at elevated temperature. The test result is reported as the time needed for the acid number to increase to 2.0 mg KOH/g due to acid formation. As the TOST test requires significant time to be completed, with the current maximum testing time being 10 000 hours, it is impractical and rarely used for in-service oil testing.

Testing of mineral oils for their susceptibility to ageing according to Baader is defined in DIN51554 [3.29] and represents a short-term test for prediction of lubricant performance. It is carried out for defined period of time in access to air and in the presence of copper wire being periodically immersed in the oil sample, which acts as ageing accelerator. Two specific temperatures are used, 95 °C in case of hydraulic oils and 110 °C for insulating oils. After the test duration, visual examination of the oil sample and wire is carried out. Additionally, sludge content is evaluated together with saponification number (mg KOH/g) according to

DIN51559 [3.30] and dimensionless dielectric dissipation factor according to DIN57370 [3.31].

3.3.2. Commonly employed experiments for investigation of IL lubricants stability

The above described standard test methods have been developed for comparison studies of conventional lubricants performance. As ILs can possess superior stabilities over even fully formulated lubricants, depending on their structural design, the conventional methods are not suitable for ILs stability evaluation. Apart from the metal catalysts, water and oxygen, these standard tests apply temperatures ranging from 95 to 150 °C, as conventional lubricating oils often fail above 150 °C temperature.

Until now, the most applied technique for evaluation of IL stability is the thermo-gravimetric analysis (TGA), commonly carried out under inert atmosphere [3.32-3.37]. It is based on recording of the sample weight change throughout the applied temperatures using fast heating rates, e.g., 10 °C/min. However, these short-term experiments lead to significant data variances, as the results obtained depend among other on the material of sample pan used, sample amount applied and IL hygroscopicity. Additionally, TGA method will overestimate IL stability in case of slow degradation rate mechanisms due to fast heating rates applied or even fail to detect IL degradation in the case of degradation mechanisms not resulting in mass loss.

In the work presented by Pisarova et al. [3.38, 3.39] for the investigation of IL long-term stabilities, combined experimental effects of the above described standard tests were utilized; (1) water and air presence, (2) copper and other alloys, such as CuSn8P and 100Cr6, employed in tribology (3) stepwise temperature increase applying temperatures at 150, 175 and 190 °C with each subsequent temperature step of seven days duration applied to the same IL sample bulk. These severe conditions proved appropriate to observe the degradation processes taking place in the selected IL lubricants.

3.3.3. Routine analysis for condition monitoring of conventional lubricants

Standard test method for acid number (AN) evaluation belongs to one of the most common lubricant analysis and it is described by ASTM D974 [3.40] and ASTM D664 [3.41]. This analysis can serve for additive depletion monitoring, as some additives such as zinc dialkyldithiophosphate (ZDDP) cause initial AN decrease as they are being consumed. Once the additives are depleted, the AN starts to increase due to acidic compounds formation as the

oil oxidizes. Information about acid number is obtained by titration method either using color indicator or by potentiometric titration and the result is expressed in mg KOH/g.

Measurement of oil viscosity is another way for oil degradation monitoring and is defined in the ASTM D445 [3.42] and ASTM D7042 [3.43]. As the oils average molecular weight increases, viscosity of the oil rises as it is related to the size of the molecules present. Viscosity changes can be also related to the shearing of viscosity modifier polymers or to the events of contamination, e.g., due to fuel dilution. Viscosity results are provided either in the form of dynamic viscosity determined commonly in milli-Pascal per second (mPa·s) or as kinematic viscosity in centi-Stoke (cSt).

The water content in oil can be monitored by coulometric Karl Fischer titration described in ASTM D6304 [3.44]. It is important to follow the water level changes, as water can adversely affect lubricants by promoting oxidation reactions, corrosion processes and can lead to depletion of some additives. Obtained results are provided in mg/kg or as weight percents.

Fourier transform infrared (FT-IR) spectroscopy described in ASTM E2412 [3.45] provides overall information about the oil condition and is complementary to physical and chemical property tests. This method is able to identify contaminants, such as water or soot, to monitor additive depletion and to follow the oil chemistry changes, such as oxidation and nitration processes. All covalent chemical bonds absorb IR radiation and exhibit characteristic IR absorptions. An IR spectrum is usually measured from 4000 to 600 cm^{-1} , while oil oxidation provides characteristic signals around 1740 cm^{-1} , the presence of nitration products is indicated by signals in the region of 1600 to 1640 cm^{-1} immediately next to the oxidation products. Sulphation process can be detected between 1180 and 1120 cm^{-1} . As used oil IR spectra are very complex with some overlapping signals, it is often necessary to measure also the starting (i.e. mostly fresh) oil sample to obtain easier ways to show the changes of the IR spectra in the time course.

3.4. References

- [3.1] Totten GE. Fuels and lubricants handbook: technology, properties, performance, and testing. 1st ed. Glen Burnie, Maryland: ASTM International; 2003.
- [3.2] Stepina V, Vesely V. Lubricants and special fluids. 1st ed. Bratislava: ALFA publishers; 1992.
- [3.3] Mortier RM, Fox MF, Orszulik ST. Chemistry and technology of lubricants. 3rd ed. London: Springer; 2010.
- [3.4] Minami I. Ionic liquids in tribology. *Molecules* 2009; 14:2286-2305.

- [3.5] Bermudez MD, Jimenez AE, Sanes J, Carrion FJ. Ionic liquids as advanced lubricant fluids. *Molecules* 2009; 14:2888-2908.
- [3.6] Siedlecka EM, Czerwicka M, Stolte S, Stepnowski P. Stability of ionic liquids in application conditions. *Curr Org Chem* 2011; 15:1974-1991.
- [3.7] Meine N, Benedito F, Rinaldi R. Thermal stability of ionic liquids assessed by potentiometric titration. *Green Chem* 2010; 12:1711-1714.
- [3.8] Chowdhury A, Thynell ST. Confined rapid thermolysis/FTIR/ToF studies of imidazolium-based ionic liquids. *Thermochim Acta* 2006; 443:159-172.
- [3.9] Hao Y, Peng J, Hu S, Li J, Zhai M. Thermal decomposition of allyl-imidazolium-based ionic liquid studied by TGA-MS analysis and DFT calculations. *Thermochim Acta* 2010; 501:78-83.
- [3.10] Ohtani H, Ishimura S, Kumai M. Thermal decomposition behaviors of imidazolium-type ionic liquids studied by pyrolysis-gas chromatography. *Anal Sci* 2008; 24:1335-1340.
- [3.11] Minami I, Kamimura H, Mori S. Thermo-oxidative stability of ionic liquids as lubricating fluids. *J Synth Lubr* 2007; 24:135-147.
- [3.12] Keil P, Kick M, König A. Long-term stability, regeneration and recycling of imidazolium-based ionic liquids. *Chem Ing Tech* 2012; 6:859-866.
- [3.13] Liebner F, Patel I, Ebner G, Becker E, Horix M, Potthast A, Rosenau T. Thermal aging of 1-alkyl-3-methylimidazolium ionic liquids and its effect on dissolved cellulose. *Holzforschung* 2010; 64:161-166.
- [3.14] Kroon MC, Buijs W, Peters CJ, Witkamp GJ. Quantum chemical aided prediction of the thermal decomposition mechanisms and temperatures of ionic liquids. *Thermochim Acta* 2007; 465:40-47.
- [3.15] Chowdhury S, Mohan RS, Scott JL. Reactivity of ionic liquids. *Tetrahedron* 2007; 63:2363-2389.
- [3.16] Baranyai KJ, Deacon GB, MacFarlane DR, Pringle JM, Scott JL. Thermal degradation of ionic liquids at elevated temperatures. *Aust J Chem* 2004; 57:145-147.
- [3.17] Morrison RT, Boyd RN. *Organic chemistry*. 6th ed. Englewood Cliffs, New Jersey: Prentice-Hall; 1992
- [3.18] Sowmiah S, Srinivasadesikan V, Tseng MC, Chu YH. On the chemical stabilities of ionic liquids. *Molecules* 2009; 14:3780-3813.
- [3.19] Anderson JL, Ding R, Ellern A, Armstrong DW. Structure and properties of high stability geminal dicationic ionic liquids. *J Am Chem Soc* 2005; 127:593-604.

- [3.20] Ngo HL, LeCompte K, Hargens L, McEwen AB. Thermal properties of imidazolium ionic liquids. *Thermochim Acta* 2000; 357-358:97-102.
- [3.21] Crosthwaite JM, Muldoon MJ, Dixon JK, Anderson JL, Brennecke JF. Phase transition and decomposition temperatures, heat capacities and viscosities of pyridinium ionic liquids. *J Chem Thermodyn* 2005; 37:559-568.
- [3.22] Wooster TJ, Johanson KM, Fraser KJ, MacFarlane DR, Scott JL. Thermal degradation of cyano containing ionic liquids. *Green Chem* 2006; 8:691-696.
- [3.23] Fredlake CP, Crosthwaite JM, Hert DG, Aki SNVK, Brennecke JF. Thermophysical properties of imidazolium-based ionic liquids. *J Chem Eng Data* 2004; 49:954-964.
- [3.24] Huddleston JG, Visser AE, Reichert WM, Willauer HD, Broker GA, Rogers RD. Characterization and comparison of hydrophilic and hydrophobic room temperature ionic liquids incorporating the imidazolium cation. *Green Chem* 2001; 3:156-164.
- [3.25] ASTM D5846, 2012 (2007), "Standard test method for universal oxidation test for hydraulic and turbine oils using the universal oxidation test apparatus", ASTM International, West Conshohocken, PA, 2012, DOI: 10.1520/D5846-07R12, www.astm.org.
- [3.26] ASTM D4871, 2011, "Standard guide for universal oxidation/thermal stability test apparatus", ASTM International, West Conshohocken, PA, 2011, DOI: 10.1520/D4871-11, www.astm.org.
- [3.27] ASTM D2272, 2011, "Standard test method for oxidation stability of steam turbine oils by rotating pressure vessel", ASTM International, West Conshohocken, PA, 2011, DOI: 10.1520/D2272-11, www.astm.org.
- [3.28] ASTM D943, 2010e1 (2004a), "Standard test method for oxidation characteristics of inhibited mineral oils", ASTM International, West Conshohocken, PA, 2010, DOI: 10.1520/D0943-04AR10E01, www.astm.org.
- [3.29] DIN 51554-1, 1978, "Testing of mineral oils; test of susceptibility to ageing according to Baader; purpose, sampling, ageing", DIN Deutsches Institut für Normung e. V., Berlin, Germany, 1978, www.din.de.
- [3.30] DIN 51559-1, 2009, "Testing of mineral oils - determination of the saponification number – part 1: saponification numbers above 2, colorindicator titration", DIN Deutsches Institut für Normung e. V., Berlin, Germany, 2009, www.din.de.
- [3.31] DIN 57370-1, 1978, "Insulating oils; new insulating oils for transformers and switch gear", DIN Deutsches Institut für Normung e. V., Berlin, Germany, 1978, www.din.de.

- [3.32] Seeberger A, Andresen AK, Jess A. Prediction of long-term stability of ionic liquids at elevated temperatures by means of non-isothermal thermogravimetric analysis. *Phys Chem Chem Phys* 2009; 11:9375-9381.
- [3.33] Arellano IHJ, Guarino JG, Paredes FU, Arco SD. Thermal stability and moisture uptake of 1-alkyl-3-methylimidazolium bromide. *J Therm Anal Calorim* 2010; 2:725-730.
- [3.34] Muhammad N, Man ZB, Bustam MA, Mutalib MIA, Wilfred CD, Rafiq S. Synthesis and thermophysical properties of low viscosity amino acid-based ionic liquids. *J Chem Eng Data* 2011; 56:3157-3162.
- [3.35] Heym F, Etzold BJM, Kern C, Jess A. Analysis of evaporation and thermal decomposition of ionic liquids by thermogravimetric analysis at ambient pressure and high vacuum. *Green Chem* 2011; 13:1453-1466.
- [3.36] Ferreira AF, Simoes PN, Ferreira AGM. Quaternary phosphonium-based ionic liquids: thermal stability and heat capacity of the liquid phase. *J Chem Thermodyn* 2012; 45:16-27.
- [3.37] Bittner B, Wrobel RJ, Milchert E. Physical properties of pyridinium ionic liquids. *J Chem Thermodyn* 2012; 55:159-165.
- [3.38] Pisarova L, Gabler Ch, Doerr N, Pittenauer E, Allmaier G. Thermo-oxidative stability and corrosion properties of ammonium based ionic liquids. *Tribol Int* 2012; 46:73-83.
- [3.39] Pisarova L, Steudte S, Doerr N, Pittenauer E, Allmaier G, Stepnowski P, Stolte S. Ionic liquid long-term stability assessment and its contribution to toxicity and biodegradation study of untreated and altered ionic liquids. *J Eng Tribol* 2012; 226:903-922.
- [3.40] ASTM D974, 2012, "Standard test method for acid and base number by color-indicator titration", ASTM International, West Conshohocken, PA, 2012, DOI: 10.1520/D0974-12, www.astm.org.
- [3.41] ASTM D664, 2011a, "Standard test method for acid number of petroleum products by potentiometric titration", ASTM International, West Conshohocken, PA, 2011, DOI: 10.1520/D0664-11A, www.astm.org.
- [3.42] ASTM D445, 2012, "Standard test method for kinematic viscosity of transparent and opaque liquids (and calculation of dynamic viscosity)", ASTM International, West Conshohocken, PA, 2012, DOI: 10.1520/D0445-12, www.astm.org.
- [3.43] ASTM D7042, 2012a, "Standard test method for dynamic viscosity and density of liquids by Stabinger viscometer (and the calculation of kinematic viscosity)", ASTM International, West Conshohocken, PA, 2012, DOI: 10.1520/D7042-12A, www.astm.org.

[3.44] ASTM D6304, 2007, "Standard test method for determination of water in petroleum products, lubricating oils, and additives by coulometric Karl Fischer titration", ASTM International, West Conshohocken, PA, 2007, DOI: 10.1520/D6304-07, www.astm.org.

[3.45] ASTM E2412, 2010, "Standard practice for condition monitoring of used lubricants by trend analysis using Fourier transform infrared (FT-IR) spectrometry", ASTM International, West Conshohocken, PA, 2010, DOI: 10.1520/E2412-10, www.astm.org.

4. Applied analytical techniques for IL degradation studies

The routine analysis applied for condition monitoring of conventional lubricants, apart from IR spectroscopy, are unspecific methods not applicable for lubricant degradation studies on the molecular level. Even though IR spectroscopy can reveal lubricant structural changes (e.g., functional group changes), its sensitivity is lower than that of mass spectrometry (MS) techniques. IR spectroscopy combined with MS analysis was employed in IL confined rapid thermolysis to study evolved species [4.1-4.4] and MS as the main analytical tool was applied in the most of other studies aiming to elucidate IL degradation processes which will be discussed further below.

4.1. Time-of-flight mass spectrometry (TOF-MS)

4.1.1. Laser desorption/ionization (LDI)

Laser desorption/ionization technique was developed for solid or liquid samples that are not volatile under vacuum [4.5, 4.6]. Sample solution or the liquid itself is deposited directly by a syringe or glass/metal tip onto designated areas of usually stainless steel plate used as sample target; thus the technique requires only simple sample preparation. By transferring several samples at once into the ion source, the total analysis time is kept short. Prepared sample spots should be homogeneous, flat and thin to avoid decrease of mass spectrometric resolution and insufficient mass spectrum quality [4.7]. In case of inhomogeneous sample spots, mass spectra of insufficient quality are obtained and the operator has to search for so called “sweet” spots to obtain sufficient signal to noise ratio intensities. Therefore, automated approach using rastering for data acquisition to obtain reproducible mass spectra cannot be applied and the analysis time is prolonged.

Analytes are ablated from the sample target surface by means of laser irradiation and sample desorption and ionization occurs in created plume [4.5]. Laser irradiation at a certain wavelength is either absorbed by the analyte or a thermal spike is generated in case of infrared lasers, hence the laser wavelength does not have to be matched to the sample [4.5, 4.6]. Focused laser pulses deliver energy packets (mJ to J) onto a small area (5 to 200 μm) in a very short time (ps to ns). Lasers employed either emit short pulses in ultraviolet region (UV); such as nitrogen laser with 337 nm wavelength and Nd:YAG laser with 355 nm (triplicated) and 266 nm (quadruplicated) wavelengths or longer pulses in infrared region (IR) are applied; with carbon dioxide laser using 10.6 μm wavelength and Er:YAG laser using 2.8 μm wavelength [4.7].

LDI is suitable for many low to medium molecular mass analytes (<1 kDa) and produces mainly singly charged ions as well as derived fragment ions, hence produced mass spectra are beneficial for analysis of complex mixtures [4.5-4.8]. Oligosaccharides, peptides and polymers are commonly analyzed samples with LDI technique. Ionic liquids despite having inherited ionic character are scarcely analyzed by LDI approach. The work carried out by Zabet-Moghaddam et al. characterizing intact ILs [4.9], studies by Dessiaterik et al. of species evolved after IR and UV ablation of intact ILs [4.10] and analysis by Pisarova et al. investigating IL long-term stabilities [4.11, 4.12] have successfully applied LDI as desorption/ionization method of choice. LDI is a pulsed technique and is therefore well suited to be combined with a time-of-flight (TOF) mass analyzer to record mass spectra by simultaneous ion detection in a short time using micro-channel plate [4.5-4.7].

4.1.2. Matrix-assisted laser desorption/ionization (MALDI)

MALDI technique extends the possibilities of LDI towards analysis of intact large molecules (of several kDa), such as peptides, proteins or polymers, and thermally labile compounds as it protects analytes from degradation and extensive fragmentation. In contrast to LDI, analytes do not absorb the laser irradiation themselves, but the desorption/ionization process is carried out by use of matrix molecules strongly absorbing at the applied laser wavelength [4.1, 4.2]. Therefore, matrix choice has to be matched with the type of laser applied.

In case of the most widely used UV lasers, matrices are aromatic based small organic molecules with hydroxyl- and carboxyl-functional groups whereas in case of IR lasers, urea and alcohols are applied [4.5, 4.8, 4.13]. Matrices can be classified as acidic (H^+ donors), the most popular being α -cyano-4-hydroxycinnamic acid (CHCA) and 2,5-dihydroxybenzoic acid (DHB) and as neutral ones, suitable for analytes with acid labile bonds, such as trihydroxyacetophenone (THAP) and Co nanoparticles in glycerol [4.6, 4.14]. Another matrix differentiation is based on the amount of energy transferred to analytes, where so called “hot” matrices deliver more energy leading to multiply charged ions whereas “cold” matrices support formation of singly charged ions and are more beneficial for labile compounds and in case of molecular weight determination. Additionally, a novel matrix type based on ionic liquids, being more homogenous than solid matrices, have been studied extensively in the last years with promising results for analysis of peptides, proteins, carbohydrates, polymers, etc. [4.15-4.19].

Appropriate matrix selection, matrix concentration and matrix to analyte mixing ratio together with sample preparation technique have to be optimized empirically [4.5]. For successful

sample preparation, vacuum stable matrix lacking chemical reactivity is a necessity, high quality volatile solvent miscible with both matrix and analyte have to be used and furthermore acid addition can be desirable for improved ionization in the positive ion mode [4.5, 4.6]. Generally, the sample is mixed with a large molar excess of matrix molecules in order to separate analyte molecules from each other and hinder the formation of aggregates and clusters. Correct sample deposition ($\leq 1 \mu\text{L}$) onto a sample holder is a critical preparation step as the crystallized surface morphology affects obtained mass spectra quality [4.5, 4.6, 4.8, 4.13]. Several sample spot preparation techniques have been established. In case of “volume technique”, matrix and sample solutions are pre-mixed before their mixture aliquot is placed on the sample target whereas during “dried droplet” preparation, separate matrix and sample solution aliquots are added onto the sample target and are mixed before drying at ambient temperature. “Thin layer” technique consists of applying first layer of matrix solution which is let to crystallize and subsequently sample solution is added on the top of matrix layer and dried at room temperature [4.5, 4.8].

The prepared sample target is loaded into the mass spectrometer and after sufficient vacuum is established the matrix-assisted laser desorption/ionization process takes place. The laser beam is focused on the sample spot and applied laser energy absorbed by the matrix is optimized for matrix threshold irradiance, so matrix excitation and desorption occurs. Due to localized sublimation, matrix and intact analyte expands into the gas phase “matrix plume”. The matrix assists in the sample ionization, which must contain easily ionized atoms or groups, via electron, proton transfer and chemical processes which occur in the gas phase [4.5, 4.6, 4.8, 4.13, 4.20]. These ionization processes are still not fully understood.

The most common ions produced are singly charged radical cations $[\text{M}]^+$, protonated molecules $[\text{M}+\text{H}]^+$ and their $[\text{M}-\text{H}]^-$ negative deprotonated molecular analogues providing molecular weight information. Additionally, some adducts with alkali metal ions $[\text{M}+\text{Na}]^+$, multiply charged ions, and very few fragments are created [4.5, 4.6, 4.13, 4.20, 4.21]. The mass spectrum is acquired for each laser pulse and to obtain a long-lasting stable signal, sample target is moved to continuously expose fresh sample. The acquired mass spectra are subsequently averaged for acquisition of reproducible mass spectra [4.5, 4.6, 4.20].

Among the advantages of MALDI technique is its high sensitivity, possibility to measure large intact biomolecules and potential sample re-analysis. Even though MALDI has good tolerance to low concentration of salts, but high concentrations can interfere with the sample desorption and ionization process. Other undesired effects are: large degree of chemical noise

at low m/z range, lower sensitivity and resolution for high m/z analytes, low shot-to-shot reproducibility and strong dependence on the sample preparation [4.5, 4.13, 4.21].

4.1.3. Time-of-flight mass spectrometer (TOF) and applied analyzing modes

4.1.3.1 Linear time-of-flight (LTOF) mass analyzer

The TOF analyzer is appropriate for separation of high molecular weight analytes, so it is best suited for so-called “soft” ionization techniques of pulsed nature having well-defined start time, such as LDI and MALDI [4.5, 4.13, 4.21].

The ions formed are expelled and accelerated from the source towards the field-free flight tube by acquiring the same kinetic energy. In the field free region the ions are separated according to their velocities due to their different mass to charge values and hence are dispersed in time. The lower the ion’s mass the higher its velocity and the faster it reaches the detector [4.5]. The schematic description of the MALDI-LTOF principle is presented in the Figure 1.

As in all mass spectrometers, calibration is required to convert the measured physical property into a mass-to-charge (m/z) value. In TOF analyzers the m/z ratio is determined by measuring the time it takes for ion to move through the field-free region between the source and the detector [4.5, 4.13]. The better the flight time determination the better the m/z determination, currently nanosecond time resolution is a routine. In the most cases mass calibration with only two reference points of measured flight time for ions with known m/z ratio is sufficient to correlate the time scale with m/z values [4.5, 4.8, 4.21]. Hence, the ion’s m/z ratio can be calculated from a measurement of its flight time t according to the following equation:

$$\frac{m}{z} = \left(\frac{2eV_s}{L^2} \right) t^2 \quad \text{equation (1)}$$

where m/z means mass to charge ratio, e^- stands for electron charge, V_s represents accelerating voltage, t is the time of flight and L is the flight path, whereas V_s and L are constant for given spectrometer.

An advantage of TOF analyzers is its high ion transmission efficiency leading to very high sensitivity, as almost all ions formed are detected. Also the analysis speed is very high, so the mass spectra recorded are a sum of several hundred individual spectra. Resolution in mass spectrometry is defined as: $R = m/\Delta m$, where m stands for ion mass and Δm represents peak width at the 50 % peak height. Mass resolution in TOF analyzer is proportional to the flight time, thus can be increased by longer flight tubes, but this has practical limitations (requires high and homogenous vacuum) or by lower acceleration voltage, however then sensitivity is

reduced. To have sufficiently high resolution and high sensitivity, flight tube length of 1 to 2 m and acceleration voltage of at least 10 kV is required. As mass resolution is also affected by ion's time, space and kinetic energy distribution originating from applied pulsed desorption/ionization technique, delayed pulsed extraction and reflectron have been developed to obtain even higher resolutions and mass accuracy [4.5, 4.8].

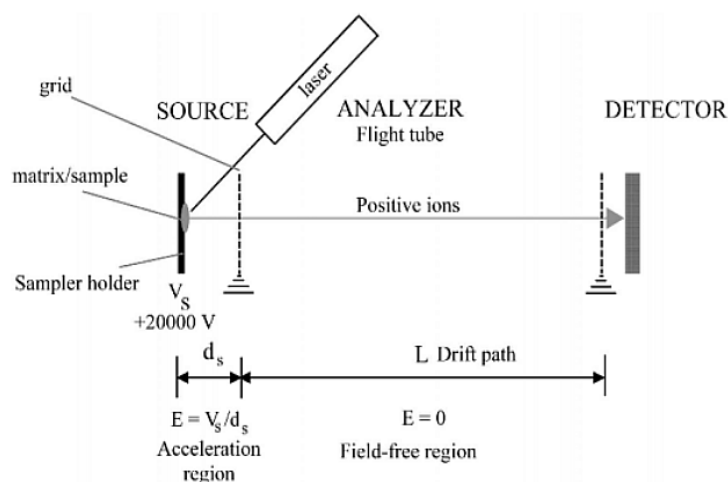


Figure 1. Schematic description of MALDI-LTOF mass spectrometer principle [4.5].

4.1.3.2 Delayed (or pulsed) extraction

To reduce kinetic energy dispersion of ions with the same m/z ratio formed in the ion source a time delay (ns to μ s) is introduced before their extraction from the ion source. The extraction pulse transmits more energy to the ions which remained longer in the source, so these initially less energetic ions join the more energetic ones at the detector. Hence, energy dispersion is corrected and the resolution is improved by adjusting the time delay and pulse amplitude. As the optimal pulse voltage and time delay are mass dependent the mass calibration procedure becomes more complicated and can only be optimized for part of the mass range at a time [4.5, 4.8].

4.1.3.3 Reflectron time-of-flight (RTOF) mass analyzer

Another way to improve TOF mass resolution is the use of an electrostatic reflector called reflectron. The reflectron lenses with a voltage cascade create retarding field that acts as an ion mirror deflecting the ions and sending them back through the flight tube in the opposite direction. The reflectron is located behind the field-free region opposed to the ion source and the reflectron detector is usually positioned adjacent to the ion source to capture the reflected ions [4.5].

The single-stage reflectron consists of equally spaced ring electrode series creating linear homogeneous electric field and corrects only for the initial kinetic energy dispersion of ions with the same m/z ratio as described in the Figure 2. The dual stage or curve field reflectron use is also important in the case of metastable ions. Ions with more kinetic energy penetrate reflectron deeper, consequently spending longer time in the reflectron and therefore reaching the detector at the same time as the slower ions with the same m/z . The reflectron thus improves resolution by flight path increase without changing the spectrometer dimension. However, the mass resolution increases at the expense of sensitivity and mass range limitation [4.5, 4.8].

The performance of the reflectron may be improved by use of the curved field reflectron which provides a retarding field increasing in a nonlinear manner and causing decrease of heavy ions penetration distance. The ions with broader kinetic energy range can be adequately focused at the same time, avoiding the need to adjust reflectron potential for particular m/z . However, curved field reflectron causes more ion losses than the linear field reflectron [4.5, 4.13].

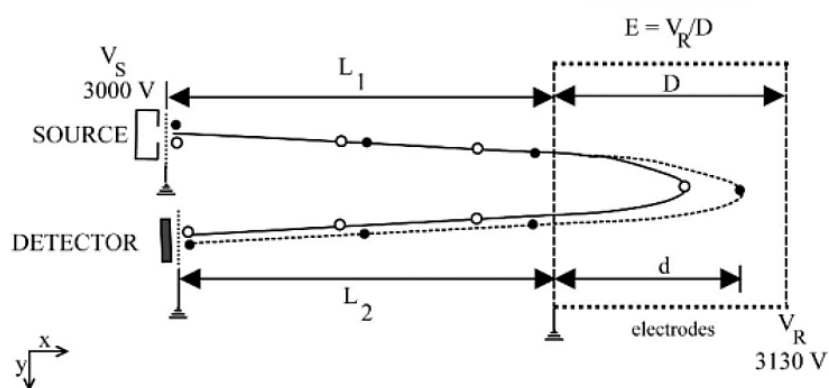


Figure 2. Schematic description of RTOF mass analyzer principle [4.5].

4.1.3.4 Post-source decay (PSD)

Post-source decay (PSD) occurs when intact ions leave the source with sufficient excess of internal energy causing them to decay in the field-free region. The process corresponds to metastable ion fragmentation. Activation of these ions occurs due to direct photon/molecule interactions or multiple collisions in the expanding matrix plume. These collisions can be controlled by extraction field strength, as its increase leads to rise of ion-neutral collision energy and thus the ion's internal energy [4.5].

When ions decay after acceleration and before entering the reflectron, created product ions have the same velocity as their precursor ion, thus have the same flight time. Therefore they

cannot be resolved in LTOF analyzer as they all reach detector at the same time, which leads to loss of mass resolution and sensitivity [4.5].

Tandem TOF mass spectrometers consisting of short linear TOF and reflectron TOF as the second mass analyzer have been designed. Selection of the precursor ion is obtained by a deflection gate situated between the source and the reflectron or in front of the reflectron. Potential is applied to eliminate other than precursor and its fragment ions traveling at the same velocity. Reflectron induces kinetic energy focusing and time dispersion of fragment ions having different mass. The optimum reflectron potential has to be adjusted for each ion's mass by subsequent voltage scanning unless a curved field reflectron is used, allowing single step recording of the complete PSD spectrum [4.5].

4.1.3.5 High-energy collision induced dissociation (HE-CID)

When structure elucidation is desired, dissociation of analyte may also be induced by more controlled experiment such as collision-induced dissociation. Selected precursor ions are accelerated by a several kilovolt-potential and enter the collision cell placed between two analyzers. Precursor ions then collide with static neutral gas molecules and excitation occurs by energy transferred during collisions. If sufficient internal energy is gained, most of the structurally viable dissociations occur and product ions are formed. Helium is the most commonly used collision gas. However, more efficient transfer of energy is reached by using heavier gasses, such as argon and xenon, leading to collision yield increase [4.5, 4.6, 4.8].

4.2. High performance liquid chromatography coupled to electrospray ionization linear ion trap orbitrap mass spectrometry (HPLC-ESI-LIT-orbitrap-MS)

4.2.1. High performance liquid chromatography (HPLC)

HPLC is differentiated from traditional liquid chromatography due to superior separation achieved by use of small diameter columns packed with small size particles and thus requiring high pressures (~ 150 bars). Typical analytical stainless steel HPLC column is 15 to 30 cm long, with internal diameter of 2 to 5 mm and particle size between 3 to 10 μm , which offers good compromise between column capacity, resolution and separation speed [4.22]. HPLC systems utilizing even smaller particles (< 2 μm) result in need of very high pressures (up to 1000 bars) and are defined as ultra high performance/pressure liquid chromatography (UHPLC) due to increase in resolution and sensitivity. The advantage of using smaller particle size is greater surface area enhancing analyte-particle interactions, so efficient

separation is achieved in shorter time. UHPLC columns, having even smaller diameter, lead to decrease in solvent consumption however at the expense of limited loading capacity [4.23]. HPLC separation modes can be based on analyte differences in polarity (partition chromatography), size (size exclusion chromatography), charge (ion exchange chromatography), or specific affinity (affinity chromatography) towards the stationary phase. The most common HPLC separation mode is the partition chromatography based on differences in compound polarities. The column stationary phase is based on tightly packed very fine solid spherical beads of silica or polymer with bonded stationary phase of desired functional groups on their surface. In principle any compound that has affinity to the stationary phase can be separated on the column. HPLC is especially suitable for separation of non-volatile and thermally labile compounds [4.22-4.24]. HPLC as a method of choice was applied to study IL stability under gamma radiation by Rouzo et al. [4.25] and effect of H₂O₂ and UV irradiation on imidazolium ILs was investigated by Czerwicka et al. [4.26]. The HPLC studies by Pisarova et al. [4.12] and Keil et al. [4.27] focused on IL long-term stability evaluation by degradation products detection and quantification.

Sample solution, as a complex mixture, is introduced into the sample loop and injected as a narrow band onto the column head by the mobile phase flow. Separation of individual components along the column is achieved due to differences in their affinity towards the stationary and mobile phase. The analyte distributed between the mobile and stationary phase would reach equilibrium if not disturbed by continuous pumping of fresh solvent down the column. Sample components move further apart as they pass the column due to different time they spent in the stationary phase, acquiring different retention times. Analytes with the highest affinity towards the column packing stay longest on the column and elute as the last ones, as analyte movement occurs only in the mobile phase. Successful separation of all mixture components requires optimized analytical conditions, such as column packing and mobile phase type, column length and diameter, mobile phase flow and column temperature. Analytes exit the column as separated bands due to differences in their interactions and enter the detector. The time it takes for the analyte to travel from injection until the detector is defined as a retention time. The separated compounds appear in the detector as peaks at their different retention times. The signals obtained from the detector are plotted versus the analysis time in chromatograms used for qualitative and quantitative evaluations [4.8, 4.22-4.24].

The HPLC system is composed of some basic components, such as mobile phase reservoir, pump system, flow and pressure regulator, injection unit, column, detector and waste

reservoir, connective tubing and computer. Pumps have to ensure delivery of constant and pulse-free mobile phase flow. It is also important to use degassed solvents to avoid gas bubbles and highly purified reagents of HPLC grade to avoid impurities as these can ruin the analysis. Use of porous stainless steel disc filter (frit) keeps the possible impurities from entering the packed column. Additionally, zero dead volume column fittings have to be used to ensure minimal band broadening [4.23, 4.24].

4.2.1.1. Normal and reverse phase chromatography

Normal and reverse phase chromatography are terms used to describe relative polarities of the stationary and mobile phase. Relative solvent polarities are determined using the polarity index. Separation can be optimized by varying either the polarity of the column or the mobile phase. If the solvent polarity is more alike the stationary phase polarity, then compounds will elute more rapidly. If the polarity difference is increased, then the retention time will decrease or increase depending on analyte affinity towards the mobile and stationary phase. Mobile phase additives used for pH modification and ion pairing reagents also modify the separation [4.23, 4.24].

In the normal phase HPLC highly polar stationary phase, such as alumina or silica is used with non-polar mobile phase such as hexane. Thus, the least polar analyte is eluted first and by increasing the mobile phase polarity the retention time is decreased [4.24].

In the reverse phase HPLC silica beads are modified to create a non-polar surface by attachment of longer hydrocarbon chains, commonly of C₁₈ length. Polar mobile phase is used, such as water, methanol or acetonitrile. Hence, the most polar analyte is eluted first while the non-polar compound elution will be slowed down due to its van der Waals interactions with the stationary phase hydrocarbon groups. Stationary phase columns of intermediate polarity are also used, with functionalities based on phenyl, cyano, or diol-groups offering additional separation selectivity [4.23, 4.24].

4.2.1.2. Isocratic and gradient separation mode

A separation in which the mobile phase composition remains constant throughout the analysis is called isocratic elution. During isocratic separation the eluted peak widths are increasing linearly with the retention time. Gradient elution is used for more complex mixtures by applying increase of the mobile phase strength throughout the separation process. Highly retained analytes are eluted faster having narrower peaks, so the resolving power is not affected. The applied gradient can be of linear, step-wise, convex or concave nature. Solvent

gradient needs to be done slowly enough to be reproducible, and the column must be re-equilibrated before the next injection [4.23, 4.24].

4.2.2. Electrospray ionization (ESI)

ESI as another “soft” ionization technique is suitable for analysis of thermally labile samples and even of non-covalent biomacromolecular complexes which are ionized intact directly from their solutions at atmospheric pressure. High molecular mass analytes can be ionized by ESI, such as proteins, nucleic acids and polymers currently up to 18 MDa, if efficient desolvation is reached [4.28]. Analytes are either present in the solution as pre-formed ions or as neutral compounds which can be ionized by presence of electrolytes, such as Na⁺ ions via adduct formation. However, protonation/ deprotonation is the main source of charging for biological molecules with several protonation or deprotonation sites, hence pH optimization is important for their stabilization [4.5, 4.13, 4.20, 4.21, 4.29].

Sample solution passes through small conductive capillary held at high voltage, typically of 3 to 5 kV relative to the counter-electrode. The required voltage has to be optimized as it depends on capillary diameter and the solvents used. Mostly polar solvents, such as methanol, acetonitrile or their mixtures with water are applied, while the higher the solvent boiling point the higher the capillary voltage is required. The counter-electrode is a plate with an orifice leading to mass spectrometric sampling system [4.5, 4.8, 4.20, 4.21, 4.29].

In the case of positive ion monitoring, the conductive capillary is held at the positive potential so the negative ions are held back and the positive ions are drawn away from the capillary. Low pH values can promote the positive ion formation. Due to potential difference between the capillary and the counter electrode an intense electric field is created at the capillary tip. Enrichment of positive charged analyte ions near the surface of the liquid meniscus occurs. Increase of a cone surface at the capillary tip is resisted by liquid surface tension. When the surface tension is disturbed by applied solvent dependent onset voltage, a Taylor cone is formed and sample solution is dispersed into a fine highly charged aerosol droplets. Coaxially flowing inert gas can enhance the nebulization process, which was frequently called ion spray. Created droplets of solvent and analytes possess a net positive charge and are dragged through a heated transfer capillary towards the mass analyzer entrance. The droplets formed continuously shrink due to solvent evaporation and ultimately form gas phase ions by two proposed mechanisms [4.5, 4.13, 4.20, 4.21, 4.29].

4.2.2.1. Proposed models of gas phase ion formations

In the case of smaller molecular weight analytes of less than 1 kDa mass, so-called ion evaporation model applies. Once the electric field on the droplet surface becomes large enough, ions located at the droplet surface are able to desorb. In the mixture of components, higher sensitivity is reached for those compounds located at the surface as these can mask those analytes which are soluble in the bulk. By this model mainly singly charged ions are generated [4.5].

Charge residue model applies to molecules larger than 1 kDa which are not able to desorb from the droplet surface. These larger molecules are able to carry multiple charges if they contain several ionizable sites. As the solvent evaporates, the droplet size is shrinking and hence the surface charge density increases. Once the charge repulsion overcomes the droplets surface tension, Coulombic explosion occurs resulting in production of smaller droplets that continue to undergo this process. Eventually multiply charged ions are completely desolvated due to entire solvent evaporation [4.5, 4.8, 4.13, 4.20, 4.29].

Multiply charged ions formed by the ESI process have advantage for high molecular weight compounds analyses by mass spectrometers with limited m/z range as they appear at much lower m/z values due to carrying higher number (z) of charges. Additionally, their molecular weight measurement can be based on each multiply-charged ion [4.5, 4.8, 4.13, 4.20, 4.21].

Advantage of ESI is its sensitivity to the concentration rather than to total quantity of sample injected in the ion source. The sensitivity is increasing when the flow entering the source is decreasing, so when flow rates above 500 $\mu\text{L}/\text{min}$ are used, the sensitivity is reduced. Among ESI shortcomings is the continuous sample consumption, hence some of the sample is wasted and no re-analysis is possible. Also ion suppression effects are susceptible to occur in presence of high salt concentrations (>1 mM), hence especially biological samples need to be desalted [4.5, 4.21].

4.2.2.2. HPLC-ESI-MS on-line coupling

ESI as a continuous ionization method is suitable for direct coupling to liquid separation methods such as HPLC. As ESI is a concentration dependent technique with linear correlation over several orders of magnitude between the ions yield and the analyte concentration, it does not have to be supplied with high flow rates. When ESI is coupled to nano-HPLC large sensitivity increase is gained [4.5, 4.8, 4.13, 4.23].

However, HPLC methods have to be modified when coupled to ESI, by means of avoiding high buffer concentrations, presence of salts and surfactants as these induce ion suppression

and cause source contamination. In order to maintain good sensitivity, the electrolyte concentration should not exceed 10 mM concentration limit. Indeed, volatile buffers and pH modifiers, such as formic or acetic acid should be preferred to avoid source deposits formation and problems in ionization processes. ESI does not tolerate well non-polar solvents. Mobile phase composition should be based on volatile organic solvents, such as acetonitrile, as solvent choice in HPLC will have an immense effect on the mass spectrum obtained. Hence, compromise between sufficient HPLC separation and efficient electrospray ionization should be reached [4.5, 4.8, 4.13].

As HPLC with ESI coupling can tolerate flow rates up to 1 mL/min, solvents have to be efficiently eliminated in order to produce gas-phase ions and maintain vacuum requirements of mass analyzers. If analyte ions are produced in form of clusters with solvent molecules, detection sensitivity and quantitative analysis are affected. To avoid cluster formation, enhance droplet desolvation has to be applied either by counter-current heated dry gas (curtain gas) or by ion passage through heated transfer capillary [4.5, 4.8, 4.29].

Special ESI-MS interface is necessary to transfer the ions from ionization chamber held at atmospheric pressure to the high vacuum region of mass spectrometer. Gradual pressure reduction is achieved by differential pumping system with intermediate vacuum and vacuum compartment being separated by use of skimmer lenses (cones) with very small orifices. The width of the orifices has to provide for sufficient sensitivity while maintain the vacuum.

ESI source can be oriented towards the mass spectrometer entrance (sampler cone) either in axis or orthogonal configuration, which is more compatible with higher flow rates but introduces discrimination based on mass or charge [4.5, 4.13].

4.2.3. Linear ion trap orbitrap mass spectrometry (LIT-orbitrap-MS)

The formed gas-phase ions have to be separated according to their mass-to-charge ratio (m/z) in the mass analyzer. Upon entering the mass spectrometer, ions are focused by use of skimmer lenses and focusing multipoles (ion guides), e.g., octapoles. These multipoles are followed by gating lens which regulates the amount of injected ions as too many ions induce space charge effects and too few lead to sensitivity loss. For positive ions the gating lens is held under negative potential during ion injection and is switched to positive potential once the desired amount of ions is reached [4.5].

4.2.3.1. Linear ion trap (LIT) mass analyzer

Ion trap is a mass analyzer able to trap ions in two or three dimensions by use of oscillating electric field hence can be classified as 2D (linear) or 3D (Paul) ion trap. The advantage of later developed linear ion trap (LIT) is higher ion trapping capacity leading to less susceptibility to space charge effects as ions are focused along the central line rather than around a point which occurs in Paul ion trap. The trapping efficiency of LIT is more than 50 % compared to 5 % for the Paul ion trap. Due to this fact, LIT offers increase of the sensitivity and the dynamic range [4.5, 4.30].

LIT geometry is more similar to quadrupole mass analyzer than to Paul ion trap as it is based on rods divided into 3 segments. Quadrupolar field restricts the ions oscillations in the radial dimension and the end segments reflect the ions forward and backward in the axial dimension. The LIT is held at 10^{-5} mbar as the present cooling gas (He) serves for ions cooling by means of their kinetic energy reduction as a result of collisions with neutral gas molecules. The ions stored in LIT can be either ejected radially through two slots in opposite rods or axially towards the orbitrap. By radial ejection two detectors are used to monitor all expelled ions at low (unit) resolution [4.5, 4.30-4.32]. The schematic description of LIT mass analyzer is provided in Figure 3.

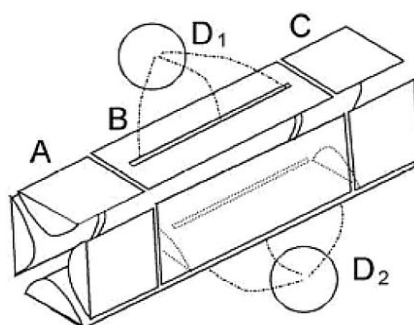


Figure 3. Schematic description of LIT mass analyzer with the central segment B enclosed by two end segments A and C. The central LIT segment enables radial ion ejection through two slots which are detected by two detectors D_1 and D_2 [4.5].

In the LIT, soft fragmentation in the time domain over several generations (MS^n) can be performed by; (1) mass selective ejection of all ions apart from the precursor ones, (2) ions kinetic energy increase due to vibrational excitation and (3) ions fragmentation due to effective collisions with present neutral gas molecules. Hence, LIT can be used independently or in combination with orbitrap to obtain high resolution full or product ion mass spectra [4.5, 4.30-4.32].

4.2.3.2. Orbitrap mass analyzer and integrated detection

Ions from the LIT are accelerated into the transfer octapole and through the gate plate enter the ion trap called C-trap (bent quadrupole) which consists of hyperbolic rods and two end lenses with slits for ion transport [4.32]. The C-trap serves for ion cooling by collisions with nitrogen gas molecules and forms thin long thread of ions along its curved axis. Rapid (μs) and orthogonal ions ejection is followed by vertical ion beam deflection in order to eliminate transport of cooling gas (N_2) into the orbitrap. The ions are accelerated to acquire high kinetic energy and form tight packets before entering the orbitrap [4.5, 4.30-4.32].

The orbitrap is in principle electrostatic ion trap operating in pulsed fashion with large space charge capacity and trapping volume. It consists of barrel shaped outer electrode cut into two equal parts separated by a small gap which serves for ion injection and coaxially placed central spindle shaped electrode as described in Figure 4. In the case of positive ions, negative electrostatic voltage of several kilovolts is applied to the central electrode, while the outer electrode is held at ground potential. The tangentially injected ions are subjected to electrodynamic squeezing to prevent their collisions with the central electrode, which voltage is monotonically lowered. The electric field increase is applied until all ions of the desired m/z , arriving as short packets, are injected. The injected ions start to orbit and oscillate on the stable trajectories along the central axial electrode (z direction). The ion packets of different m/z coherently oscillate at their respective frequencies and have to remain in phase. Ion collisions with background gas molecules result in ion packet dephasing or even in ion loss, hence orbitrap is held at 10^{-10} mbar to avoid signal intensity decrease. The axial frequency of ions harmonic oscillations is directly linked to their m/z ratio and more importantly it is completely independent of the ions kinetic energy and spatial spread as can be seen below,

$$\omega = \sqrt{\left(\frac{z}{m}\right) k} \quad \text{equation (2)}$$

where ω is frequency of axial ions oscillations, z represents ions charge, m stands for ions mass and k describes field curvature [4.5, 4.30-4.32].

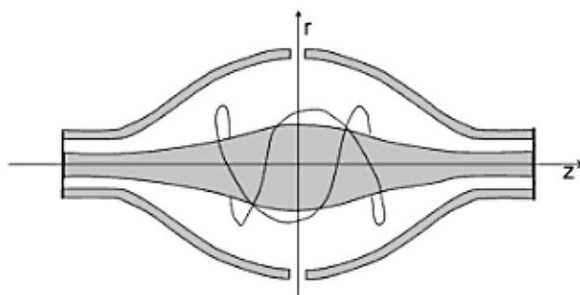


Figure 4. Schematic description of orbitrap mass analyzer composed of outer barrel shaped electrode with coaxially aligned central spindle shaped electrode. The tangentially injected ions coherently oscillate on the stable trajectories around the central electrode [4.5].

The broadband image current induced by ions oscillations is detected once the central electrode is stabilized after electrodynamic squeezing process. The total image current is the sum of individual currents. The signal is detected by the outer electrodes, amplified and converted from the time domain by fast Fourier transformation into the mass spectrum. As the ions motion is very coherent, it enables sensitive detection as well as improvement in mass resolution and mass accuracy. The orbitrap resolution increases linearly with the acquisition time reaching a maximum mass resolution of over 100 000 FWHM. The mass accuracy has been demonstrated as 5 ppm based on external calibration and 2 ppm using internal calibration. Mass accuracy indicates how closely is the measured m/z related to the theoretical m/z and is expressed in millimass units (mmu) or in parts per million (ppm). High mass accuracy together with high resolution is significant for determination of elemental composition. The large dynamic range of orbitrap is over 10^3 within a spectrum and over 10^5 between spectra. The mass range is limited by the use of the LIT and is either m/z 50-2000 or m/z 200-4000 [4.5, 4.30-4.32].

The normal acquisition cycle time in the orbitrap is 1 s and during this period other operations can be performed in LIT as a result of fast ion transmission. Hence, two LIT low-resolution spectra and one orbitrap high-resolution spectrum can be obtained within 1 s. Thus, the LIT-orbitrap hybrid instrument combines the LIT tandem capability with the high resolution and mass accuracy of the orbitrap [4.5, 4.32].

4.3. Headspace cold trap gas chromatography electron ionization mass spectrometry (HS-CT-GC-EI-MS)

4.3.1. Headspace and cold trap techniques

Headspace sampling is an auxiliary sample introduction technique of gas chromatography for analysis of volatile organic compounds. It is especially suitable for solid or liquid matrices from which volatile analytes can be released into the gas phase above the matrix (headspace). Thus, this technique enables increase of the analysis selectivity and sensitivity. Samples are placed into gas-tight closed headspace vials and exposed to optimized and controlled temperature for reproducible analysis. The analyte partition coefficient and volumes of both phases determine the amount of the analyte released into the gas phase. After the equilibrium is reached between the two phases or after a defined amount of time, the aliquot of the headspace phase is directly injected into the gas chromatograph for subsequent chromatographic analysis [4.33-4.35].

Cold trap provides cryogenic concentration (focusing) of the injected gas sample followed by rapid thermal desorption to deliver narrow sample vapor band into the column. This results in generation of sharp, well resolved GC peaks, reproducible retention times and peak areas. The cryo-trap consists of a small heating/cooling chamber installed inside the GC oven, just under the GC injection port. Liquid nitrogen is utilized to permit the trapping of volatiles down to -180 °C [4.33-4.35].

4.3.2. Capillary gas chromatography (GC)

Gas chromatography (GC) is analytical separation technique applicable for analysis of sufficiently volatile and thermally stable organic compounds. The analyzed sample, of liquid or solid form, is commonly introduced into the GC as a solution in volatile organic solvent, such as hexane or dichloromethane. Additionally, gaseous samples can be directly analyzed, solid samples can undergo pyrolysis and non-volatile or thermally labile compounds can be treated by chemical derivatization in order to become suitable for GC measurement. Ionic liquid analytes were studied by several authors using pyrolysis gas chromatography approach in order to identify volatile products evolved after short-term thermal treatment [4.36-4.38]. Thermal degradation products of 1-alkyl-3-methyl-imidazolium based ILs were studied by Liebner et al. [4.39] identifying imidazole, N-methylimidazole and N-alkylimidazoles as the main products, whereas dimeric substituted imidazoles carrying methylene bridge are elucidated as the secondary products. Degradation products evolved due to 1-butyl-3-methyl-

imidazolium chloride treatment in Fenton-like system were studied by Siedlecka et al. [4.40] where imidazolones and their 18 hydroxyl substituted analogues were detected. Headspace gas chromatography analysis of volatile degradation products evolved under long-term thermo-oxidative stress of several ammonium based ILs revealed a presence of abundant gaseous species, such as oxidation products of IL side chains, alkylated IL anions and amines with their secondary degradation products, as stated by Pizarova et al. [4.41]. Qualitative and quantitative analysis of complex mixtures can be performed as GC offers wide applicability range and great instrumental versatility [4.22, 4.33, 4.42].

GC system consists of several components; gas supply system, injection port, column mounted into GC oven, detector and data acquisition system. GC mobile phase is an inert gas (He, H₂) called “carrier gas” as it serves for transfer of analytes through the separation column. Apart from inertness, the carrier gas must be of high purity, as impurities and moisture adversely affect the separation process. To regulate the carrier gas flow and therefore applied pressure, appropriate regulators and controllers are used in the gas chromatograph [4.22, 4.33].

Several injection techniques have been developed to introduce the sample vapors into the column as a narrow band, using heated deactivated glass vaporization chambers called liners. These are inserted into the injection port which should be kept about 50 °C higher than the boiling point of the least volatile sample component in order to avoid discrimination during sample vaporization. Sample introduction is a crucial GC step affecting sensitivity and resolution of the analysis. Slow injections and oversized samples lead to peak broadening and hence to decrease in sensitivity and column capacity [4.22, 4.33].

4.3.2.1. Split and splitless injection techniques

The carrier gas in the injector port is divided into three streams; (1) septum purge to sweep away any contamination from the sealing septum, (2) split flow directed outside from the chromatograph via split valve and (3) carrier gas flow portion transferring the remaining sample vapors towards the separation column [4.33].

The sample size is diminished during the split injection by eliminating most of the sample vapors via the split vent to acquire sample size compatible with the column capacity, preventing the column overload. Commonly applied split ratios range from 1:50 to 1:500 depending on the column diameter and stationary phase thickness, so only a very small sample fraction reaches the column. A purge control valve has to ensure reproducibility of the sample portion arriving into the column for quantification purposes [4.22, 4.33].

Splitless injection is especially beneficial for analysis of trace components in the sample mixture. During the sample injection the split vent is closed, so almost the entire volume of sample vapors is transferred into the column. After an optimized short amount of time, the split vent is opened again, so residual solvent vapors can be eliminated in order to prevent solvent peak tailing which can mask closely eluting analytes. Also solvent type and initial column temperature affect the separation efficiency; thus splitless injection requires optimization of several parameters [4.33].

In most gas chromatography applications the traditional packed columns were replaced by more efficient open tubular capillary columns. The open tubular capillary columns are generally made of fused silica quartz coated on the outside with a polyimide for improved durability. The GC column is characterized by the type of stationary phase used, its film thickness (μm), the column inner diameter (mm) and the column length (m). The carrier gas flows in the capillary columns can range from 1 to 25 mL/min [4.22, 4.33].

The sample separation in GC is based on the analyte interactions with the stationary phase as they are carried through the column in the flow of inert gas. The stationary phase selection is crucial and should be based on the character of sample components to be analyzed. The type of stationary phase determines the elution order of the analytes. If the appropriate stationary phase is selected, analytes will successively elute from the column due to their different affinities towards the stationary phase, while the least interacting analyte will exit the column as the first one [4.22, 4.33].

4.3.2.2. Gas-solid and gas-liquid chromatography

The stationary phase in GC capillary columns is based either on solid porous or on viscous liquid material, so the sample separation in the column is due to either gas-solid or gas-liquid interactions in the column [4.33].

Porous layer open tubular (PLOT) columns are used in the case of gas-solid based chromatography. The separation mechanism occurs as a result of differences in analytes physical adsorption towards the solid adsorbent, such as aluminium oxide. The analytes separation is affected by their molecular weight, stereometry, the sorbent pores geometry and the column temperature. PLOT columns are mainly used where separation of low-molecular-weight volatiles and gases is required, such as air components, carbon monoxide and nitrogen oxides [4.22, 4.33].

In the case of separation based on gas-liquid interactions, the liquid stationary phase is either directly uniformly coated on the column walls (WCOT columns) or immobilized by use of solid support (SCOT columns). SCOT columns have greater sample capacity but worse separation efficiency than WCOT columns. The stationary film of liquid phase has to be nonvolatile, thermally stable and chemically inert. The most applied stationary phase material is polydimethyl siloxane with 100% methyl groups for non-polar interactions or with fraction of methyl groups substituted by functional groups, such as phenyl, cyanopropyl to obtain wider range of polarities. Polyethylene glycol based stationary phases offer additional selectivity. Generally applies, that the stationary phase polarity should match the sample polarity [4.22, 4.33].

Capillary columns can get contaminated due to impurities present in the gas supply or in the sample. Therefore column conditioning by periodical temperature increase or column solvent rinse is carried out. To avoid a loss of stationary phase due to this treatments, the stationary phase is either chemically bonded or cross-linked in order to avoid column bleeding [4.22].

To separate mixture of components, these have to possess sufficiently different affinities towards the applied stationary phase. The analyte retention time depends on its affinity to the stationary phase and its thickness, selected carrier gas flow and the column temperature. These parameters have to be optimized in order to achieve desired separation within the shortest time [4.22, 4.33].

4.3.2.3. Isothermal and gradient temperature program

Column temperature has to be efficiently controlled to a several tenths of a degree by oven thermostat in order to obtain reproducible results. The optimal oven temperature is determined experimentally with the respect to separation efficiency required and range of analyte boiling points. Isothermal analysis, applying constant column temperature throughout the analysis, is sufficient for samples with narrow range of boiling points. When analyzing samples with wide boiling point range, gradient temperature program increasing either continuously or in step manner is applied. This provides shorter analysis time, and thus more efficient separation especially for the later eluting analytes. As the separated analytes elute from the column, their retention time is recorder and plotted versus their signal intensity in the obtained chromatogram [4.22, 4.33].

4.3.3. Electron ionization (EI)

Electron ionization is a “hard” ionization technique during which gas phase molecules ionization occurs via high-energy electron beam bombardment. These electrons are emitted from metal wire (filament) acting as a cathode which is heated by a passing current controlling the number of emitted electrons. The emitted electrons acquire certain energy, generally of 70 eV, depending on the potential difference applied between the cathode and the anode. The lowest potential difference during which the sample ionization occurs is called first ionization potential. The formed high-energy electrons are accelerated across the ion source towards the anode and collide with the gas molecules present in the ionization chamber [4.5, 4.8, 4.20, 4.22].

For most organic molecules the threshold energy leading to ionization is approximately 10 eV (1st ionization potential), but as not all of the electron energy is transferred to the molecule during collisions, higher electron energies of 70 eV are used. The transferred energy causes loss of the molecule (M) valence electron (e^-) and so the formation of molecular ion (radical cation M^+) occurs. The molecular ion carries the information about the compounds mass. The excess of molecule internal energy can further lead to uni-molecular decompositions, hence variety of smaller fragment ions is observed in the mass spectrum. The extent of fragmentation depends on the molecule bond strengths and the fragment ions internal energy and stability [4.5, 4.20].

The obtained fragment ions provide structural information for compound identification even in the absence of molecular ion due to extensive fragmentation. The obtained EI mass spectra are very reproducible and characteristic for a compound (molecular finger print); therefore by use of mass spectral libraries produced with electrons of 70 eV energy, the analytes can be easily identified based on pattern recognition [4.5, 4.20, 4.22].

4.3.3.1. Open split and direct GC-EI-MS coupling

As the gas chromatography can separate complex mixtures with high resolution and mass spectrometry is able to efficiently identify separated compounds, the coupling of GC-MS is highly beneficial. As the mass spectrum of mixture is difficult to interpret, it is essential that the analytes are eluted and ionized subsequently in a stepwise manner. These complementary techniques both require samples in the gas phase; however they have to be properly interfaced as GC operates under pressure while MS works under vacuum. Currently, two approaches are applied to interface the GC-MS coupling, based on open-split and direct coupling systems [4.5, 4.8, 4.20, 4.22, 4.42].

In the case of open-split coupling, the GC column and the MS deactivated interface capillary are inserted into small diameter tube held in a T-shaped housing kept at atmospheric pressure. This housing is filled with helium to avoid oxidation of eluting compounds and the MS capillary is heated to avoid sample condensation. The portion of GC eluent is pumped away and only part of the sample amount reaches the MS ion source. However, the amount of analyte entering the mass spectrometer is important as it affects the instrument detection limit. The advantage is the reduced gas load for the pump system, but at the expense of sensitivity and the possibility of column exchange without breaking the mass spectrometer vacuum [4.5, 4.8, 4.20].

Direct coupling enables passing of the entire eluent flow to the MS source, if compatible flows (1 to 2 mL/min) and high capacity vacuum pumps ensure low operating pressure in the ion source. The capillary column is directly inserted into the ion source via heated small diameter tube to avoid condensation. Since the gas chromatography is performed between the injector held at atmospheric pressure and the ion source held at vacuum, the column of sufficient length has to be used. As the entire flow is directed to the MS ion source, the detection sensitivity is increased, however the column exchange becomes more complicated [4.5, 4.8, 4.20, 4.42].

4.3.4. Quadrupole mass analyzer

Quadrupole mass analyzer consists of four perfectly parallel aligned circular or hyperbolic metallic or metallized electrode rods. The two opposite quadrupole rods are connected into pairs and experience the alternation of positive and negative potentials. Schematic description of the quadrupole mass analyzer is provided in the Figure 5. As quadrupole acts as a mass filter, this oscillating electric field enables only resonant ions of a particular m/z to follow stable oscillating pathway along the z -axis and reach the detector. The m/z value transmitted is determined by the radio frequency (RF) and direct current (DC) voltages applied to the rods. All ions above or below the set m/z value are discharged on the quadrupole rods. To obtain a mass spectrum over selected m/z range, the RF and DC fields are scanned, either by potential or frequency, so all ions sequentially become resonant and reach the detector [4.5, 4.8, 4.13, 4.20].

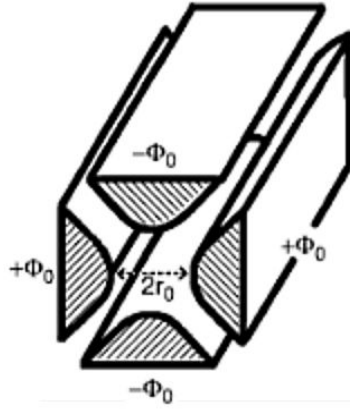


Figure 5. Schematic description of quadrupole mass analyzer with four electrodes connected into two pairs subjected to alternating potentials [4.5].

In detail, the trajectory of an ion will be stable as long as its x and y coordinates remain less than r_0 , so until it does not collide with the quadrupole rods. Two functions a and q define ions stability areas across a range of varying direct current value U and a radiofrequency value V_{RF} , as shown below,

$$U = a_u \frac{m \omega^2 r_0^2}{z \ 8e} \quad \text{equation (3)}$$

$$V = q_u \frac{m \omega^2 r_0^2}{z \ 4e} \quad \text{equation (4)}$$

where r_0 is a radius of an imaginary cylinder that fits in the center of the rods and ω is the angular frequency of the RF field. The last terms of both U and V_{RF} equations are held constant for a given quadrupole instrument [4.5, 4.8].

Graphical representation of q parameter, related to RF voltage versus a parameter, related to DC voltage is known as the Mathieu stability diagram, described in Figure 6. The regions below the obtained curves are the areas of stable ions trajectories. Ions of different m/z are successively scanned along the line by increasing the magnitude of the RF and DC voltages while keeping the U/V_{RF} ratio constant to maximize the achievable mass resolution [4.5, 4.8, 4.13, 4.21].

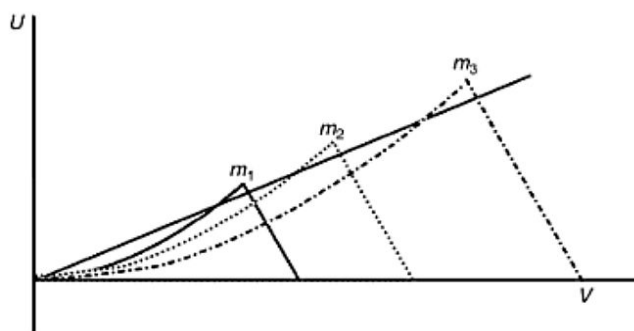


Figure 6. Mathieu stability diagram describing stability areas of ions with mass increasing in order $m_1 < m_2 < m_3$. Ions are successively scanned along the operating line [4.5].

Quadrupole mass spectrometers usually operate at unit resolution over the whole mass range, so are able to separate two ions being 1 mass unit apart. This categorizes quadrupoles as low-resolution instruments with mass accuracy reaching several hundreds of ppm. Depending on the quadrupole physical parameters, the upper m/z limit can reach maximum detectable m/z value of 4000 [4.5, 4.8, 4.13, 4.21].

Quadrupole is a real mass-to-charge ratio analyzer as it does not depend on the ions kinetic energy. The ions leaving the source are only accelerated by one to a few hundred eV to enable quadrupole scans to be obtained over the desired m/z range. The quadrupole scan speed is very high and can reach 1000 Da/s or more, so it is well suited for coupling with capillary GC, as around 10 mass spectra can be obtained throughout the capillary GC peak. Quadrupole analyzers are robust, easy to handle and low cost instruments [4.5, 4.8, 4.13, 4.21, 4.42].

4.4. References

- [4.1] Chowdhury A, Thynell ST. Confined rapid thermolysis/FTIR/ToF studies of imidazolium-based ionic liquids. *Thermochim Acta* 2006; 443:159-172.
- [4.2] Chowdhury A, Thynell ST. Confined rapid thermolysis/FTIR/ToF studies of triazolium-based energetic ionic liquids. *Thermochim Acta* 2007; 466:1-12.
- [4.3] Chowdhury A, Thynell ST, Lin P. Confined rapid thermolysis/FTIR/ToF studies of tetrazolium-based energetic ionic liquids. *Thermochim Acta* 2009; 485:1-13.
- [4.4] Chowdhury A, Thynell ST. Confined rapid thermolysis/FTIR/ToF studies of methyl-amino-triazolium-based energetic ionic liquids. *Thermochim Acta* 2010; 505:33-40.
- [4.5] De Hoffmann E, Stroobant V. *Mass spectrometry: principles and applications*. 3rd ed. Chichester, West Sussex, UK: Wiley; 2007.

- [4.6] Walker KL, Wilkins ChL. Laser mass spectrometry. In: Settle FA, editor. Handbook of instrumental techniques for analytical chemistry. Upper Saddle River, New Jersey, USA: Prentice Hall; 1997, 665-682.
- [4.7] Lee MS. Mass spectrometry handbook. 1st ed. Hoboken, New Jersey, USA: Wiley; 2012.
- [4.8] Downard K. Mass spectrometry: A foundation course. 1st ed. Cambridge, UK: Royal society of chemistry; 2004.
- [4.9] Zabet-Moghaddam M, Krueger R, Heinzle E, Tholey A. Matrix-assisted laser desorption/ionization mass spectrometry for the characterization of ionic liquids and the analysis of amino acids, peptides and proteins in ionic liquids. *J Mass Spectrom* 2004; 39:1494–505.
- [4.10] Dessiaterik Y, Baer T, Miller RE. Laser ablation of imidazolium based ionic liquids. *J Phys Chem A* 2006; 110:1500-1505.
- [4.11] Pisarova L, Gabler Ch, Doerr N, Pittenauer E, Allmaier G. Thermo-oxidative stability and corrosion properties of ammonium based ionic liquids. *Tribol Int* 2012; 46:73-83.
- [4.12] Pisarova L, Steudte S, Doerr N, Pittenauer E, Allmaier G, Stepnowski P, Stolte S. Ionic liquid long-term stability assessment and its contribution to toxicity and biodegradation study of untreated and altered ionic liquids. *J Eng Tribol* 2012; 226:903-922.
- [4.13] Manz A, Pamme N, Iossifidis D. Bioanalytical chemistry. 1st ed. Covent Garden, London, UK: Imperial College Press; 2004.
- [4.14] Tanaka K, Waki H, Ido Y, Akita S, Yoshida Y, Yoshida T. Protein and polymer analyses up to m/z 100 000 by laser ionization time-of flight mass spectrometry. *Rapid Commun Mass Spectrom* 1988; 2:151-153.
- [4.15] Zabet-Moghaddam M, Heinzle E, Lasasosa M, Tholey A. Pyridinium-based ionic liquid matrices can improve the identification of proteins by peptide mass-fingerprint analysis with matrix-assisted laser desorption/ionization mass spectrometry. *Anal Bioanal Chem* 2006; 384:215-224.
- [4.16] Tholey A, Heinzle E. Ionic (liquid) matrices for matrix-assisted laser desorption/ionization mass spectrometry: applications and perspectives. *Anal Bioanal Chem* 2006; 386:24-37.
- [4.17] Crank JA, Armstrong DW. Towards a second generation of ionic liquid matrices (ILMs) for MALDI-MS of peptides, proteins and carbohydrates. *J Am Soc Mass Spectrom* 2009; 20:1790-1800.

- [4.18] Berthod A, Crank J A, Rundlett KL, Armstrong DW. A second-generation ionic liquid matrix-assisted laser desorption/ionization matrix for effective mass spectrometric analysis of biodegradable polymers. *Rapid Commun Mass Spectrom* 2009; 23:3409-3422.
- [4.19] Gimenez E, Benavente F, Barbosa J, Sanz-Nebot V. Ionic liquid matrices for MALDI-TOF-MS analysis of intact glycoproteins. *Anal Bioanal Chem* 2010; 398:357-365.
- [4.20] Van Bramer SE. An introduction to mass spectrometry. Department of chemistry, Chester, Pennsylvania, USA; 1998.
- [4.21] Glish GL, Vachet RW. The basics of mass spectrometry in the twenty-first century. *Nature* 2003; 2:140-150.
- [4.22] Skoog DA, West DM, Holler FJ, Crouch SR. Fundamentals of analytical chemistry. 8th ed. Belmont, California, USA: Brooks/Cole; 2004.
- [4.23] McMaster MC. HPLC: A practical user's guide. 2nd ed. Hoboken, New Jersey, USA: Wiley; 2007.
- [4.24] Brown P, DeAntonis K. High-performance liquid chromatography. In: Settle FA, editor. Handbook of instrumental techniques for analytical chemistry. Upper Saddle River, New Jersey, USA: Prentice Hall; 1997, 665-682.
- [4.25] Rouzo G, Lamouroux Ch, Bresson C, Guichard A, Moisy P, Moutiers G. Hydrophilic interaction liquid chromatography for separation and quantification of selected room-temperature ionic liquids. *J Chromatogr A* 2007; 1164:139-144.
- [4.26] Czerwicka M, Stolte S, Mueller A, Siedlecka EM, Golebiowski M, Kumirska J, Stepnowski P. Identification of ionic liquid breakdown products in an advanced oxidation system. *J Hazard Mater* 2009; 15:478-483.
- [4.27] Keil P, Kick M, Koenig A. Long-term stability, regeneration and recycling of imidazolium-based ionic liquids. *Chemie Ingenieur Technik* 2012; 84:859-866.
- [4.28] Snijder J, Rose RJ, Veessler D, Johnson JE, Heck AJR. Untersuchung von 18 MDa großen Viruspartikeln mit nativer Massenspektrometrie. *Angew Chem* 2013; 125:4112-4115.
- [4.29] Cole RB. Electrospray and MALDI mass spectrometry: fundamentals, instrumentation, practicalities, and biological applications. 2nd ed. Hoboken, New Jersey, USA: Wiley; 2010.
- [4.30] Makarov A. Electrostatic axially harmonic orbital trapping: a high performance technique of mass analysis. *Anal Chem* 2000; 72:1156-1162.
- [4.31] Hu Q, Noll RJ, Li H, Makarov A, Hardman M, Cooks RG. The orbitrap: a new mass spectrometer. *J Mass Spectrom* 2005; 40:430-443.

- [4.32] Makarov A, Denisov E, Kholomeev A, Balschun W, Lange O, Strupat K, Horning S. Performance evaluation of a hybrid linear ion trap/orbitrap mass spectrometer. *Anal Chem* 2006; 78:2113-2120.
- [4.33] Van Sant MJ. Gas chromatography. In: Settle FA, editor. *Handbook of instrumental techniques for analytical chemistry*. Upper Saddle River, New Jersey, USA: Prentice Hall; 1997, 125-146.
- [4.34] McNair HM, Miller JM. *Basic gas chromatography*. 2nd ed. Hoboken, New Jersey, USA: Wiley; 2009.
- [4.35] Kolb B, Ettre LS. *Static headspace - gas chromatography: theory and practice*. 2nd ed. Hoboken, New Jersey, USA: Wiley; 2006.
- [4.36] Baranyai KJ, Deacon GB, MacFarlane DR, Pringle JM, Scott JL. Thermal degradation of ionic liquids at elevated temperatures. *Aust J Chem* 2004; 57:145-147.
- [4.37] Wooster TJ, Johanson KM, Fraser KJ, MacFarlane DR, Scott JL. Thermal degradation of cyano containing ionic liquids. *Green Chem* 2006; 8:691-696.
- [4.38] Ohtani H, Ishimura S, Kumai M. Thermal decomposition behaviors of imidazolium-type ionic liquids studied by pyrolysis-gas chromatography. *Anal Sci* 2008; 24:1335-1340.
- [4.39] Liebner F, Patel I, Ebner G, Becker E, Horix M, Potthast A, Rosenau T. Thermal aging of 1-alkyl-3-methylimidazolium ionic liquids and its effect on dissolved cellulose. *Holzforschung* 2010; 64:161-166.
- [4.40] Siedlecka ME, Golebiowski M, Kumirska J, Stepnowski P. Identification of 1-utyl-3-methylimidazolium chloride degradation products formed in Fe(III)/H₂O₂ oxidation system. *Chem Anal (Warsaw)* 2008; 53:943-951.
- [4.41] Pisarova L, Totolin V, Gabler Ch, Doerr N, Pittenauer E, Allmaier G, Ichiro M. Insight into degradation of ammonium-based ionic liquids and comparison of tribological performance between selected intact and altered ionic liquid. *Tribology International* 2013; <http://dx.doi.org/10.1016/j.triboint.2013.02.020> (In Press).
- [4.42] Hites RA. Gas chromatography mass spectrometry. In: Settle FA, editor. *Handbook of instrumental techniques for analytical chemistry*. Upper Saddle River, New Jersey, USA: Prentice Hall; 1997, 609-626.

5. Applied methods for IL (eco)toxicity and biodegradability assessment

In order to implement IL lubricants into large scale applications, it is important to assess their impact on human and environment as not only technical requirements but also Registration, Evaluation, Authorization and Restriction of Chemicals (REACH) legislation requirements have to be fulfilled. Thus, the environmental impact of ILs have to be investigated by means of their (eco)toxicological impact on different biological test systems of varying complexity and their biodegradability has to be assessed. As the test batteries commonly applied to assess ILs are generally performed in water environments, the water solubility of ILs to the required level is a necessity.

5.1. Acetylcholinesterase inhibition assay

Acetylcholinesterase inhibition assay represents the least complex test system working on molecular level utilizing acetylcholinesterase enzyme, an important biomarker for central nervous system of higher organisms to study IL inhibitory potential. IL exhibit structural similarity to acetylcholine substrate as they are mainly based on quaternary ammonium cations and hence can act as acetylcholinesterase inhibitors. High throughput screening test with isolated acetylcholinesterase enzyme is based on colorimetric assay using 5,5'-dithio-bis-(2-nitrobenzoic acid) (DTNB) dye reduction by enzymatically formed thiocholine moiety from the acetylcholine iodide substrate as described by Stock et al. [5.1].

Studies carried out by Stock et al. [5.1], Ranke et al. [5.2] and Arning et al. [5.3] led to conclusion that IL cationic moieties with longer side chain length are those responsible for acetylcholinesterase inhibition and that the aromatic head groups, such as imidazolium and pyridinium are strong inhibitors whereas as stated by Stolte et al. [5.4] and Pisarova et al. [5.5] ammonium based ILs with short alkyl chains and with implemented polar functional groups show no inhibition effects. Apart from fluorine containing anions, such as $[\text{PF}_6]^-$, IL anion moieties do not contribute to the enzyme inhibition as concluded by Matzke et al. [5.6].

5.2. Cell viability assay with IPC-81 cells

Cell viability assay is used to evaluate cytotoxicity of compounds by using mammalian cell culture and represents biological system with higher complexity. Cytotoxicity test using leukemia rat cell line IPC-81 is based on colorimetric assay measuring cells ability to reduce

2-(4-iodophenyl)-3-(4-nitrophenyl)-5-(2,4-disulphophenyl)-2-H-tetrazolium monosodium salt (WST-1) reagent as described by Ranke et al. [5.7].

Ranke et al. [5.7, 5.8] and Torrecilla et al. [5.9] investigated the influence of IL cation side chain lengths and concluded that the ILs with longer alkyl side chains exhibit higher cytotoxicity due to their increased hydrophobicity, which is in consistency with studies of other chemicals. Also anions can contribute to the IL cytotoxicity by means of their hydrophobicity or hydrolytic instability as stated by Stolte et al. [5.5, 5.10]. Implementation of polar functional groups into the IL alkyl side chains, such as hydroxyl or nitrile groups, decreases the cytotoxicity effect of ILs [5.5, 5.11-5.13].

5.3. Luminescence inhibition assay with the marine bacterium *Vibrio fischeri*

Luminescence inhibition assay uses marine bacteria *Vibrio fischeri*, a unicellular organism capable of emitting bioluminescence as part of its metabolism process, hence indicating cells viability. Changes in the bioluminescence intensity provide indication of chemicals cytotoxicity towards *Vibrio fischeri* bacteria and are detected photometrically as described in more detail within DIN EN ISO 11348 ecotoxicological standards [5.14]. Therefore, it is possible to study environmental effects of ILs towards aquatic organisms due to their potential breakthrough from wastewater treatment plants.

Couling et al. [5.15] concluded that toxicity of ILs towards *Vibrio fischeri* decreases in the following order; imidazolium > pyridinium > ammonium as it correlates with the number of N atoms in the cation. The clear contribution of IL cation alkyl chain length increase to IL cytotoxicity was confirmed by Ranke et al. [5.7] and Pernak et al. [5.16] as the hydrophobic chains disrupts the cells lipophilic membrane. Not only the length of the alkyl chain but also the number of alkyl chains attached to the cation leads to IL cytotoxicity increase as stipulated by Docherty et al. [5.17], and Stolte et al. [5.18] assigned the organism membranes being the primary target of IL toxic action. General contribution of anion moiety towards *Vibrio fischeri* cytotoxicity is low [5.7, 5.19].

5.4. Acute immobilization assay with *Daphnia magna*

Crustacean *Daphnia magna* serves as test organism for studies of toxicity effects towards invertebrates, hence represents an important link between microbial and higher trophic level. Aquatic toxicity of compounds can be determined following the Organization for Economic Co-operation and Development (OECD) guideline 202: *Daphnia sp.*, acute immobilization test and reproduction test [5.20]. Animals not older than 24 h are incubated with the substance

for either 24 or 48 h. At the end of the test, the EC₅₀ value of a substance is determined as a concentration needed to immobilize 50% of the *Daphnia magna*.

Couling et al. [5.15] stated that the IL toxicity towards *Daphnia magna* increases with the amount of aromatic nitrogen atoms in IL cation, the link between the toxicity and the alkyl chain length was observed also by Yu et al. [5.21], additionally suggesting oxidative stress as the significant mechanism of IL toxic effect. Imidazolium based ILs were found to be much more toxic than non-chlorinated conventional organic solvents, such as methanol and also more toxic than chlorinated solvents, such as chloroform, however less toxic than imidazolium based cationic surfactants [5.22, 5.23]. Oxygen introduction to the IL cation side chain results in a large decrease of IL toxicity, which is thus lower than that of chlorinated solvents, however still higher than that of non-chlorinated solvents [5.24-5.26]. In the studies of Stolte et al. [5.4], it was shown that depending on the type of oxygen based functional group in IL cation side chain, the IL aquatic toxicity ranges greatly. Thus, ILs with ether functional group were classified as harmful and even toxic to aquatic organisms whereas ILs containing hydroxyl functional group were not harmful to aquatic organisms.

5.5. Ready biodegradability according to OECD 301F manometric respirometry

Ready biodegradability of compound is determined in an aerobic aqueous medium following the Organization for Economic Co-operation and Development (OECD) guideline 301F: manometric respirometry [5.27]. The investigated compound is inoculated by activated microbial sludge and incubated under aerobic conditions in the dark for 28 days or until the biodegradation curve reaches a plateau. The biodegradability is determined by the oxygen consumption and can be measured manometrically. A substance is classified as readily biodegradable when biodegradation reaches a minimum of 60% within 28 days.

Pyridinium was evaluated as the most biodegradable IL cation moiety, fully mineralizing within 28 days and suitable for biodegradable IL structural design [5.12, 5.28-5.30], whereas imidazolium moiety was found to be only partially biodegradable [5.31]. The trend of biodegradation based on cation alkyl chain length is as follows; alkyl chains shorter than C₄ are not biodegradable, rate of biodegradation increases with alkyl chain elongation up to C₁₂, while longer side chains show inhibitory effects towards the inoculum [5.22, 5.31, 5.32]. Polar functional groups incorporated into the short IL side chains do not always improve IL biodegradation in the same way [5.31], it was shown that hydroxyl group leads to ready biodegradability of ammonium ILs while ether functional group hinder the ammonium IL biodegradation [5.4, 5.5]. In contrary, ester groups were reported to increase imidazolium

based ILs biodegradation, as they represent sites susceptible to enzymatic attacks [5.33, 5.34]. Fluorinated anions like [NTF2] could not be readily biodegraded [5.22, 5.35], while octylsulfate anion is recommended in further IL structural design as readily biodegradable anion moiety [5.34].

5.6. References

- [5.1] Stock F, Hoffmann J, Ranke J, Stoermann R, Ondruschka B, Jastorff B. Effects of ionic liquids on the acetylcholinesterase – a structure-activity relationship consideration. *Green Chem* 2004; 6:286-290.
- [5.2] Ranke J, Stolte S, Stoermann R, Arning J, Jastorff B. Design of sustainable chemical products – the example of ionic liquids. *Chem Rev* 2007; 107:2183-2206.
- [5.3] Arning J, Stolte S, Boesch A, Stock F, Pitner WR, Welz-Biermann U, Jastorff B, Ranke J. Qualitative and quantitative structure activity relationships for the inhibitory effects of cationic head groups, functionalized side chains and anions of ionic liquids on acetylcholinesterase. *Green Chem* 2008; 10:47-58.
- [5.4] Stolte S, Steudte S, Areitioaurtena O, Pagano F, Thoeming J, Stepnowski P, Igartua A. Ionic liquids as lubricants or lubrication additives: an ecotoxicity and biodegradability assessment. *Chemosphere* 2012; 89:1135-1141.
- [5.5] Pisarova L, Steudte S, Doerr N, Pittenauer E, Allmaier G, Stepnowski P, Stolte S. Ionic liquid long-term stability assessment and its contribution to toxicity and biodegradation study of untreated and altered ionic liquids. *J Eng Tribol* 2012; 226:903-922.
- [5.6] Matzke M, Stolte S, Thiele K, Juffernholz T, Arning J, Ranke J, Welz-Biermann U, Jastorff B. The influence of anion species on the toxicity of 1-alkyl-3-methylimidazolium ionic liquids observed in an (eco)toxicological test battery. *Green Chem* 2007; 9:1198-1207.
- [5.7] Ranke J, Molter K, Stock F, Bottin-Weber U, Poczobutt J, Hoffmann J, Ondruschka B, Filser J, Jastorff B. Biological effects of imidazolium ionic liquids with varying chain lengths in acute *Vibrio fischeri* and WST-1 cell viability assays. *Ecotoxicol Environ Saf* 2004; 58:396-404.
- [5.8] Ranke J, Mueller A, Bottin-Weber U, Stock F, Stolte S, Arning J, Stoermann R, Jastorff B. Lipophilicity parameters for ionic liquid cations and their correlation to in vitro cytotoxicity. *Ecotox Environ Saf* 2007; 67:430-438.
- [5.9] Torrecilla JS, Garcia J, Rojo E, Rodriguez R. Estimation of toxicity of ionic liquids in leukemia rat cell line and acetylcholinesterase enzyme by principal component analysis, neural networks and multiple linear regressions. *J Hazard Mater* 2009; 164:182-194.

- [5.10] Stolte S, Arning J, Bottin-Weber U, Stock F, Thiele K, Uerdingen M, Welz-Biermann U, Jastorff B, Ranke J. Anion effects on the cytotoxicity of ionic liquids. *Green Chem* 2006; 8:621-629.
- [5.11] Kumar RA, Papaiconomou N, Lee JM, Salminen J, Clark DS, Prausnitz JM. In vitro cytotoxicities of ionic liquids: effect of cation rings, functional groups, and anions. *Environ Toxicol* 2009; 24:388-395.
- [5.12] Stasiewicz M, Mulkiewicz E, Tomczak-Wandzel R, Kurmirska J, Siedlecka EM, Gołebiowski M, Gajdus J, Czerwicka M, Stepnowski P. Assessing toxicity and biodegradation of novel, environmentally benign ionic liquids (1-alkoxymethyl-3-hydroxypyridinium chloride, saccharine and acesulfamates) on cellular and molecular level. *Ecotox Environ Saf* 2008; 71:157-165.
- [5.13] Stolte S, Arning J, Bottin-Weber U, Mueller A, Pitner WR, Welz-Biermann U, Jastorff B, Ranke J. Effects of different head groups and functionalized side chains on the cytotoxicity of ionic liquids. *Green Chem* 2007; 9:760-767.
- [5.14] ISO 11348-3, 2007, "Determination of the inhibitory effect of water samples on the light emission of *Vibrio fischeri* (Luminescent bacteria test) - part 3: method using freeze-dried bacteria", ISO International Organization for Standardization, Geneva, Switzerland, 2007, www.iso.org.
- [5.15] Couling DJ, Bernot RJ, Docherty KM, Dixon JK, Maginn EJ. Assessing the factors responsible for ionic liquid toxicity to aquatic organisms via quantitative structure-property relationship modeling. *Green Chem* 2006; 8:82-90.
- [5.16] Pernak J, Sobaszekiewicz K, Mirska I. Anti-microbial activities of ionic liquids. *Green Chem* 2003; 5:52-56.
- [5.17] Docherty KM, Kulpa CF. Toxicity and antimicrobial activity of imidazolium and pyridinium ionic liquids. *Green Chem* 2005; 7:185-189.
- [5.18] Stolte S, Matzke M, Arning J, Boeschen A, Pitner WR, Welz-Biermann U, Jastorff B, Ranke J. Effects of different head groups and functionalized side chains on the aquatic toxicity of ionic liquids. *Green Chem* 2007; 9:1170-1179.
- [5.19] Romero A, Santos A, Tojo J, Rodriguez A. Toxicity and biodegradability of imidazolium ionic liquids. *J Hazard Mater* 2008; 151:268-273.
- [5.20] OECD 202, 1984, "Daphnia sp., acute immobilisation test and reproduction test", OECD The Organisation for Economic Co-operation and Development, Paris, France, 1984, www.oecd.org.

- [5.21] Yu M, Wang SH, Luo YR, Han YW, Li XY, Zhang BJ, Wang JJ. Effects of the 1-alkyl-3-methylimidazolium bromide ionic liquids on the antioxidant defense system of *Daphnia magna*. *Ecotox Environ Saf* 2009; 72:1798-1804.
- [5.22] Wells AS, Coombe VT. On the freshwater ecotoxicity and biodegradation properties of some common ionic liquids. *Org Pro Res Dev* 2006; 10:794-798.
- [5.23] Garcia MT, Gathergood N, Scammells PJ. Biodegradable ionic liquids. Part II: effect of the anion and toxicology. *Green Chem* 2005; 7:9-14.
- [5.24] Samori C, Pasteris A, Galletti P, Tagliavini E. Acute toxicity of oxygenated and nonoxygenated imidazolium based ionic liquids to *Daphnia magna* and *Vibrio fischeri*. *Environ Toxicol Chem* 2007; 26:2379-2382.
- [5.25] Samori C, Malferrari D, Valbonesi P, Montecavalli A, Moretti F, Galletti P, Sartor G, Tagliavini E, Fabbri E, Pasteris A. Introduction of oxygenated side chain into imidazolium ionic liquids: Evaluation of the effects at different biological organization levels. *Ecotox Environ Safe* 2010; 73:1456-1464.
- [5.26] Pretti C, Chiappe C, Baldetti I, Brunini S, Monni G, Intorre L. Acute toxicity of ionic liquids for three freshwater organisms: *Pseudokirchneriella subcapitata*, *Daphnia magna* and *Danio rerio*. *Ecotoxicol Environ Saf* 2009; 72:1170-1176.
- [5.27] OECD 301F, 1992, "Ready biodegradability - manometric respirometry test", OECD The Organisation for Economic Co-operation and Development, Paris, France, 1992, www.oecd.org
- [5.28] Harjani JR, Singer RD, Garcia MT, Scammells PJ. The design and synthesis of biodegradable pyridinium ionic liquids. *Green Chem* 2008; 10:436-438.
- [5.29] Docherty KM, Joyce MV, Kulacki KJ, Kulpa CF. Microbial biodegradation and metabolite toxicity of three pyridinium-based cation ionic liquids. *Green Chem* 2010; 12:701-712.
- [5.30] Pham TPT, Cho CW, Jeon CO, Chung YJ, Lee MW, Yun YS. Identification of metabolites involved in the biodegradation of the ionic liquid 1-butyl-3-methylpyridinium bromide by activated sludge microorganisms. *Environ Sci Technol* 2009; 43:516-521.
- [5.31] Stolte S, Abdulkarim S, Arning J, Blomeyer-Nienstedt AK, Bottin-Weber U, Matzke M, Ranke J, Jastorff B, Thoeming J. Primary biodegradation of ionic liquid cations, identification of degradation products of 1-methyl-3-octylimidazolium chloride and electrochemical wastewater treatment of poorly biodegradable compounds. *Green Chem* 2008; 10:214-224.

- [5.32] Docherty KM, Dixon JK, Kulpa CF. Biodegradability of imidazolium and pyridinium ionic liquids by an activated sludge microbial community. *Biodegradation* 2007; 18:481-493.
- [5.33] Gathergood N, Garcia MT, Scammells PJ. Biodegradable ionic liquids: part I. Concept, preliminary targets and evaluation. *Green Chem* 2004; 6:166-175.
- [5.34] Gathergood N, Scammells PJ, Garcia MT. Biodegradable ionic liquids. Part III: the first readily biodegradable ionic liquids. *Green Chem* 2006; 8:156-160.
- [5.35] Neumann J, Cho CW, Steudte S, Koeser J, Uerdingen M, Thoeming J, Stolte S. Biodegradability of fluoroorganic and cyano-based ionic liquid anions under aerobic and anaerobic conditions. *Green Chem* 2012; 14:410-418.

6. Publications within the thesis topic

6.1. Thermo-oxidative stability and corrosion properties of ammonium based ionic liquids

Tribology International 2012; 46:73–83



Thermo-oxidative stability and corrosion properties of ammonium based ionic liquids

Lucia Pizarova^{a,b,*}, Christoph Gabler^a, Nicole Dörr^a, Ernst Pittenauer^b, Günter Allmaier^b

^a Austrian Centre of Competence for Tribology—AC²T research GmbH, Wiener Neustadt, Austria

^b Institute of Chemical Technologies and Analytics, Vienna University of Technology, Vienna, Austria

ARTICLE INFO

Article history:

Received 24 July 2010

Received in revised form

19 January 2011

Accepted 18 March 2011

Available online 9 April 2011

Keywords:

Ionic liquids

Corrosion

Thermo-oxidative degradation

MS

ABSTRACT

Ionic liquids (ILs) as a novel and potential type of lubricants possess partly superior properties over traditional classes of lubricants. Their extremely low vapor pressure, generally high thermal stability and non-flammability suggest them for high performance applications. However, their tendency towards corrosiveness is neglected in general. The selection of three ILs was based on the aim to achieve relevant lubricant properties, in particular high oxidation stability and low corrosiveness, as well as high environmental benignity. The cations were in all cases ammonium based with and without functionalization. Bis(trifluoromethylsulfonyl)imide (NTF₂) was chosen as anion and has been replaced for one IL by methanesulfonate. Artificial aging was carried out to obtain knowledge about the lubricant long-term performance under both oxidative and humid conditions while being in contact with CuSn8P and 100Cr6 commonly used in tribology. For the evaluation of IL corrosion potential, the metal content in the IL was monitored by ICP-OES, metal specimens were examined optically and by SEM-EDX analysis. To find out the IL suitability for the long-term applications the thermo-oxidative stability of the IL has been analyzed by several mass spectrometric techniques. In this study, NTF₂ based IL – regardless of the cationic moiety – showed superior performance over methanesulfonate based IL under all conditions. In the case of 100Cr6, dry conditions lead to the lowest corrosion whereas CuSn8P caused the lowest corrosion under humid conditions. The degradation process based on thermally induced transmethylation of the IL investigated occurred only at the cationic moiety of methanesulfonate based IL. This is based on mass spectrometric investigations and indicates a contribution to the enhanced corrosiveness by means of the IL reduced stability.

© 2011 Elsevier Ltd. All rights reserved.

1. Introduction

Common ionic liquid (IL) structures for tribological applications are based on bulky asymmetrical cations and anions which have organic or semi-organic nature. IL cations are frequently based on aromatic ring systems containing hetero-atoms with typical representatives such as imidazolium as stated in a recent review by Zhou et al. dealing with the structural designs of IL lubricants. They also brought up the issues of IL as lubricating oil and identified corrosion and thermo-oxidation as two bottlenecks to be solved before really large-scale applications can be realized [1].

Together with the tribological properties also emphasis on the environmental aspects has to be taken into account. The anion moiety in most cases does not contribute significantly to the IL toxicity properties with the exception of frequently used anions in tribological applications based on fluorinated structures, such

as bis(trifluoromethylsulfonyl)imide (NTF₂) and tris(pentafluoroethyl)trifluorophosphate (FAP). For IL cations, shortening of the chain length and introducing polar functional groups were recommended to significantly reduce possible (eco)toxicological risks [2,3]. Choline based quaternary ammoniums were identified as cations for the design of highly promising biodegradable IL [4].

Due to some exceptional IL properties they represent equivalent or even superior class of compounds in comparison to the classical lubricant formulations and their performance. The outstanding properties comprise negligible vapor pressure, non-flammability, very low melting points down to –80 °C and good oxidative stability which predestine them for the high temperature and high vacuum applications. Due to the vast variety of structural possibilities and combinations of cation and anion the aforementioned does not apply as general rule for all IL structures. Hence tremendous research efforts are still necessary to understand the structural prerequisites for applications in general and tribological applications in particular. The reviews by Minami [5] and Bermúdez et al. [6] deal extensively with the potential and applicability of IL as novel lubricants focusing on their structure–performance relationships.

* Corresponding author at: AC²T research GmbH, Viktor Kaplan-Straße 2, 2700 Wiener Neustadt, Austria. Tel.: +43 2622 81600 152.
E-mail address: pizarova@ac2t.at (L. Pizarova).

Besides the favorable lubricant properties of IL their inclination towards corrosiveness is also known. The progress of corrosion heavily depends on the chemical structures of IL, impurities present in IL, type of material in contact and application conditions such as temperature, access to air and different amounts of water to mention the most important environmental influencing factors. The most applied techniques to study the corrosion phenomena of IL are weight loss and electrochemical methods for quantification together with scanning electron microscopy with energy-dispersive-X-ray spectrometer (SEM-EDX) and X-ray photoelectron spectroscopy (XPS) to understand the corrosion processes on a qualitative level [7,8]. Bardi et al. [9] and Perissi et al. [10] investigated the corrosion resistance of ASI1018, ASI304, Inconel 600 based on Ni, and Naval Brass being in contact with IL constituted from fluorinated anion moieties with various cation counter ions. Results from surface analysis by XPS, SEM-EDX and secondary ion mass spectrometry (SIMS) suggested that the decomposition products of the IL form an interaction layer on the metal surfaces. This conclusion was unambiguously confirmed by the presence of significant amounts of elements originating from the IL studied.

Oxidative stability of IL based lubricant is among the most desired prerequisites for applicability in tribosystems. In contrast to well explored long-term behavior of traditional lubricant classes there is still a vast lack of knowledge in the case of the long-term IL performance. Recently, a review has been published dealing with IL as novel solvents and summarizing the knowledge about their chemical stabilities with emphasis on imidazolium cation [11]. Widely used attempts to study the IL stability were carried out by means of thermo-gravimetric analysis associated with weight loss. However, the obtained data vary significantly and do not provide information about chemical nature of the degradation products originating from IL decomposition [12]. In order to find out the molecular structure and composition of the IL degradation products and to elucidate the possible degradation pathways on the molecular level sophisticated high end analytical techniques such as mass spectrometry (MS) have to be applied. The application of MS to investigate IL is still a rare approach. However, some researchers have already characterized the IL in the fresh condition mostly by electrospray ionization mass spectrometry (ESI-MS) [13,14]. To our best knowledge, there is only one publication dealing with the applicability of laser desorption/ionization (LDI) and matrix-assisted laser desorption/ionization (MALDI) mass spectrometry applied to IL while treating them as analytes and not as matrix components. Zabet-Moghaddam et al. [15] stated that these methods are suitable for straightforward characterization of IL in both positive and negative ion mode.

In this publication, the performance of three IL with variation of cation and anion moieties resulting in different hydrophobicity or hydrophilicity, respectively, has been compared. Structural variation was aimed to lower the (eco)-toxicological impact but to maintain the lubricant stability and low corrosion potential. The specially designed small-scale artificial aging method was developed and applied to accelerate the IL degradation progress and to evaluate the corrosion potential of two types of alloys used in tribological applications under influence of air and water.

The corrosion progress was monitored by inductively coupled plasma with optical emission spectrometry (ICP-OES) to track the presence of metal within the IL. The metal specimens were examined by optical means and by a scanning electron microscope equipped with an energy-dispersive-X-ray spectrometer (SEM-EDX).

In this research work, the IL was also characterized by high end mass spectrometry techniques using laser desorption/ionization time-of-flight mass spectrometry (LDI-TOF-MS), matrix-assisted laser desorption/ionization time-of-flight mass

spectrometry (MALDI-TOF-MS) and electrospray ionization ion trap mass spectrometry (ESI-IT-MS). The optimization and comparison of these desorption/ionization techniques for IL were carried out and the most suitable and straightforward mass spectrometry technique was applied to identify subsequently degradation products and to develop the aging mechanism.

Furthermore, the expected findings gained from the structural determination of the degradation products could give insight into the corrosion mechanism of IL, in particular whether degradation products may contribute to IL corrosiveness. Additionally, more reliable information about the long-term performance of IL is anticipated when carrying out corrosion experiments under more severe conditions and for a longer period in comparison with standardized corrosion tests with durations of some hours [16]. Based on the structural prerequisites of the studied IL it could be expected that the most hydrophobic IL would possess a significantly lower corrosiveness compared to less hydrophobic IL.

2. Experimental

2.1. Ionic liquids selected

Besides technical requirements, the impact on the environment of a lubricant has to be taken into account. Thus, the structural design of the selected IL was carried out to confer sustainability due to legislative regulations such as REACH [17] in Europe.

Three ionic liquid structures (IL1–3) were provided through custom synthesis on request carried out by IoLiTec (Ionic Liquids Technologies, Heilbronn, Germany). The cation moieties are based on quaternary ammonium with and without functionalization on one side chain. The implementation of the hydroxyl group has the aim to lower the IL hydrophobicity and hence to lower the expected ecotoxic impact. The use of bis(trifluoromethylsulfonyl)imide as anion represents a conventional choice often used in tribological applications. But due to the generally known environmental hazardous properties of NTF₂ [3] the attempt has been made to replace the anion by a structure of lower toxicity. Methanesulfonate was selected, but at the same time the thermo-oxidative stability of the IL should be preserved. The selected IL structures are presented in Table 1 and their purity is stated (given by the supplier).

2.2. Artificial aging and corrosion evaluation

Artificial aging in lubrication science usually utilizes the application of harsh but short-term conditions to the lubricant sample in order to accelerate the degradation process. This way, a correlation with natural aging – meaning all kinds of deterioration happening to the lubricant in application – for an estimation of the long-term performance of a lubricant is tried. Besides other prerequisites, the knowledge about the lubricant long-term performance together with possible corrosion potential has to be obtained for the successful implementation of a lubricant in the practical application.

Iron based alloy 100Cr6 and copper based alloy CuSn8P were selected as common materials used in tribological applications in order to monitor the corrosion potential of the selected IL. Table 2 provides the content of minor elemental components of the above mentioned alloys.

Specimens of both materials were cut with the dimensions 5 mm × 5 mm × 5 mm, and polished on all sides. The specimens were cleaned with toluene, petroleum ether and carefully dried immediately prior to use. The vessels for carrying out the artificial aging experiments represent conventional glass laboratory test tubes that were thoroughly cleaned prior to washing by methanol,

Table 1
Summary of investigated ionic liquids and their purity provided by the supplier IoLiTec.

IL	Name	Structure	Purity
IL1	Butyl-trimethyl-ammonium bis(trifluoromethylsulfonyl)imide		99% Halides <100ppm
IL2	Choline bis(trifluoromethylsulfonyl)imide		99% Halides 80ppm
IL3	Choline methanesulfonate		98% Halides <100ppm

Table 2
Summary of CuSn8P and 100Cr6 alloy minor elemental components in percentage. Content of major components Cu and Fe, respectively, varies according to the overall content of minor elements stated by term “is balance” in both cases.

CuSn8P	Element	Cu	Sn	P	Zn	Ni	Fe	Pb	Other
	From	Is balance	7.5	0.1	–	–	–	–	–
	To (%)		9	0.4	0.3	0.3	0.1	0.05	0.3
100Cr6	Element	Fe	Cr	C	Mn	Si	Mo	P	S
	From	Is balance	1.35	0.93	0.25	0.15	–	–	–
	To (%)		1.60	1.05	0.45	0.35	0.10	0.025	0.015

toluene and petroleum ether and subsequently dried. Each metal specimen was subsequently immersed in each IL. An additional artificial aging without the presence of a metal was also carried out. The ratio of IL in grams to the metal specimen area in cm² was chosen 1:1 (weight/area) to ensure the direct performance comparison. The influence of air in the “open” experiment carried out in open test tubes and the influence of defined 1.5% of water content in IL carried out in “closed” test tubes (melting of the tubes to close the reaction chamber) during closed (“defined humidity”) experiment, respectively, were selected to simulate the effect of typical application conditions in lubrication field. In the case of artificial aging without a metal, only the “open” experiment was chosen.

Artificial aging without a metal specimen was carried out in three subsequent artificial aging steps of which each lasted 7 days with subsequent temperature steps at 150 °C (starting temperature), 175 °C (temperature increase after 7 days) and 190 °C (temperature increase after 14 days after start) always followed by IL sampling. While using metal specimens, two subsequent 7 day artificial aging steps at 150 and 175 °C were applied to the IL. The third artificial aging step at 190 °C has been omitted due to progressed corrosion already monitored after the second artificial aging step at 175 °C by ICP-OES measurements.

A common laboratory oven was used for temperature stepping and samples were cooled in a desiccator prior to aliquot sample removal, taking place after each 7 day artificial aging step. In the case of a decrease of the water content below 1.5% (determined by Karl-Fischer method), a calculated amount of water was added to restore the initial water content. The variations of the artificial aging procedures are summarized in Table 3.

Representative aliquots of artificially aged IL samples were analyzed by ICP-OES to monitor the metal content in the IL during the corrosion progress. Karl-Fischer measurements were done to monitor the water level during artificial aging. After the final artificial aging

Table 3
Overview of all applied variations of artificial aging experiments.

General condition	Artificial aging parameters	Temperature (°C)		
		150	175	190
“Open”	Air	✓	✓	✓
	CuSn8P	✓	✓	–
“Closed” (melted tube)	100Cr6	✓	✓	–
	CuSn8P	✓	✓	–
	100Cr6	✓	✓	–

step the metal specimens were cleaned with 2-propanol, toluene and petroleum ether, dried and examined/documentated by optical means using Canon EOS 450 D camera (Tokyo, Japan) with AFMacro lens magnification system (Voigtländer, Fürth, Germany). Subsequently, the scanning electron microscope Philips XL30 ESEM-FEG equipped with an energy-dispersive-X-ray spectrometer (SEM-EDX) was applied in order to determine the topography and the elemental composition of the metal surfaces affected. First the area scan has been carried out to analyze the overall composition of the surface and subsequently often if of interest the spot scan has been applied to analyze particular crystals of interest. The attempt to monitor IL structural changes throughout the aging has been carried out by Fourier transform infrared (FT-IR) spectrometrical measurements using a Bruker Tensor 27 FT-IR spectrometer (Ettlingen, Germany).

2.3. Mass spectrometric measurements

In order to understand and evaluate the corrosion process the information about lubricant degradation mechanisms on the molecular level is a valuable asset. Mass spectrometric measurements were utilized as highly sensitive technique in order to identify the possible IL degradation products. Aged IL samples were centrifuged for 2 min at 12000 rpm with an Eppendorf centrifuge model 5415D (Eppendorf, Hamburg, Germany) to avoid the transfer of dispersed metal parts originating from the corrosion process into the mass spectrometer. IL aliquots of fresh and aged samples of 3–5 µl were dissolved in 1 ml of methanol to prepare the stock solutions in concentration range of 0.3–0.5% (v/v). Two mass spectrometric approaches and instrument types have been chosen for IL structural characterization: a Shimadzu Biotech TOF² MALDI/LDI tandem time-of-flight (TOF) instrument (Shimadzu Biotech Kratos Analytical, Manchester, UK) with a curved-field reflectron as MS2 allowing high energy (20 keV) collision induced dissociation (CID), post source decay (PSD) and

a Bruker Esquire 3000^{plus}-ESI-IT-MS device (Bruker Daltonics, Bremen, Germany) allowing multistage low energy CID.

The MALDI/LDI mass spectrometer was equipped with a nitrogen laser operating at a wavelength of $\lambda=337$ nm and a repetition rate of 20 Hz. A stainless steel MALDI-MS target was used and the following MALDI matrices were chosen to examine IL samples: 2,4,6-trihydroxyacetophenone (THAP) and α -cyano-4-hydroxy cinnamic acid (CHCA) which were both purchased from Sigma-Aldrich (St. Louis, MO, USA).

5 mg of THAP were dissolved in 1 ml of methanol. Subsequently, 20 μ l of the prepared solution was mixed with the same volume of the IL methanolic stock solution. Finally, 0.8 μ l of this mixture was applied onto the MALDI target and allowed to dry at room temperature (RT).

In the case of CHCA, 5 mg MALDI-MS matrix was dissolved in a acetonitril/methanol mixture 1:1 (v/v) containing 0.1% of trifluoroacetic acid TFA (Pierce, Rockford, IL, USA). Subsequently, by using thin layer technique, 1 μ l of prepared matrix was applied onto the MALDI-MS target and allowed to dry at RT, afterwards 1 μ l of IL methanolic stock solution was applied on the prepared matrix layer (spot with crystallized MALDI-MS matrix) and dried.

The approach of UV laser desorption ionization (LDI) technique was chosen as an alternative to MALDI. In the case of LDI, the methanolic solution of the corresponding IL was applied directly to the multiple-use stainless steel target without any MALDI-MS matrix and the solvent was evaporating at RT. The analysis of aged samples was done by means of the LDI-TOF-MS approach and every sample was examined in the both positive and negative ion mode with an m/z range from 1 to 1000. Mass spectra were acquired at least from 300 individual laser shots using the raster scanning. For structural determination the PSD experiments were carried out selecting a precursor ion with a window of ± 2 Da from the monoisotopic precursor ion and the PSD spectrum is based on 500 single laser shots. In the case of CID experiments helium was used as collision gas at collision energy of 20 keV and each CID spectrum is based on 1000 single laser shots.

ESI-IT-MS experiments were carried out in the direct infusion mode by applying a 2 μ l/min flow of the methanolic IL solution with a concentration of 0.003% (v/v). The experimental conditions of the ion source were: dry gas temperature, 250 °C; capillary voltage, 4.4 kV; all other voltages were optimized for maximum analyte ion transmission. The m/z range selected was from m/z 30 to 750, with a maximum accumulation time of 400 ms. All mass spectra were acquired in profile mode and one analytical scan represented the average of three microscans. Representative mass spectra were collected for at least 1 min in both positive and negative ion mode. An overview summarizing the elemental composition of IL

representative moieties (cation and anion) and their monoisotopic masses is provided in Table 4.

3. Results and discussion

Chemical deterioration of the artificially aged IL has been tried to be monitored by FT-IR. Applying FT-IR spectra of aged lubricants are compared with that of the unused lubricant. Due to the fact that no valuable data were gained from IL aging by this conventional oil analytical method, no results are shown.

The IL degradation has been evaluated by the above mentioned MS techniques in detail obtaining useful data.

3.1. Identification of ionic liquid degradation products by mass spectrometry

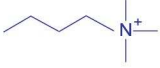
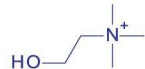
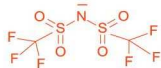
In lubrication science, mass spectrometrical measurements can considerably contribute to the evaluation of aging behavior of lubricants: it allows the identification of degradation products to better understand the behavior of lubricants on the molecular level, e.g. the thermo-oxidative stability and the corrosion behavior of IL as discussed in this paper.

3.1.1. Comparison of mass spectrometric desorption/ionization techniques for IL

The most crucial and well-known part by using LDI- and MALDI-TOF-MS is the sample preparation step. Preparation of the sample spots on the MALDI target was carried out as described in Section 2. The homogeneous crystallization is a prerequisite for obtaining representative mass spectra. Unsatisfactory crystallization by thin layer technique was yielded when the prepared CHCA matrix was subsequently treated with IL methanolic stock solution. The reason for this behavior might be related to the destruction of the crystal layer by IL.

The IL desorption/ionization properties using the THAP and CHCA matrices in case of MALDI- and LDI-TOF-MS technique were compared by the evaluation of the resulting mass spectra acquired from fresh IL. Comparing the mass spectra obtained with LDI (plain deposition of the methanolic IL solution and evaporation of solvent) and MALDI-MS technique a few general conclusions could be made for small molecular weight analytes as the selected IL:LDI with a UV laser provides mass spectra with a low 'chemical' background and without additional ions originating from the applied MALDI matrix. LDI also gives rise to fragment ions at higher signal intensities in both positive and negative ion mode due to higher laser energy input (thermo-induced fragmentation) in comparison to MALDI

Table 4
Summary of IL representative moieties with their elemental compositions and calculated monoisotopic masses.

IL representative moieties	Elemental composition	Monoisotopic mass (Da)
	C ₇ H ₁₈ N	116.14392
	C ₅ H ₁₄ NO	104.10754
	C ₂ F ₆ NO ₄ S ₂	279.91730
	CH ₃ O ₃ S	94.98029

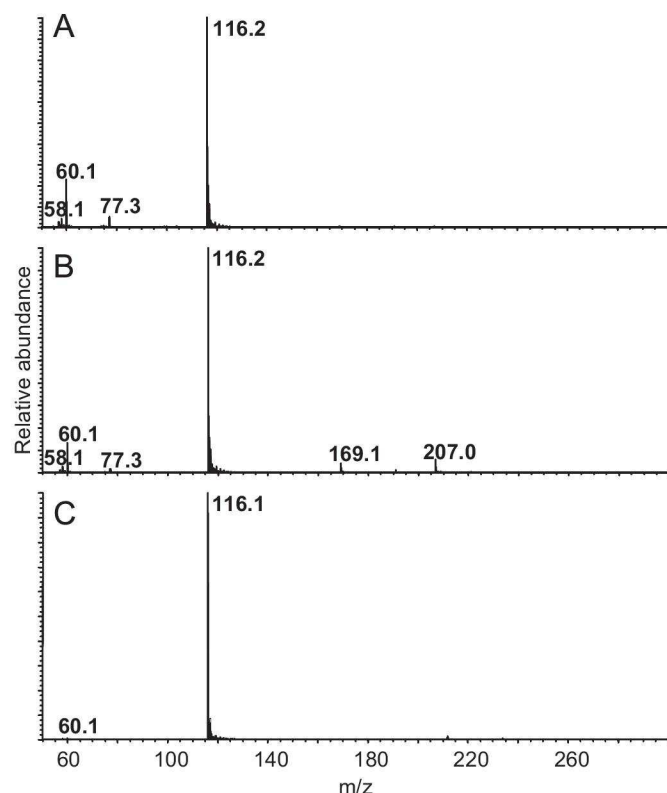


Fig. 1. Mass spectra of fresh butyl-trimethyl-ammonium bis(trifluoromethylsulfonyl)imide (IL1) obtained in positive ion mode by different methods of desorption/ionization: LDI (A), MALDI using THAP as matrix applying the volume technique (B) and MALDI using CHCA as matrix applying the thin layer technique (C).

when using the two matrices (a so-called ‘cold’ MALDI-MS matrix – THAP, and a ‘hot’ matrix – CHCA). More laser energy does not improve the situation in MALDI, but it results in more pronounced increase of MALDI matrix related ion intensities without improving the abundance of ionic liquid fragment ions in both positive and negative ion mode.

Fig. 1 shows the mass spectra of IL1 obtained by LDI- and MALDI-MS using THAP and CHCA as matrix. In all cases the base peak is related to the cation species of IL1 at m/z 116. The intensity of fragment ions at m/z 60 and 58 originating from butyl-trimethyl-ammonium moiety of IL1 is diminished by using the MALDI-MS technique. In the case of the application of THAP for MALDI-MS in Fig. 1(B) a protonated matrix ion is present at m/z 169. The ion at m/z 207 corresponds to a potassiated THAP matrix ion. The ion at m/z 77 does not originate from butyl-trimethyl-ammonium as is corroborated by MS/MS analysis shown in Fig. 2(A) in the following Section 3.1.2. In the negative ion mode, problematic desorption/ionization of the methanesulfonate anion (IL3) resulted in very low signal intensities under LDI condition and did not improve by using higher laser power or switching to MALDI-MS. Based on the above observations, LDI-TOF-MS was preferably applied to the artificially aged IL samples for further structural elucidation.

3.1.2. Structural determination of the observed IL clusters and fragment ions

To confirm the origin of the fragment ions from a particular precursor ion representing the IL cation, post source decay (PSD) and collision-induced dissociation (CID) were chosen using LDI-MS. The term post-source decay (PSD) refers to the fragmentation of precursor ions (e.g. protonated molecular ions or preformed molecular ions) resulting in product ions during their flight in the

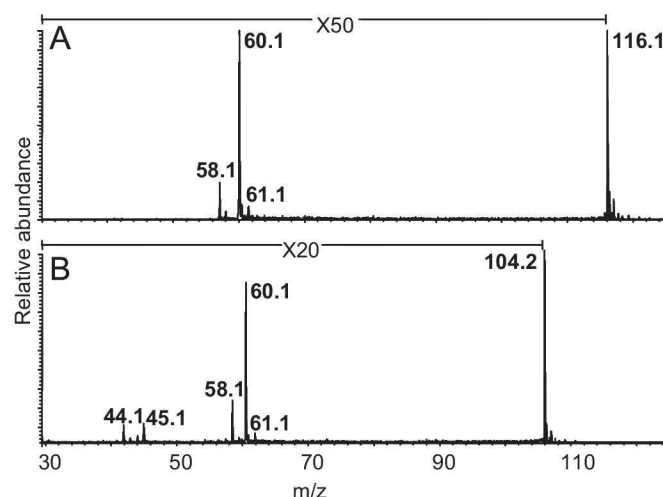


Fig. 2. PSD spectrum in the positive ion mode of butyl-trimethyl-ammonium in fresh IL1 (precursor ion m/z 116) (A), and CID spectrum of choline in fresh IL3 (precursor ion m/z 104) (B). LDI was used to generate the precursor ions in both cases. Spectra confirm the origin of the fragment ions from the precursor ions representing IL cations. Magnifications of $50\times$ and $20\times$ relating to the absolute abundance of m/z 116 and m/z 104, respectively, illustrated by ‘zoom in’ to show all fragment ions present.

mass spectrometric analyzer (TOF). CID is a mechanism by which selected precursor ions (e.g. molecular ions) are allowed to collide with neutral gas molecules which results in fragmentation of the precursor ion into smaller fragments. CID and PSD and the fragment ions produced are used for structural confirmation. Fig. 2 shows the PSD spectrum of the cation of IL1 (Fig. 2(A)) and the CID spectrum of the cation of IL3 (Fig. 2(B)). The PSD spectrum of the precursor ion at m/z 116, representing butyl-trimethyl-ammonium cation of IL1, confirmed the formation of fragment ions at m/z 61, 60 and 58, which could be observed in the full scan mass spectrum, too. In the case of CID of IL3, choline as precursor ion at m/z 104, fragment ions were observed at m/z 61, 60, 58, 45 and 44. The fragment ions originating from choline precursor ion are characterized in Section 3.1.3, showing the suggested fragmentation pathway based on cleavage of alkyl moieties.

Additionally, also cluster ions formed only from ionic liquid ions when using MALDI-MS were mostly found by applying THAP as MALDI matrix in both positive and negative ion mode. For example, in the positive ion mode the cluster composed of IL2 moieties has been observed at m/z 488 corresponding to two choline cations and one NTF_2 anion. When studying IL3 in the negative ion mode a cluster ion at m/z 294 has been attributed to one choline cation and two methanesulfonate anions. In contrast, combined cluster ions of MALDI-MS matrix anion with IL cations were observed by using CHCA matrix. To confirm the identity of the observed cluster ions, PSD was applied for structural elucidation (data not shown). Cluster ions originating from ammonium based ionic liquids and from ionic liquids together with matrices, respectively, by applying MALDI technique have been observed. This finding is in agreement with Zabet-Moghaddam et al. [15] who investigated higher molecular weight imidazolium based IL with various anions.

3.1.3. Structural determination of the IL degradation products

IL samples from the final artificial aging steps under all conditions studied (see Table 3) were selected for LDI-TOF mass spectrometric analysis in both positive and negative ion mode. The acquired mass spectra of IL1 and IL2 containing NTF_2 anion have not revealed any degradation products under all artificial

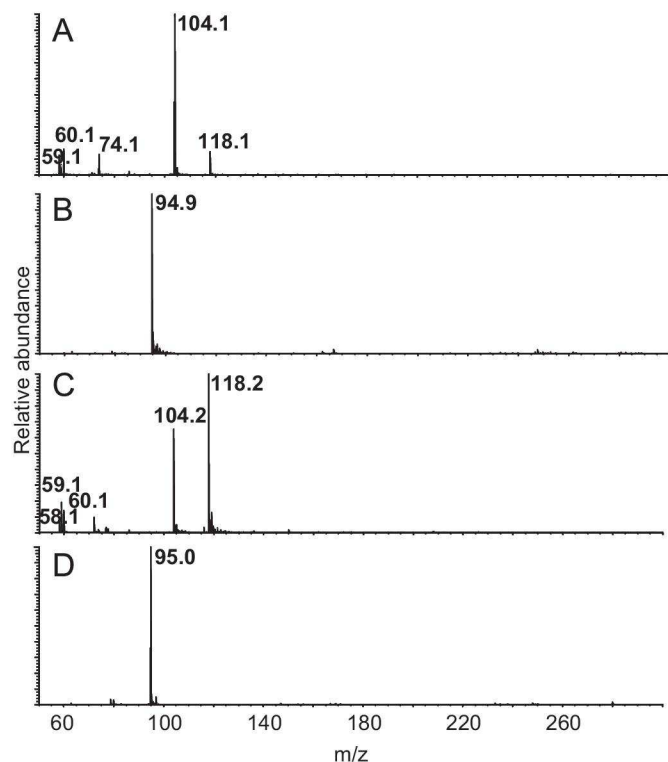


Fig. 3. LDI mass spectra of IL3 artificially aged in contact with 100Cr6 at 175 °C (m/z 104 choline in A, m/z 95 methanesulfonate in B) and IL3 aged without the addition of a metal specimen at 190 °C artificial aging step (m/z 104 choline in C, m/z 95 methanesulfonate in D). Measurements in both positive and negative ion mode show the increased abundance of the age-related product at m/z 118 representing methylated choline but no age-related product(s) of the methanesulfonate anion.

aging conditions studied neither in positive nor in negative ion mode.

The only IL that turned out to be prone to thermally induced degradation was choline methanesulfonate (IL3). The transmethylation of IL3 choline moiety was observed in all artificial aging experiments and progressed with the subsequent artificial aging steps. Fig. 3(A) and (C) depicts the degradation product of choline found at m/z 118 and the unaffected choline m/z 104, respectively. No degradation product was observed in the negative ion mode, only the methanesulfonate ion is present at m/z 95 as shown in Fig. 3(B) and (D).

For the confirmation of the structure of the degraded choline of IL3 CID spectra were acquired from the aged product sample from the precursor ion m/z 118 and can be seen in Fig. 4. The precursor ion yielded fragmentation ions at m/z 102, 86, 74, 60, 59, 58, 43, 42. These fragment ions were attributed to structures which allowed elucidating the entire fragmentation pathways and are summarized in Fig. 5(B). Unaffected choline yielded a fragmentation pattern (Fig. 5(A)) with fragmentation ions at m/z 60 and 58 corresponding with that of methylated choline. However, clearly different fragmentation ions providing most valuable structural information at m/z 59 and especially 86 corresponding to neutral loss of methanol gave strong evidence for the changed chemical structure of choline due to thermally induced transmethylation.

ESI-IT-MS is another MS technique used to obtain additional information concerning the formation of IL degradation products during artificial aging. In particular, ESI-IT-MS was used to study IL samples from the final artificial aging step carried out at 190 °C under air (without the addition of a metal specimen). Due to the high temperature IL were exposed to the harshest conditions (oxygen, water and temperature) and so the most pronounced degradation

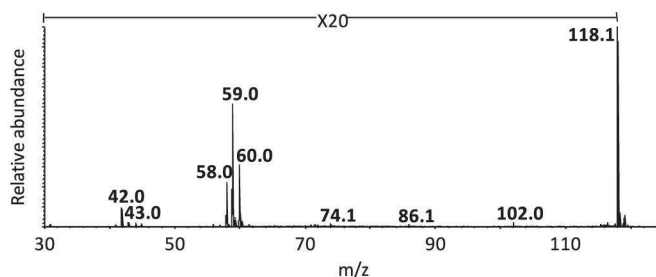


Fig. 4. CID spectrum of the methylated choline (m/z 118). Spectrum was generated by LDI-TOF/RTOF-MS in the positive ion mode from the precursor ion m/z 118. Methylated choline was found in all artificially aged samples of IL3.

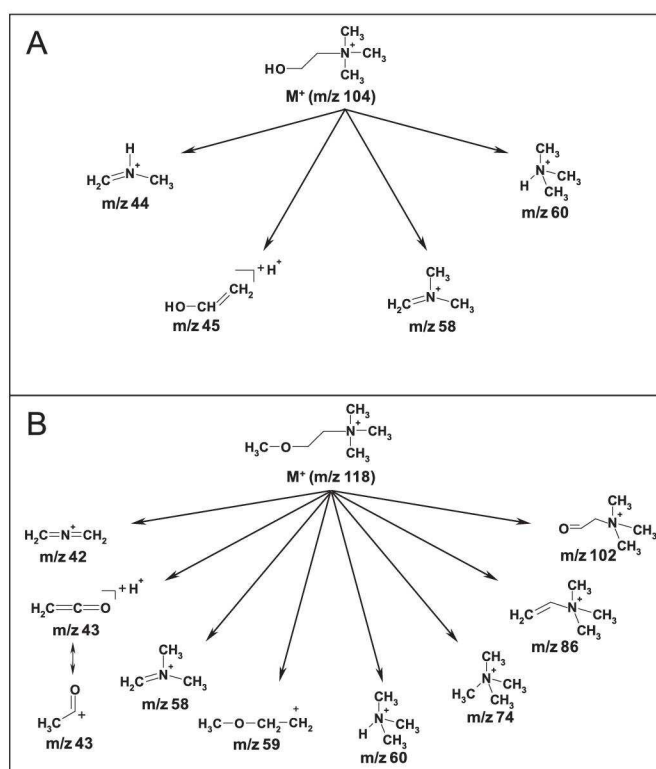


Fig. 5. Fragmentation pathways based on the measured CID spectra of artificially aged choline methanesulfonate (precursor ion m/z 104 is non-fragmented choline) (A), and methylated choline found in the same sample of choline methanesulfonate (precursor ion m/z 118) (B) both obtained by LDI-TOF/RTOF-MS.

reactions were supposed to take place. However, this analytical approach did not reveal any additional degradation products present in the artificially aged IL sample (hence data not shown).

Summing up, the application of LDI-TOF-MS in combination with CID analysis has been successfully applied for small ionic liquid moieties and confirmed the origin of the fragment ions as shown for fresh and artificially aged IL3. Furthermore, the mass spectrometrical investigation enabled the suggestion of fragmentation pathways for choline and thermally degraded choline.

Bis(trifluoromethylsulfonyl)imide and methanesulfonate which were chosen as anions in this research work showed no evidence for degradation reactions/products under the artificial aging conditions and monitored by means of analytical methods applied. Artificial aging experiments confirmed the superior stability of the NTF₂ based IL [5]. The degradation occurred at the IL3 cation moiety due to thermally induced transmethylation of the choline leading to (2-methoxyethyl)trimethyl-ammonium formation. Based on the above mentioned findings, the bis(trifluoromethylsulfonyl)imide anion appears to confer the stability

to the choline cation as no degraded choline was detected. Consequently it is proposed that ionic liquid properties should be jointly interpreted to elucidate synergies and antagonisms between anion and cation moieties.

3.2. Monitoring of metal corrosion by IL

As an indicator of corrosion progress the metal contents in the IL samples were analyzed after each artificial aging step by means of ICP-OES technique. A summary of the metal contents found for all artificial aging experiments is presented in Table 5. The results clearly show that corrosiveness was dependent on several parameters: IL chosen, material being in contact, temperature and water. For example, NTF₂ based IL (IL1 and IL2) caused lower corrosion in comparison with IL3 under all conditions. Usually, an increase of temperature promotes corrosion. 100Cr6 showed good corrosion resistance when immersed in IL1 and IL2. But when adding water to the IL, corrosion increased by about three orders of magnitude. IL3 exerts severe corrosion on both CuSn8P and 100Cr6 under all conditions.

After the final artificial aging step the metal specimens were cleaned as stated in Section 2.2 and examined by optical means as shown in Table 6 (dark upper faces due to photographic adjustments). In comparison with freshly polished specimens the appearance of all metal specimens was affected by the contact with IL at elevated temperatures. Especially, specimens immersed in IL3 were characterized by severe surface damage.

The mass loss of each specimen was investigated and the results are presented in Fig. 6 for CuSn8P alloy and in Fig. 7 for 100Cr6 alloy, respectively. Substantial mass loss was found for CuSn8P and 100Cr6 specimens that were in contact with IL3 in both “open” and “closed” conditions. A qualitative comparison of the results for mass loss with those for metal content in IL in Table 5 shows a good correspondence.

3.2.1. Corrosion evaluation with applied CuSn8P alloy—“open” condition

Under the condition of “open” artificial aging a lower corrosion potential of CuSn8P alloy is observed for IL containing NTF₂

Table 5

Summary of the metal contents in ILs as corrosion indicator during the artificial aging experiments. In the case of CuSn8P the copper content was measured and regarding 100Cr6 the amount of iron was measured by ICP-OES.

IL	Name	Alloy	ICP-OES	“Open” experiment		“Closed” experiment	
				150 °C	175 °C	150 °C	175 °C
IL1	Butyl-trimethyl-ammonium NTF ₂	CuSn8P	Cu (ppm)	90	1100	90	220
IL2	Choline NTF ₂			6	640	30	20
IL3	Choline methanesulfonate			3500	86000	8400	16000
IL1	Butyl-trimethyl-ammonium NTF ₂	100Cr6	Fe (ppm)	2	2	2900	6300
IL2	Choline NTF ₂			2	1	1700	4500
IL3	Choline methanesulfonate			8100	38000	7700	14000

Table 6

Overview of metal specimens after the final artificial aging step examined optically after cleaning step with 2-propanol, toluene and petroleum ether. Specimens of both materials have approximate dimensions of 5 mm × 5 mm × 5 mm.

IL	Name	Alloy	Opened experiment	Closed experiment
			175°C	175°C
IL1		CuSn8P		
IL2	Choline			
IL3	Choline Methanesulfonate			
IL1	Butyl-trimethyl-ammonium NTF ₂	100Cr6		
IL2	Choline NTF ₂			
IL3	Choline Methanesulfonate			

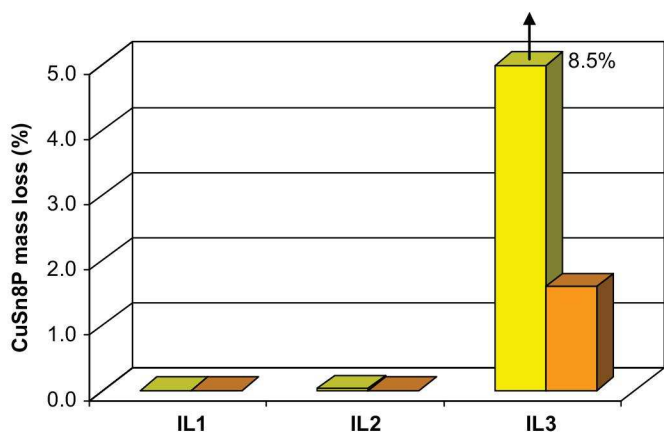


Fig. 6. Mass loss of CuSn8P specimens after last artificial aging step at 175 °C. Results for “open” experiments (air), marked yellow, and for “closed” experiments with defined water content (humid), marked orange. (For interpretation of the references to color in this figure legend, the reader is referred to the web version of this article.)

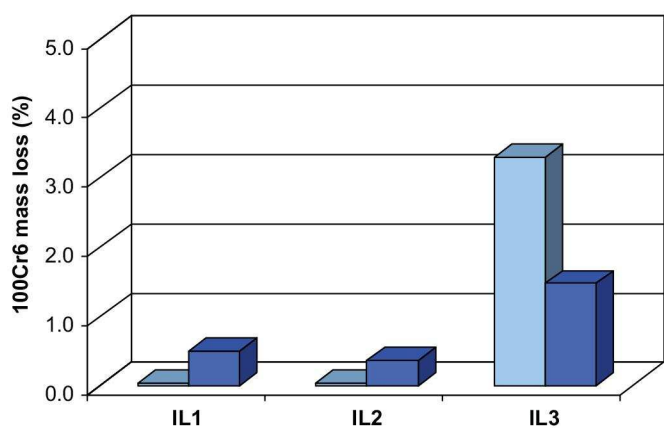


Fig. 7. Mass loss of 100Cr6 specimens after last artificial aging step at 175 °C. Results for “open” experiments (air), marked light blue, and for “closed” experiments with defined water content (humid), marked dark blue. (For interpretation of the references to color in this figure legend, the reader is referred to the web version of this article.)

anions (IL1 and IL2) even though the copper content indicates already an advanced level of corrosion, especially at 175 °C (Table 5).

SEM-EDX analyses of CuSn8P surface resulting from artificial aging with IL1 (used as obtained) revealed a layer of rough structure mainly composed of carbon, oxygen, fluorine and sulfur. This suggests that parts of the layer originate from the IL itself. This conclusion is in agreement with the findings of Bardi et al. [9] and Perissi et al. [10]. However, they stated that the interaction layers are formed by decomposition products of IL, which was not confirmed by our study using MS of artificially aged IL as discussed in Section 3.1.3. Currently, it cannot be definitively excluded that volatile but corrosive degradation products were formed during artificial aging. Such volatiles would have been lost under the “open” experimental conditions. As no evidence for the formation of volatile degradation products of IL was found, one would conclude that either no degradation products evolved or all degradation products had low boiling points.

IL2 used as obtained in the corrosion experiment interacted with the CuSn8P alloy in a different way: a structured layer covered the whole surface of the specimen being clearly different from the composition described for immersion in IL1. The main elements found were copper and oxygen, hence suggesting the

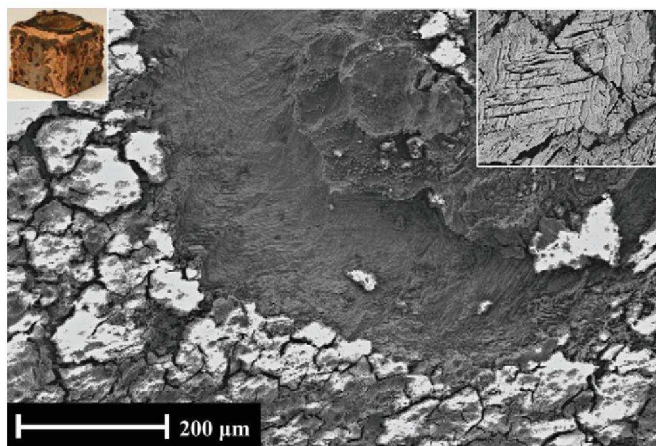


Fig. 8. Corrosion shown at a magnification of 100 × together with rupture lines seen at a magnification of 500 × (upper right corner inset) is revealed by SEM of CuSn8P specimen surface (upper left corner inset) after being in contact with pure IL3 in “open” artificial aging experiment.

formation of copper oxide. No carbon, fluorine or sulfur was present (monitored by EDX) indicating that IL was not directly involved in the formation of a reaction layer.

The behavior of IL3 in contact with the copper alloy differs significantly from the other two investigated ILs. Choline methanesulfonate (IL3) exhibited a very corrosive behavior already at the first stage of artificial aging at 150 °C and the corrosion proceeded rapidly to a tremendous extent. As shown in Fig. 8 after final artificial aging step, the specimen surface was significantly damaged, which is in agreement with the high copper content measured by ICP-OES in the IL and the high mass loss. The corroded CuSn8P surface indicates both the etching type of corrosion and the formation of the so-called “rupture” lines alongside of the lamellar grains of CuSn8P (Fig. 8).

Bright spots of IL3 affected surface were found in SEM-EDX images as a result of a heavily charged non-conductive surface with a significantly higher content of Sn compared to the surrounding area. This suggests the formation of non-conductive tin oxide by an etching mechanism, when only Sn is left out on the surface and oxidized. Such an etching mechanism was also proposed for copper material in contact with 1-hexyl-3-methyl-imidazolium tetrafluoroborate reported by Zhou et al. [1]. It can be suggested that the etching could be caused by attack of degraded IL3 choline moiety as confirmed by MS analysis and discussed in Section 3.1.3.

3.2.2. Corrosion evaluation with applied CuSn8P alloy—“closed” (with defined humidity) condition

In the case of humid environment with defined water content of 1.5% in IL, low copper contents were measured in IL1 and IL2 containing NTF₂. Unexpectedly, ICP-OES of IL1 and IL2 showed that CuSn8P remained unaffected and even indicated lower corrosion than under “open” condition with presence of air (Table 5).

SEM-EDX analysis of CuSn8P specimen surface resulting from artificial aging with IL1 with 1.5% of water content gave again a layer mainly formed by carbon, oxygen, fluorine and sulfur, most probably originating from the IL itself. The layer was brittle and peels off easily. Beneath the brittle layer the microstructure of the unaffected substrate material became visible and was confirmed by SEM-EDX spot analysis.

A similar surface composition but with a different – crystalline – structure was found for CuSn8P immersed in IL2 with 1.5% of water content. The SEM image in Fig. 9 clearly shows that the surface is covered by crystals of various sizes. When studying these crystals at higher magnifications they easily melted due to the higher energy

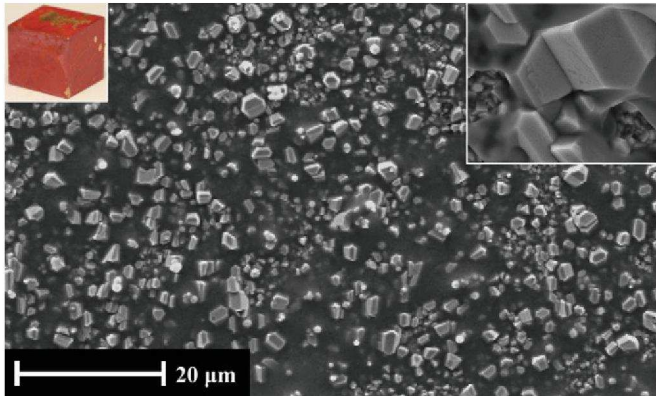


Fig. 9. SEM image of CuSn8P after being in contact with IL2 containing 1.5% water (upper left corner inset) reveals crystal growth of various sizes at a magnification of $1000\times$. These crystals readily melt during SEM analysis at a magnification of $10,000\times$ (upper right corner inset) due to higher energy electron beam.

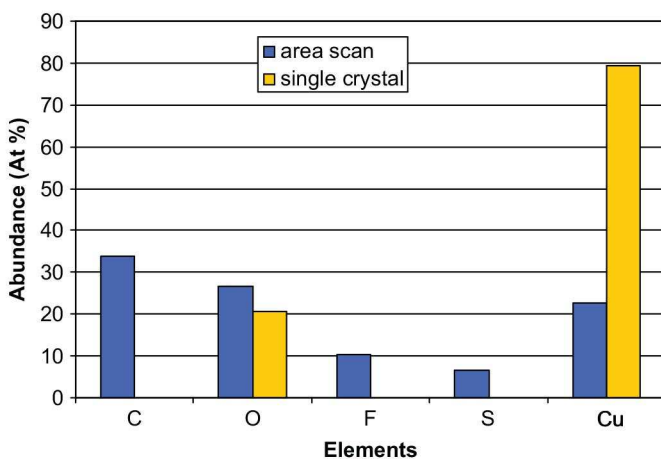


Fig. 10. EDX analysis of CuSn8P specimen surface from last artificial aging step at 175°C after being in contact with IL2 containing 1.5% water. Area scan covered an area of $95\times 125\mu\text{m}^2$ of the surface shown in Fig. 9. Spot scan was done of one larger crystal of copper oxide.

impact of the electron beam. The spot analysis of a selected single crystal revealed that the main elements are copper and oxygen whereas the matrix surrounding the crystals consists of carbon, fluorine and sulfur as can be seen in Fig. 10.

The lower corrosion potential also of choline methanesulfonate (IL3) with 1.5% of water content is supported by ICP-OES, showing roughly 5.5 times lower copper content in comparison to artificial aging with pure IL3 in “open” experiment. Also specimen weight loss throughout the artificial aging is significantly lower and optical appearance of the metal specimen supports lower corrosion as well. The surface revealed by SEM-EDX is severely etched but not to such an extent as observed for IL3 artificially aged in air.

Summing up, choline NTF₂ (IL2) seems to have lower corrosion potential in comparison to the butyl-trimethyl-ammonium NTF₂ (IL1) in contact with CuSn8P alloy under both artificial aging conditions in air and with addition of water, respectively. Furthermore, the results suggest that IL1 creates surface layers composed of IL moieties both under “open” and closed, humid conditions. On the contrary, artificial aging of IL2 resulted in the formation of copper oxide layer or copper oxide crystals embedded into a matrix composed of IL moieties. The methanesulfonate anion and/or the reduced stability of IL3 choline moiety leading to (2-methoxyethyl)trimethyl-ammonium formation

seem to be responsible for the enhanced corrosion behavior when compared to the IL1 and IL2 containing NTF₂ anions.

3.2.3. Corrosion evaluation with applied 100Cr6 alloy—“open” condition

The iron contents of IL with 100Cr6 measured after final artificial aging step in contact with air are for all three ILs considerably lower than the copper content during artificial aging with CuSn8P alloy (Table 5). Low corrosion extent of 100Cr6 monitored by means of iron content in artificially aged IL was particularly observed in the case of NTF₂ containing IL (IL1 and IL2). The combined results obtained by ICP-OES and SEM-EDX revealed no severe attack of the 100Cr6 surface when immersed in pure IL1 and IL2.

Surface analysis of the metal specimen immersed in IL1 showed that the surface was completely covered with evenly distributed small structures at a magnification of $10,000\times$. The EDX area scan found a high content of oxygen in the surface which suggests the formation of iron oxide as main corrosion product.

SEM-EDX of 100Cr6 specimen removed from aged IL2 revealed that no damage to the surface occurred as depicted in Fig. 11. The EDX area scan (area of $45\times 60\mu\text{m}^2$ of the surface shown in Fig. 11) resulted in almost 98% of iron content corresponding to the iron content of unaffected 100Cr6. Furthermore, droplets of high carbon content can be seen at a magnification of $10,000\times$ which were uniformly distributed over the entire surface. The droplets observed can be attributed to residual IL.

Choline methanesulfonate (IL3) fails again under “open” artificial aging condition in terms of stability and proves to be very corrosive. SEM-EDX analysis shows high oxygen content on the surface which indicates that the iron oxide is formed as main corrosion product.

3.2.4. Corrosion evaluation with applied 100Cr6 alloy—“closed” (with defined humidity) condition

In contrast to the artificial aging with pure NTF₂ based ILs (IL1 and IL2) showing exceptional low corrosion, a significantly higher corrosion was observed in the presence of water (defined content of 1.5%) in ILs (Table 5). Also significantly more severe corrosion was observed when compared to the artificial aging of IL1 and IL2 under the same humid conditions but in contact with CuSn8P alloy. This observation can be partially attributed to 100Cr6 itself

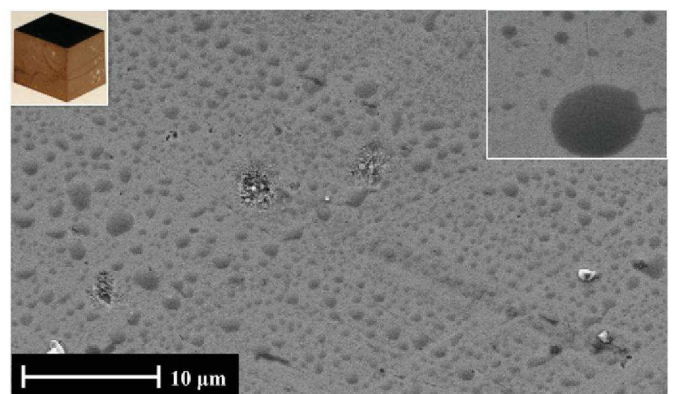


Fig. 11. SEM image of 100Cr6 specimen (upper left corner inset) immersed in IL2 during “open” artificial aging experiment. At a magnification of $2,000\times$ unaffected surface of the 100Cr6 specimen EDX analysis (not shown) revealed almost 98% of iron content supporting low corrosion. At a magnification of $10,000\times$ (upper right corner inset) small drops of high carbon content with uniform distribution over the surface were found. It is suspected that these droplets are residual IL.

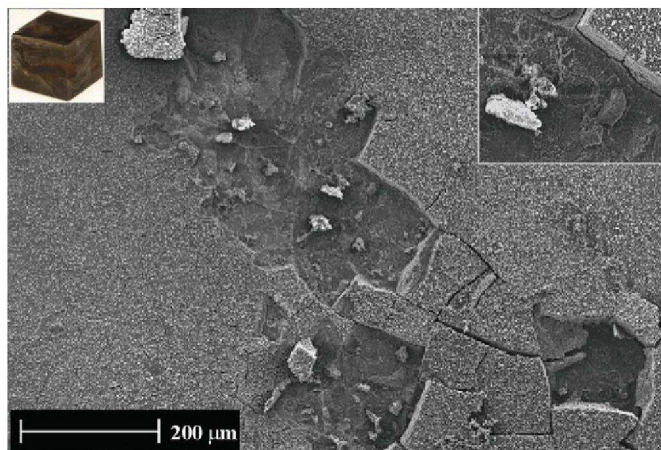


Fig. 12. SEM image of 100Cr6 immersed in IL2 containing 1.5% of water (upper left corner inset) reveals a brittle layer at the magnification of $100\times$. Furthermore, EDX analysis (not shown) revealed the presence of iron oxide. Corrosion even continued beneath the oxide layer as shown at the magnification of $500\times$ (upper right corner inset).

as it is known to be a material prone to corrosion especially under humid conditions.

The corroded (with IL1 and IL2) specimens had similar surface features in terms of oxygen and iron being the main components suggesting the presence of iron oxide. Only the crystalline structure differentiated the two surfaces from each other. In the case of IL1, the residues from corrosion were uniformly distributed over the specimen surface and the visual appearance of reddish layer proposed the presence of iron oxide. Fig. 12 clearly shows that a brittle layer of iron oxide was formed during corrosion of 100Cr6 with IL2 containing 1.5% of water and that corrosion continued beneath this layer.

The same trend as with CuSn8P was observed for 100Cr6 in IL3 where it proved to result in severe corrosion. During artificial aging of IL3 under humid conditions a porous layer consisting of iron and oxygen was formed by corrosion.

Summing up the results for 100Cr6, the corrosion potentials of butyl-trimethyl-ammonium NTF₂ (IL1) and choline NTF₂ (IL2) are in a similar range under all conditions examined (temperatures, “open” and closed conditions) examined. However, choline NTF₂ shows lower corrosion and less pronounced surface changes. Furthermore, the mass losses of the specimens after the final artificial aging step of IL1 and IL2 are comparable. The results indicate that choline NTF₂ may be less harmful in terms of corrosion. Choline methanesulfonate (IL3) showed severe corrosion under all conditions supported by mass loss, metal content in IL3 and SEM-EDX analysis. The presence of significant amounts of water leads to elevated corrosion, which is attributed to the general corrosion sensitivity of 100Cr6. Additionally, the more pronounced corrosion in the case of IL3 could be assigned to the methanesulfonate anion and/or to the reduced stability of IL3 choline moiety prone to transmethylation.

The applied experimental setup for artificial aging proved suitable to evaluate the corrosiveness of studied IL under oxidative and well-defined humid conditions. Based on the results, it can be stated that under some conditions the principle applicability of IL as lubricants is given.

4. Conclusions

Three ionic liquids (IL) were investigated for their thermo-oxidative stability and corrosiveness in a single approach by the implementation of artificial aging procedures under oxidative or well-defined humid conditions. The IL selection based on their

structures has been chosen to fulfill technical requirements for general applications as stated above and to confer environmental sustainability at the same time.

For a better understanding of the degradation mechanisms in the ILs mass spectrometry emerged as highly valuable tool to reveal chemical deterioration of lubricants. For the first time, low molecular mass analytes – starting ILs and degradation products – were successfully examined by LDI- and MALDI-TOF-MS in combination with PSD and CID for structural elucidation. LDI technique proved to be the most suitable and enabled straight forward as well as rapid structural elucidation without any kind of sophisticated sample preparation.

Using “high end” desorption/ionization mass spectrometric techniques, methylated choline has been identified as the degradation product of choline methanesulfonate leading to the formation of (2-methoxyethyl)trimethyl-ammonium which can together with methanesulfonate moiety be responsible for the severe corrosion properties of IL3 in comparison with IL1 and IL2. In contrast to IL3, NTF₂ based IL with butyl-trimethyl-ammonium (IL1) and choline (IL2) proved to be highly stable under the conditions applied. An interesting outcome was the resistance of choline towards degradation in the case of choline bis(trifluoromethylsulfonyl)imide (IL2), where, on the other hand, choline originating from choline methanesulfonate (IL3) is progressively methylated. This finding indicates again the importance that IL moieties – anion and cations – cannot be considered separately from each other due to possible synergistic effects as well as undesirable side effects. Important consideration arise which indicates that some choline based ionic liquids will not be applicable under the conditions of long-term thermo-oxidative stress, even though conferring the sustainability by lowering the (eco)toxicological impact.

Investigation of ILs and metal specimens after artificial aging revealed following findings:

- The extent of corrosion increases with increasing temperature.
- Humid conditions may lead to elevated corrosion as found for 100Cr6 but not for CuSn8P.
- Corrosiveness of ILs depends on the choice of both anion and cation. Severe corrosive attack was found for choline methanesulfonate (IL3) in all artificial aging experiments. Choline NTF₂ (IL2) revealed significantly lower corrosiveness with least pronounced specimen surface changes.
- When comparing the corrosiveness of the most hydrophobic non-functionalized IL1 and medium hydrophobic choline based IL2, IL2 performed unexpectedly less corrosive. Thus, the implementation of hydroxyl group into the cation alkyl side chain confers to less IL corrosiveness, and it delivers at the same time the benefit of lower (eco)toxicological impact to the environment.
- Surfaces affected by corrosion may form oxide layers such as copper, tin and iron oxide as well as reaction layers with IL involved.

In all attempts, IL3 showed the largest corrosion impact on the surface of both copper alloy and steel. Hence, replacement of cation and anion in IL by more environmentally benign species requires further investigation. Currently, choline NTF₂ appears as best compromise between lubricant performance in terms of thermo-oxidative stability, of low corrosiveness and of low potential ecotoxicity.

Research will continue to focus on two aspects: (1) gaining more information about the degradation process, in particular quantification of degradation products and their kinetics and (2) the impact of both (a) environmentally benign design and (b) of degradation products on tribological performance.

Acknowledgments

This work was founded by the European project within the FP7 program – Marie Curie Initial Training Network MINILUBES (216011-2) – by the European Commission. The ESI-IT-MS was made available by a grant from the Austrian Science Foundation (Grant no. P15008 to G.A.) and the LDI/MALDI-tandem MS by the Vienna University of Technology (to G.A.).

References

- [1] Zhou F, Liang Y, Liu W. Ionic liquid lubricants: designed chemistry for engineering applications. *Chem Soc Rev* 2009;38:2590–9.
- [2] Jastorff B, Mölter K, Behrend P, Bottin-Weber U, Filser J, Heimers A, et al. Progress in evaluation of risk potential of ionic liquids—basis for an eco-design of sustainable products. *Green Chem* 2005;7:362–72.
- [3] Pham TPT, Cho C-W, Yun Y-S. Environmental fate and toxicity of ionic liquids: a review. *Water Res* 2010;44:352–72.
- [4] Coleman D, Gathergood N. Biodegradation studies of ionic liquids. *Chem Soc Rev* 2010;39:600–37.
- [5] Minami I. Ionic liquids in tribology. *Molecules* 2009;14:2286–305.
- [6] Bermúdez MD, Jiménez A-E, Sanes J, Carrión F-J. Ionic liquids as advanced lubricant fluids. *Molecules* 2009;14:2888–908.
- [7] Uerdingen M, Treber C, Balser M, Schmitt G, Werner C. Corrosion behaviour of ionic liquids. *Green Chem* 2005;7:321–5.
- [8] Perissi I, Bardi U, Caporali S, Lavacchi A. High temperature corrosion properties of ionic liquids. *Corr Sci* 2006;48:2349–62.
- [9] Bardi U, Chenakin SP, Caporali S, Lavacchi A, Perissi I, Tolstogousov A. Surface modification of industrial alloys induces by long-term interaction with an ionic liquid. *Surf Interface Anal* 2006;38:1768–72.
- [10] Perissi I, Bardi U, Caporali S, Fossati A, Lavacchi A. Ionic liquids as diathermic fluids for solar trough collector's technology: a corrosion study. *Sol Energy Mater Sol Cells* 2008;92:510–7.
- [11] Sowmiah S, Srinivasadesikan V, Tseng MC, Chu Y-H. On the chemical stabilities of ionic liquids. *Molecules* 2009;14:3780–813.
- [12] Scammells PJ, Scott JL, Singer RD. Ionic liquids: the neglected issues. *Aust J Chem* 2005;58:155–69.
- [13] Alfassi ZB, Huie RE, Milman BL, Neta P. Electrospray ionization mass spectrometry of ionic liquids and determination of their solubility in water. *Anal Bioanal Chem* 2003;377:159–64.
- [14] Lesimple A, Mamer O, Miao W, Chan TH. Electrospray mass spectral fragmentation study of N, N'-disubstituted imidazolium ionic liquids. *J Am Soc Mass Spectrom* 2006;17:85–95.
- [15] Zabet-Moghaddam M, Krüger R, Heinzele E, Tholey A. Matrix-assisted laser desorption/ionization mass spectrometry for the characterization of ionic liquids and the analysis of amino acids, peptides and proteins in ionic liquids. *J Mass Spectrom* 2004;39:1494–505.
- [16] ASTM D130-10. Standard test method for detection of copper corrosion from petroleum products by the copper strip tarnish test. ASTM D130 2010, ASTM International, West Conshohocken, PA, USA, 2010.
- [17] REACH homepage of the European Commission: <http://ec.europa.eu/environment/chemicals/reach/reach_intro.htm>.

6.2. Ionic liquid long-term stability assessment and its contribution to toxicity and biodegradation study of untreated and altered ionic liquids

Journal of Engineering Tribology 2012; 226:903-922

Ionic liquid long-term stability assessment and its contribution to toxicity and biodegradation study of untreated and altered ionic liquids

Proc IMechE Part J:
J Engineering Tribology
226(11) 903–922
© AC²T Research GmbH,
Austria 2012
Reprints and permissions:
sagepub.co.uk/journalsPermissions.nav
DOI: 10.1177/1350650112451696
pij.sagepub.com


Lucia Pizarova^{1,2}, Stephanie Steudte^{3,4}, Nicole Dörr¹,
Ernst Pittenauer², Günter Allmaier², Piotr Stepnowski³ and
Stefan Stolte⁴

Abstract

In contrast to well understood degradation mechanisms in conventional lubricants generally promoted by thermo-oxidative stress, the degradation of ionic liquids is widely unknown although they are considered as promising novel types of lubricants. Hence, the ionic liquid long-term stability has been evaluated by small scale artificial alteration experiments under thermo-oxidative conditions. The ionic liquid selection was based on non-functionalized and functionalized ammonium type cations with three different counter anions. The identification of ionic liquid degradation products accomplished by high end mass spectrometric methods, namely time-of-flight/reflectron time-of-flight mass spectrometry and linear quadrupole trap-orbitrap-mass spectrometry, revealed that ionic liquids which were composed of functionalized cation moieties were prone to degradation. Furthermore, the amounts of the most abundant degradation product formed under various artificial alteration conditions have been quantified by ultra high pressure liquid chromatography coupled to electrospray ionization linear quadrupole ion trap orbitrap mass spectrometry, suggesting that the ionic liquid degradation preferably takes place at higher temperatures after a longer period of time. The proposed degradation mechanism requires the presence of nucleophilic species such as methanesulphonate anion. The (eco)toxicological impact of the selected ionic liquids have been evaluated by comprehensive toxicity studies and biodegradation experiments. As the evaluation of selected ionic liquids revealed contrary assessments from stability and (eco)toxicological studies, the need for mutual and complementary consideration of the ionic liquids for a successful implementation of ionic liquid lubricants has been disclosed.

Keywords

Ionic liquid, stability, degradation, toxicity, biodegradation, lubricant

Date received: 16 December 2011; accepted: 23 May 2012

Introduction

Ionic liquids (ILs) are organic or semiorganic salts with physicochemical properties considerably predetermined by the choice of cation and anion. Thus, they offer the possibility to obtain desired properties, such as melting point, viscosity, etc. Their vast structural variability leads to many potential applications, e.g. as electrolytes, thermal fluids or engineering fluids such as novel lubricants.^{1–6}

Implementation of ILs into large scale applications demands the fulfilment of technical requirements as well as passing the Registration, Evaluation,

¹Austrian Centre of Competence for Tribology – AC²T Research GmbH, Wiener Neustadt, Austria

²Institute of Chemical Technologies and Analytics, Vienna University of Technology, Vienna, Austria

³Department of Environmental Analysis, Faculty of Chemistry, University of Gdańsk, Gdańsk, Poland

⁴Department Sustainable Chemistry, Centre for Environmental Research and Sustainable Technology, University of Bremen, Bremen, Germany

Corresponding author:

Lucia Pizarova, Austrian Centre of Competence for Tribology – AC²T Research GmbH, Viktor-Kaplan-Straße 2, 2700 Wiener Neustadt, Austria.

Email: pizarova@ac2t.at

Authorization and Restriction of Chemicals (REACH) requirements.⁷ In accordance with REACH, extensive IL toxicity studies with different test systems comprising enzymes,⁸ mammalian cell lines,^{9–11} bacteria,^{12,13} fungi,^{13,14} algae,^{15,16} plants^{17,18} and crustaceans¹⁹ were performed. Common conclusion is that ILs with longer side chains have higher toxicity in contrast to short, polar functionalized side chains.²⁰ Less significant influence on the toxicity was shown for cation head group and anion.^{17,19,21} Nevertheless, highly fluorinated anions such as $(CF_3SO_2)_2N^-$ as well as phosphates or sulphates with long alkyl chains^{21,22} and aromatic head groups like imidazolium^{8,14} usually increase the IL toxicity. The environmental impact of a compound is also classified by its biodegradability. For example, pyridinium with ethyl and octyl side chains fully mineralize within 28 days;^{23,24} whereas, imidazolium cations are just partially biodegradable.²⁵ Thus, considering both, toxicity and biodegradation, ILs without aromatic systems, short and polar functionalized side chains and non-fluorinated anions should be preferred. Furthermore, compounds structurally based on natural substances are a promising strategy.²⁶

In the field of lubrication, favourable IL properties such as negligible vapour pressure, wide liquid range and enhanced thermal stability are beneficial assets compared to the possibilities of conventional synthetic oil lubricants. This unique set of properties predetermines ILs as suitable candidates for lubrication applications where enhanced long-term lubricant performance under high vacuum and elevated temperature are required. A review by Zhou et al.² identified the need for extensive IL long-term stability evaluation as this crucial characteristic is greatly dependent on the choice of IL moieties – also evaluated by our recent study.²⁷ The review on the IL chemical stabilities by Sowniah et al.²⁸ also refuses the presumption of generally assumed IL inertness. In the industrial lubrication field, the methods designed for evaluation of hydrocarbon-based lubricants are insufficient to study IL stability. Hence, IL stability is mostly evaluated by means of non-isothermal^{29,30} and isothermal thermo-gravimetric analysis (TGA)^{31–33} usually applied in short-term experiments. Some long-term standard test methods, e.g. rotating bomb oxidation test, have also been applied³⁴ but failed to identify the degradation products evolved. There are only a few studies making use of pyrolysis gas chromatography³⁵ and TGA combined with mass spectrometry (MS)^{36,37} to identify degradation products of imidazolium IL. However, these approaches do not simulate the conditions of long-term thermal stress as they apply high heating rates. To our knowledge, there is only one publication by Meine et al.,³⁸ dealing with the quantification of imidazolium based IL degradation products by potentiometric titration.

In our approach, small scale artificial alteration experiments have been applied with the aim to estimate IL long-term performance in industrial applications under simulated thermo-oxidative stress and to gain insight into the degradation processes. The knowledge of IL degraded species can help to better understand the mechanisms of tribochemical reactions and how friction and wear are affected. Thus, the IL matrix was selected for a better understanding of structure–property relationships by varying IL hydrophobicity, anion nucleophilicity and cation side chain functionality. The impact of copper catalyst is examined as copper is known to promote oxidation of conventional lubricants. IL stability has been evaluated by high-end MS techniques, namely laser desorption/ionization time-of-flight MS (LDI-TOF-MS) and ultra high pressure liquid chromatography coupled to electrospray ionization linear quadrupole ion trap orbitrap MS (UHPLC-ESI-LTQ-orbitrap-MS) with the aim to identify IL degradation products and to quantify the degradation products formed under different artificial alteration conditions.

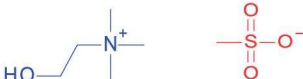
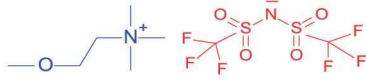
The ILs chosen were also subjected to thorough toxicity and biodegradability assessments to verify their benignity suggested by structural designs following the (eco)toxicological requirements as discussed above. This interdisciplinary assessment emphasizes the importance of an integrated approach towards IL applicability for large scale usage based on the knowledge on their chemical stabilities, toxicity and persistency in the environment of both intact and degraded IL structures.

Experimental

IL structural selection

IL1–IL6 samples were provided by IoLiTec (Ionic Liquids Technologies, Heilbronn, Germany) both as synthesis on request or as catalogue products. The cation moieties of selected IL are based on quaternary ammonium with and without alkyl side chain modification. The alkyl chain has been functionalized by polar hydroxyl or methoxy groups, respectively. The polar functional groups are aimed to lower the (eco)toxicity impact as recommended in the published literature²⁰ and discussed in the introduction part. The selected (2-hydroxyethyl)-trimethyl-ammonium cation is also known as choline being a water soluble essential nutrient. (2-methoxy-ethyl)-trimethyl-ammonium cation was selected to find out whether an increase of stability could be achieved while maintaining high polarity. The anions vary from hydrophobic bis(trifluoromethylsulphonyl)imide to hydrophilic methyl sulphate and methanesulphonate to investigate

Table 1. Overview of the investigated ILs and the purities provided by the supplier Ionic Liquids Technologies.

IL	Name	Structure	Purity	
IL1	Tributyl-methyl-ammonium methanesulphonate		98%	<500 ppm halides
IL2	Butyl-trimethyl-ammonium methanesulphonate		98%	<100 ppm halides
IL3	(2-hydroxyethyl)-trimethyl-ammonium methanesulphonate		98%	<100 ppm halides
IL4	(2-methoxyethyl)-trimethyl-ammonium methanesulphonate		98%	<100 ppm halides
IL5	(2-methoxyethyl)-trimethyl-ammonium methyl sulphate		98%	<100 ppm halides
IL6	(2-methoxyethyl)-trimethyl-ammonium bis(trifluoromethylsulfonyl)imide		99%	<1000 ppm halides

IL: ionic liquid.

structure–property relationships of IL stability. Hence, IL1–IL4 represent the variation of cation side chain with methanesulphonate anion while IL4–IL6 enable the comparison of the effect of anion variation on IL stability, toxicity and biodegradability. The complete overview of the selected IL matrix together with their purity as provided by the supplier is summarized in Table 1.

Artificial alteration experiments

In order to estimate IL long-term stability, small scale artificial alteration has been applied to the same IL sample by three steps of subsequently increasing temperature. Accordingly, artificial alteration was started at 150 °C for 7 days, then continued at 175 °C for additional 7 days and completed at 190 °C as final temperature for further 7 days.

Two parallel experiments were performed for all chosen ILs, with copper as potential oxidation catalyst, stopped after the second alteration step at 175 °C due to expected catalytic effects, and without metal presence, carried out up to the third alteration step at 190 °C, both performed under contact with air.

For carrying out the experiments, conventional glass laboratory test tubes have been used as vessels after thorough cleaning with methanol, toluene, petroleum

ether and drying with dry and oil-free compressed air. The copper catalyst represented a copper wire of 0.1 cm diameter and 3.8 cm length, cleaned with petroleum ether and dried. The ILs were used as obtained within the range 1–6 g. To ensure a direct comparison between the samples, the ratio of IL in grams to copper wire in grams was kept constant. The samples were stored in a common laboratory oven. The sampling took place at the end of each alteration step (seventh day each). The above described experiments are summarized in Table 2.

In order to study the impact of water on IL degradation, also artificial alteration experiments with Cu in the presence of 1.5% (w/w) water were carried out under ‘closed’ condition in sealed glass tube. Therefore, alteration steps at 150 °C and 175 °C were applied in accordance to the general procedure as described above (Table 2).

Experiments for degradation mechanism elucidation

For the confirmation of the previously suggested IL3 degradation mechanism based on transmethylation,²⁷ IL3 was subjected to artificial alterations performed in presence of 20% (w/w) of methyl methanesulphonate (methanesulphonic acid methyl ester), acting as supposed intermediate product and in presence of 20%

Table 2. Overview of conditions applied in the artificial alteration experiments. IL sampling took place after seventh day of each temperature step.

IL	General condition			Catalyst	Temperature		
					150 °C	175 °C	190 °C
IL1	Air	'Opened'	Continuous	–	✓	✓	✓
				Cu	✓	✓	–
IL2				–	✓	✓	✓
				Cu	✓	✓	–
IL3				–	✓	✓	✓
				Cu	✓	✓	–
IL4	20% A 20% B 1.5% water	'Closed'	Discont.	–	✓	✓	✓
				Cu	✓	✓	–
IL5				–	✓	✓	✓
				Cu	✓	✓	–
IL6				–	✓	✓	✓
				Cu	✓	✓	–
IL3	–	–	–	✓	–	–	
	–	–	–	✓	–	–	
	–	–	–	✓	✓	–	
	–	–	–	–	✓	✓	

IL: ionic liquid.

'A' stands for methyl methanesulphonate, 'B' for ethyl methanesulphonate and 'discont.' for discontinuous.

(w/w) ethyl methanesulphonate (methanesulphonic acid ethyl ester) to evaluate the reactivity of longer chain alkylation agent. The reactions were carried out in 'closed' set up in a sealed glass tube, cleaned as described previously, and only the first step at 150 °C for the duration of 7 days has been performed, due to expected fast reaction rates, once the supposed intermediate product is present. The sampling took place at the first and seventh day for the comparison of the degradation product amounts present. The methyl methanesulphonate was obtained in 99% purity as stated by the supplier Sigma–Aldrich (Vienna, Austria) and ethyl methanesulphonate in 99% purity as stated by the supplier VWR (Vienna, Austria).

For the determination of widely unknown kinetics of IL degradation, IL3 was also subjected to discontinuous artificial alteration experiments with temperatures at 175 °C and 190 °C, respectively. 'Discontinuous' means independent experiments at the stated temperature with durations of 1, 2, 5 and 7 days followed by MS analysis to monitor the build-up of degradation products. The reaction was carried out under 'closed' conditions in sealed glass tubes as already described (Table 2).

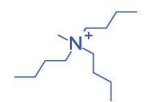
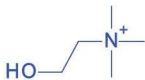
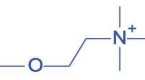
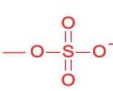
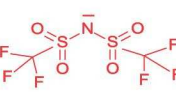
Analytical techniques

IL stability is most commonly determined by TGA at usually fast heating rates of 10 °C/min or higher and is

rarely coupled to infrared spectroscopy or MS for the identification of degradation products evolved. In order to obtain insight into the build-up of degradation products and mechanisms probably occurring under long-term thermo-oxidative stress, high-end MS techniques have been applied to the IL sampling steps from artificial alterations.

LDI-TOF/RTOF-MS approach. Fresh IL sample solutions and solutions of samples from artificial alteration steps have been prepared in the concentration range 0.5–1% (w/w) in methanol. IL methanolic solutions of 0.8 µL have been applied onto the stainless steel target and the solvent was let to dry at room temperature. As straight forward desorption/ionization approach, the ultraviolet laser desorption ionization technique has been selected using the nitrogen laser operating at a wavelength of $\lambda = 337$ nm and a repetition rate of 20 Hz. As analyser, the Shimadzu Biotech Axima TOF² LDI tandem TOF instrument (Shimadzu Biotech Kratos Analytical, Manchester, UK) has been used with a curved-field RTOF as MS2 allowing post-source decay (PSD) or alternatively high energy (20 keV) collision induced dissociation (HECID) with helium as collision gas. The instrument has been calibrated before each sample set to be measured within the m/z range of the measured analytes and while achieving a mass tolerance of 200–500 mDa. Each sample has been examined in both positive and

Table 3. Elemental composition and calculated monoisotopic mass (Da) of representative IL moieties.

IL moiety	Elemental composition	Monoisotopic mass (Da)
	C ₁₃ H ₃₀ N	200.23728
	C ₇ H ₁₈ N	116.14392
	C ₅ H ₁₄ NO	104.10754
	C ₆ H ₁₆ NO	118.12319
	CH ₃ O ₃ S	94.98029
	CH ₃ O ₄ S	110.97521
	C ₂ F ₆ NO ₄ S ₂	279.91730

IL: ionic liquid.

negative ion mode within an m/z range 1–1000 and mass spectra have been acquired at least from 500 individual unselected laser shots using the raster mode. For structural determination purposes, the PSD and HE-CID experiments were carried out while selecting a precursor ion with a mass window of ± 2 Da from the monoisotopic precursor ion. PSD spectra were based at least on 500 single laser shots (so-called profiles). In the case of HE-CID experiments, helium gas was used as collision gas at collision energy of 20 keV and each CID spectrum was based on at least 1000 single laser shots. The summary of the representative IL moieties with their elemental composition and monoisotopic mass values are compiled in Table 3.

UHPLC-ESI-LTQ-orbitrap-MS approach. All solvents were of chromatographic quality, methanol ($\geq 99.9\%$, Chromasolv grade) and water (Chromasolv grade) were obtained from Sigma–Aldrich (Vienna, Austria). Fresh ILs and IL samples from artificial alteration experiments were diluted in methanol for the final

concentration levels of 10 and 1 mg/L. The stock solution of IL4 calibration standard, identical with IL3 altered product, was prepared in methanol in a concentration of 10 mg/mL and the subsequent series of dilutions were performed to yield appropriate concentration levels of standard solutions.

For obtaining high mass accuracy mass spectra, an UHPLC-MS system consisting of Rheos Allegro UHPLC quaternary pump (ThermoScientific, Bremen, Germany), HTS PAL auto-sampler (CTC analytics, Zwingen, Switzerland), six-port Cheminert injection valve (0.25 mm bore) from VICI (Schenkon, Switzerland) and a LTQ orbitrap XL hybrid tandem MS equipped with an IonMax API ion source with the ESI probe mounted (ThermoScientific, Bremen, Germany) were used. Measurements were carried out solely in positive ion mode with the experimental conditions applied as follows: spray voltage of 4 kV, capillary voltage of 41 V, all other voltages optimized for maximum molecular ion transmission, nitrogen sheath gas with a flow rate of 40 units (no conversion in SI-units is provided by the manufacturer) and the transfer capillary temperature at 275 °C. Full scan high resolution mass spectra ($R=30,000$ FWHM at m/z 400) were collected at a selected m/z range of 50–300 with maximum injection time of 200 ms. For verification of the ion identities from full scan high resolution measurements at the same time, low energy-CID (MS/MS) was applied to the expected precursor ion mass in the second scan event. The parameters applied were as follows: isolation and activation width of 2 Da, activation time of 30 ms, normalized collision energy at 50% (100% equals 5 eV according to the manufacturer), helium as collision gas. The mass accuracy with external calibration was in the range 5–10 ppm in all measurements. For data acquisition and data processing, Xcalibur v2.0 software was used.

An aliquot of 2 μ L of each IL sample was injected onto a Kinetex PFP 2.6 μ m analytical column (50×2.1 mm² i.d.) connected to a pre-column, both from Phenomenex (Aschaffenburg, Germany) and the separation was performed at ambient temperature. The mobile phase was a binary mixture of buffer solutions prepared as follows: water with 10 mM ammonium acetate and adjusted with acetic acid to pH 4.3 (A), methanol with 10 mM ammonium acetate (B). The system was operating at gradient elution ramping from 60% to 100% B over 5 min with a 100% B column cleaning step of 5 min and with a 10 min re-equilibration phase. The flow rate was chosen at 200 μ L/min and the column dead time was calculated to be 0.61 min (method 1).

For higher sample throughput, the gradient was adjusted as follows: 60–100% B over 2 min with a 100% B column cleaning step of 2 min and with a

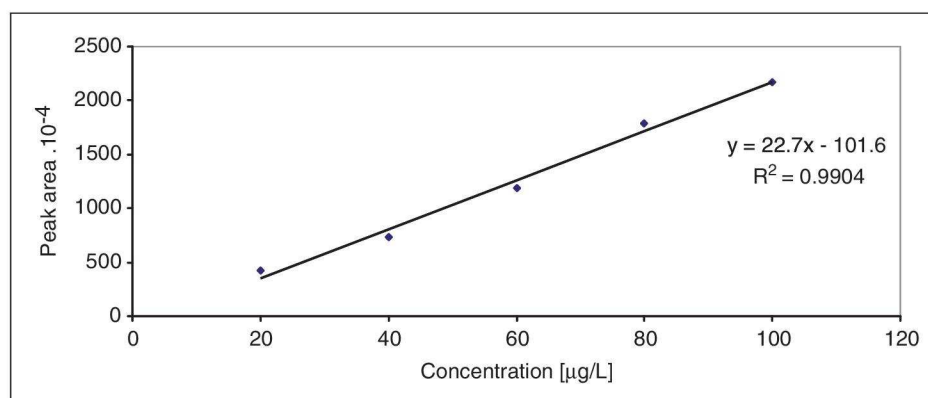


Figure 1. Calibration line (1) based on IL4 cation (identical to altered product of IL3 cation), constructed with the calibration standards in the concentration range 20–100 µg/L for low yields of altered product in IL3 samples, with a coefficient of determination R^2 equal to 0.9904.

IL: ionic liquid.

7 min re-equilibration phase. The flow rate was adjusted to 250 µL/min and the column dead time calculated to be at 0.48 min (method 2).

Quantification of the altered product in IL3 samples subjected to artificial alteration experiments was accomplished by external calibration using IL4 as calibration standard (identical to IL3 altered product). The calibration standard solutions were prepared by dilution series of IL4 stock solution prepared at 10 mg/mL to obtain the final concentration range of 20 µg/L to 1 mg/L. The samples of IL3 subjected to artificial alteration experiments as described in the previous sections as well as the samples of IL3 obtained from earlier artificial alterations²⁷ were diluted to concentrations of 10 and 1 mg/L, respectively, and injected together with the calibration standards at the same run, applying the UHPLC method 2. The corresponding peak areas of the respective standard concentration were obtained by manual integration using Xcalibur v2.0 software and the calibration curves were plotted in Microsoft Excel 2003 (Redmont, WA, USA). Linear regression was applied to the calibration data points obtained and was described by coefficient of determination R^2 and the relative SD (%RSD). These values were determined from three replicates of the quality control (QC) standard selected from calibration standard solutions. The contents of the altered product (IL4) in the samples of IL3 subjected to artificial alteration experiments were calculated from the corresponding calibration while considering the dilution factor applied and expressed as weight percentage (%) based on the weight of the IL3 sample aliquots used for quantification.

As the amount of altered sample within IL3 varied, two calibrations have been constructed from the calibration standards injected. The calibration line (1) constructed within the IL4 concentration range 20–100 µg/L with applied linear regression described by coefficient of

determination R^2 of 0.9904 and with the %RSD of 2.8 determined from three repetitions of the QC standard of 100 µg/L concentration is shown in Figure 1. The calibration line (2) constructed within the IL4 concentration range 40 µg/L to 1 mg/L, suitable for quantification of higher yields of IL3 altered product, with applied linear regression described by coefficient of determination R^2 of 0.9965 and with the %RSD of 3.7 determined from three repetitions of the QC standard of 100 µg/L concentration is shown in Figure 2.

Toxicity and biodegradability assessment

Chemicals. Cell culture media, sera and phosphate buffer were purchased from Invitrogen Life Technologies (Frankfurt, Germany) and WST-1 reagent was obtained from Roche Diagnostics (Mannheim, Germany). Dimethylsulphoxide (DMSO), trifluoroacetic acid, 5,5'-dithio-bis-(2-nitrobenzoic acid) (DTNB), bovine serum albumin (BSA), KH_2PO_4 , K_2HPO_4 , $\text{Na}_2\text{HPO}_4 \cdot 2\text{H}_2\text{O}$, $\text{CaCl}_2 \cdot 2\text{H}_2\text{O}$, $\text{MgSO}_4 \cdot 7\text{H}_2\text{O}$ and FeCl_3 were received from Sigma–Aldrich (St Louis, MO, USA). Acetonitrile, NH_4Cl , NaCl , KOH , acetylcholine esterase (AChE, obtained from electric eel) and acetylthiocholine were purchased from Fluka (Buchs, Switzerland) and NaHCO_3 from GIBCO BRL (Eggenstein, Deutschland).

AChE inhibition assay. The inhibition of acetylcholinesterase was measured using a colorimetric assay based on the reduction of the dye DTNB by the enzymatically formed thiocholine moiety from the AChE substrate acetylthiocholine iodide. The assay is described in detail by Stock et al.⁸ Briefly, a dilution series of the test substances in phosphate buffer (0.02 M, pH 8.0) containing maximum 1% methanol was prepared directly in the wells of a 96-well microtitre plate. DTNB

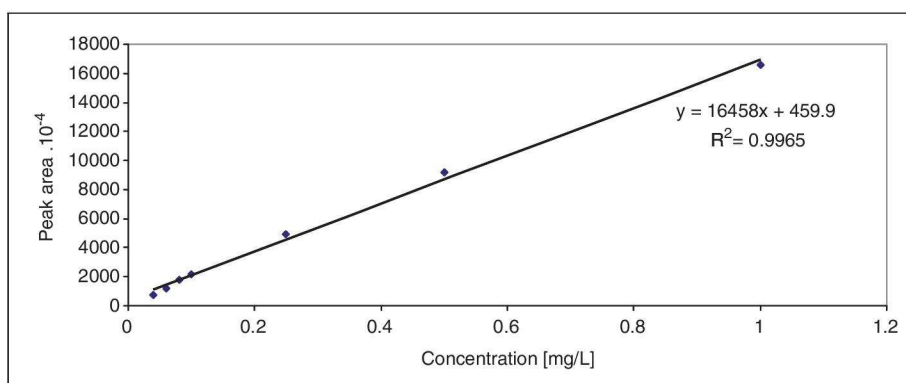


Figure 2. The calibration line (2) based on IL4 cation being identical to altered product of IL3 cation, constructed with the calibration standards in the concentration range from 40 $\mu\text{g/L}$ to 1 mg/L for higher yields of altered product in IL3 samples, with a coefficient of determination R^2 equal to 0.9965.

IL: ionic liquid.

(2 mM, 0.185 mg/L NaHCO_3 in phosphate buffer pH 8.0) and the enzyme (0.2 U/mL, 0.25 mg/mL BSA in phosphate buffer pH 8.0) were added to each well. The reaction was started by the addition of acetylthiocholine iodide (2 mM in phosphate buffer). The final concentrations were 0.5 mM of DTNB and acetylthiocholine iodide and 0.05 U/mL of AChE, respectively. Each plate contained blanks (no enzyme) and control samples (without substance, no toxicant). Enzyme kinetics was measured at 405 nm at 30 s intervals in a microplate reader (MRX, Dynatech Laboratories, Chantilly, Virginia, USA) for 5 min. The enzyme activity was expressed as the slope of optical density (OD/min) from a linear regression. The relative toxicity of the samples was expressed as percentage of enzymes activity compared to the control samples.

Cell viability assay with IPC-81 cells. Cytotoxicity was determined for the promyelocytic leukemia rat cell line IPC-81.³⁹ Cultures of IPC-81 were grown in medium (with L-glutamine, without NaHCO_3 , supplemented with 1% penicillin–streptomycin and 1% glutamine, pH 7) with 10% horse serum at 37 °C (5% CO_2) developed by Roswell Park Memorial Institute (RPMI).

The cytotoxicity assay was carried out according to Ranke et al.⁹ Cell viability was measured using a colorimetric assay for 96-well plates with 2-(4-iodophenyl)-3-(4-nitrophenyl)-5-(2,4-disulphophenyl)-2 H-tetrazolium monosodium salt (WST-1) reagent. Each plate contained blanks (no cells), controls (no toxicants) and substance in 1:1 (v/v) dilution series. Stocks of ILs were prepared in culture medium with 0.5% DMSO to improve solubility of the substances. This DMSO concentration has been proven not to be cytotoxic. For the test, IPC-81 cells in a concentration of 15×10^5 cells/mL (in RPMI with 8% fetal calf

serum) were incubated for 44 h in 96-well plates in the presence of substance and for additional 4 h in the presence of WST-1 reagent. Cell viability as the ability to reduce WST-1 was observed photometrically at 450 nm in a microplate reader (MRX, Dynatech Laboratories, Chantilly, Virginia, USA). Cytotoxicity of the compounds was expressed as percentage of cell viability measured as WST-1 reduction compared to controls. Each dose response curve was recorded for at least nine parallel dilution series on three different 96-well plates. Positive control samples with carbendazim (Sigma–Aldrich, St Louis, MO, USA) were checked in regular intervals.

Luminescence inhibition assay with the marine bacteria *Vibrio fischeri*. The bioluminescence inhibition assay with the marine bacterium *Vibrio fischeri* (*V. fischeri*) was performed according to DIN EN ISO 11348-2.⁴⁰ The freeze-dried bacteria were purchased from Dr Lange (Düsseldorf, Germany). In order to exclude pH effects, a phosphate buffer (0.02 M, pH 7.0, including 2% sodium chloride) was used to prepare a solution of 200 mg/L of the selected substances. The freeze-dried bacteria were rehydrated according to the test protocol after which 500 μL of the bacteria solution were pre-incubated for 15 min at 15 °C with the thermostat LUMISTherm (Dr Lange, Düsseldorf, Germany). The initial luminescence has been measured, 500 μL of the sample were added and after incubation time of 30 min, the luminescence was measured again using LUMISTox 300 (Dr Lange, Düsseldorf, Germany). The relative toxicity of the samples was expressed as the percentage of luminescence compared to control samples. The tests were carried out at least twice for each substance with two replicates per concentration and at least four control samples (2% NaCl solution, phosphate buffered).

Acute immobilization assay with *Daphnia magna*. The 48 h acute immobilization test with the crustacean *Daphnia magna* (*D. magna*) was assessed using the commercially available Daphtoxkit F (MicroBioTest, Gent, Belgium) referred to in Organization for Economic Co-operation and Development (OECD) guideline 202.⁴¹ The detailed description how to perform this assay is given in the supplier's standard operational procedure.⁴² The tests with neonates less than 24 h old obtained by the hatching of ephippia, were performed at 20 °C in the dark. Five pre-fed animals were incubated with the substances in 10 mL of mineral medium, included in the Daphtoxkit F. The numbers of immobilized or dead organisms were checked after 24 and 48 h. The relative toxicity of the samples was expressed as the percentage of not affected organisms compared to control samples. For each substance, five different concentrations of the IL in five replicates and five control samples were investigated. All the experiments were performed at least twice. The sensitivity of the organisms to K₂Cr₂O₇ (Sigma–Aldrich, St Louis, MO, USA) was checked routinely once a new batch of organisms was obtained.

Effect data modeling. Dose response curve parameters and plots were obtained using the drift software package (version 0.05-92) for the R language and environment for statistical computing.⁴³

Ready biodegradability according to OECD 301F Manometric respirometry. The manometric respirometry test was performed according to OECD guideline 301F.⁴⁴ The biological oxygen demand of the substance was determined for 28 days using BOD TRAK (Hach Lange, Düsseldorf, Germany). Acquired from the wastewater treatment plant at Delmenhorst (Germany), the inoculum was filtered and aerated for 5 days before use. A mineral medium containing final concentrations of 85 mg KH₂PO₄/L, 217.5 mg K₂HPO₄/L, 221.3 mg Na₂HPO₄·2H₂O/L, 17 mg NH₄Cl/L, 36.4 mg CaCl₂·2H₂O/L, 22.5 mg MgSO₄·7H₂O/L and 0.25 mg FeCl₃/L (pH 7.2) was added to the filtrate. The samples containing inoculated media and 50 mg/L substance were prepared, as well as blank samples (inoculated media without test substance). Here, a bacteria number of 10⁶ cells/mL was applied determined by Paddle-Tester (Hach Europe, Düsseldorf, Germany). The flasks containing vessels with KOH to ensure absorption of the carbon dioxide evolved were closed with gas tight stoppers and stored in the dark at 20 °C. The oxygen consumption was determined manometrically. Biodegradation of the substance was calculated by the oxygen uptake for the substance (corrected by the oxygen demand of the blank samples) with respect to the theoretical oxygen demand (ThOD) of the

substance and the amount of substance present in the sample as stated in equation (1)

$$\% \text{ biodegradation} = \frac{\text{O}_2 \text{ uptake (s)} - \text{O}_2 \text{ uptake (b)}}{c \text{ (s)} \cdot \text{ThOD (s)}} \cdot 100 \quad (1)$$

where *s* represents the substance, *b* stands for blank, oxygen uptake is in mg/L, substance concentration *c* is expressed in mg/L and ThOD is described in mg(O₂)/mg(s) unit.

Results and discussion

IL altered product identification by LDI-TOF/RTOF-MS

Non-functionalized ammonium-based IL1 and IL2. IL1 and IL2 based on non-functionalized IL cation moieties proved to be stable under all artificial alteration conditions, without and with copper as catalyst in both positive and negative ion mode (no data is shown).

(2-methoxyethyl)-trimethyl-ammonium based IL4–IL6. The series of ILs based on (2-methoxyethyl)-trimethyl-ammonium cation with *m/z* 118 (IL4–IL6) subjected to artificial alterations with and without copper showed in positive ion mode the presence of altered product at *m/z* 104 with low-signal intensity. The signal intensity of this altered product has not significantly changed throughout the artificial alteration under both conditions. For comparison, the mass spectra of IL4–IL6 from the third alteration step at 190 °C without copper presence are shown in Figure 3.

Spectra obtained by a TOF analyser are of low mass accuracy. In order to gain more structural information, the observed mass at *m/z* 104 has been selected as precursor ion in the HE-CID experiment for generating the corresponding CID fragmentation spectrum as shown in Figure 4. The obtained spectrum was subsequently compared with the HE-CID spectrum of fresh IL3 cation of *m/z* at 104. The fragments obtained from both *m/z* 104 precursor ions are identical and hence the altered product is identified as (2-hydroxyethyl)-trimethyl-ammonium moiety, i.e. the choline cation.

The corresponding fragmentation pathway based on the obtained HE-CID spectra with fragment ions at *m/z* 60, 58, 45 and 42 were successfully attributed to the structures and are summarized in Figure 5. The elucidated product ions from fragmentation further supports the identification of the (2-hydroxyethyl)-trimethyl-ammonium as altered product of IL4–IL6.

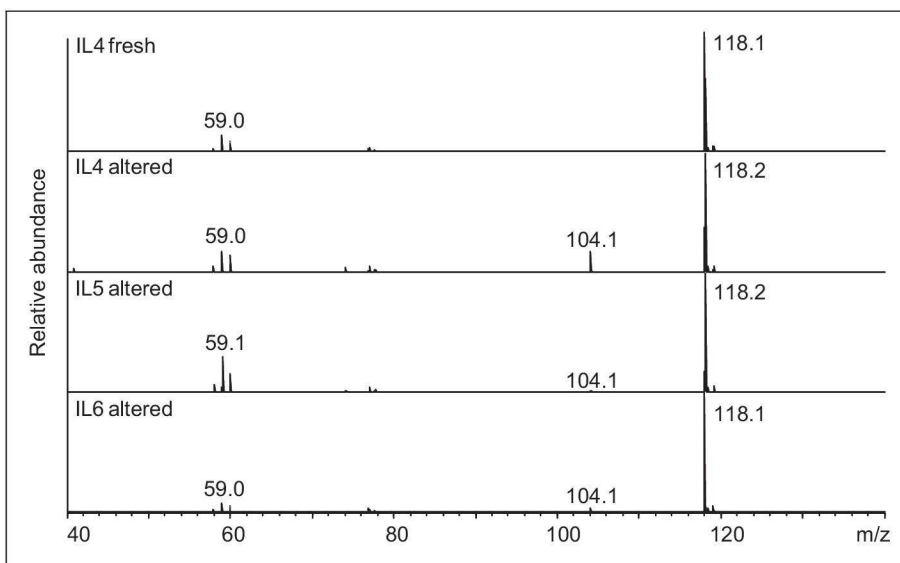


Figure 3. LDI mass spectra in positive ion mode of IL4–IL6 obtained from third artificial alteration step at 190 °C, sampled after seventh day, showing the presence of altered product at m/z 104. In the LDI spectrum of fresh IL4, no mass at m/z 104 was present, as well as it was not detected for fresh IL5 and IL6 (data not shown).

LDI: laser desorption ionization; IL: ionic liquid.

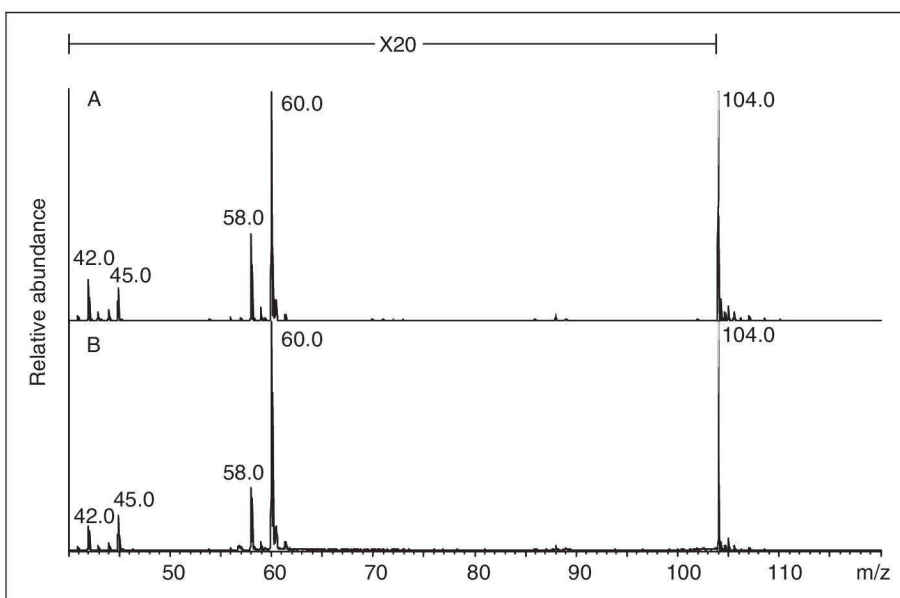


Figure 4. HE-CID spectra in positive ion mode of IL3 (2-hydroxyethyl)-trimethyl-ammonium cation at m/z 104 (A) compared with the HE-CID spectra of altered product at m/z 104 observed in IL4, IL5 and IL6 series based on (2-methoxyethyl)-trimethyl-ammonium cation (B). The fragments from both precursor ions at m/z 104 are identical, identifying the degradation product as (2-hydroxyethyl)-trimethyl-ammonium moiety.

HE-CID: high energy collision induced dissociation; IL: ionic liquid.

The presence of (2-hydroxyethyl)-trimethyl-ammonium as degradation product suggests that the degradation mechanism based on demethylation occurs during the IL4–IL6 artificial alteration. Hence, it cannot be excluded that the demethylation can take place directly

from the quaternary ammonium leading to volatile tertiary amines as altered product. However, volatile tertiary amines are difficult to be detected under the measurement setup of high vacuum LDI-TOF-MS in presence of quaternary ammonium cations.

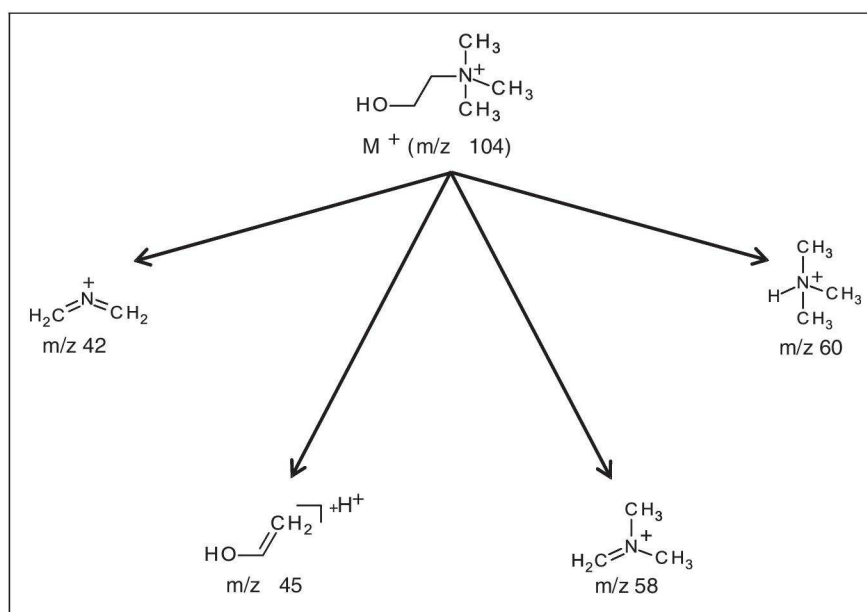


Figure 5. Product ions from fragmentation of (2-hydroxyethyl)-trimethyl-ammonium moiety identified as degradation product in IL4, IL5 and IL6 samples from artificial alteration experiments based on HE-CID using a LDI-TOF/RTOF-MS.

IL: ionic liquid; HE-CID: high energy collision induced dissociation; and LDI-TOF/RTOF-MS: laser desorption ionization time-of-flight/reflectron time-of-flight mass spectrometry.

In the negative ion mode, the anions of IL4 and IL6 were stable throughout the artificial alteration experiment. But the methyl sulphate anion moiety of IL5 at m/z 111 was hydrolysed in all cases which resulted in the formation of hydrogen sulphate occurring at m/z 97 as can be seen in Figure 6. The methyl sulphate instability in aqueous solution leading to hydrolysis was already stated by Wasserscheid et al.⁴⁵ However, no water has been added in the experiments. Hence, IL was only possible to react with atmospheric moisture and water already dissolved in IL. The observed ion at m/z 79 does not correspond to fresh or to altered IL anion moiety and can be attributed to a background anion.

(2-hydroxyethyl)-trimethyl-ammonium based IL3. All sampling steps from the artificial alterations of IL3 were measured in both positive and negative ion modes. In the negative ion mode, methanesulphonate performed as stable anion moiety under all conditions (data not shown). In the positive ion mode, a degradation product at m/z 118 has been detected in all cases additionally to the authentic IL3 cation at m/z 104. The degradation product intensities at m/z 118 under the examined artificial alteration experiments are summarized in Figure 7.

In order to obtain structural information of the present degradation product at m/z 118, the IL3 sample from the last artificial alteration step at 190 °C has been subjected to HE-CID experiment which enables

pronounced fragmentation of the m/z 118 precursor ion. The HE-CID spectrum with the obtained product ions important for structural confirmation is shown in Figure 8.

In our previous research with alteration experiments under different conditions, the IL3 degradation product at m/z 118 was elucidated as (2-methoxyethyl)-trimethyl-ammonium moiety supported by the CID spectrum where low signal intensity ions at m/z 43, 74, 86 and 102 have been detected with very high and time consuming number of laser pulses.²⁷ However, spectra based on lower number of laser pulses and of low mass accuracy allow the detection of product ions occurring only in higher abundances. Thus, such spectra generated from the altered product at m/z 118 could easily lead to ambiguous data interpretation. Hence, two possible fragmentation pathways can be suggested based on the data obtained as it is depicted in Figure 9, revealing (carboxymethyl)-trimethyl-ammonium moiety as well as (2-methoxyethyl)-trimethyl-ammonium moiety, both products of reasonable degradation mechanisms.

As shown, the product ion at m/z 59 can represent fragment carrying information of the alkyl chain functionalization. Thus, for unambiguous confirmation of the identity of chemical structures in general and of the degradation product at m/z 118 in detail, high mass accuracy spectra have been acquired by UHPLC-ESI-LTQ-orbitrap-MS as further discussed below.

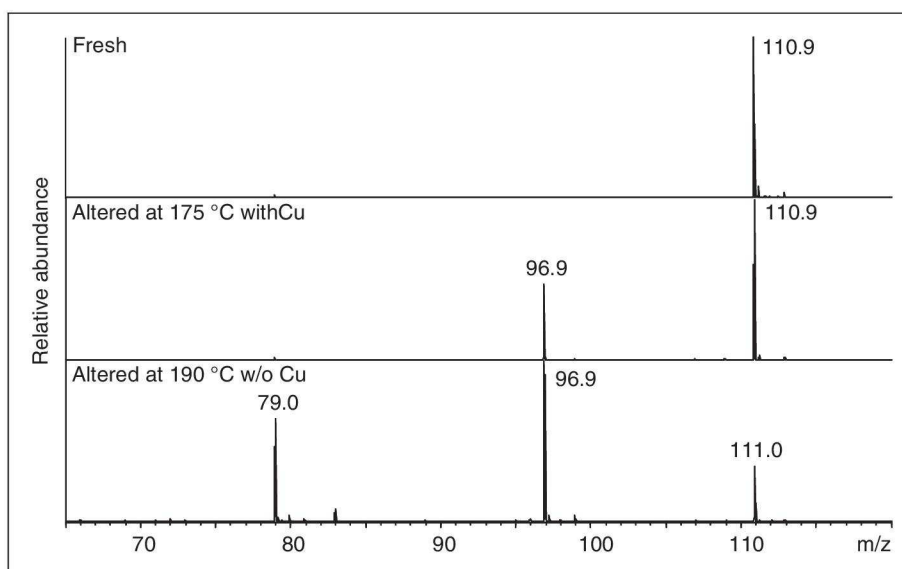


Figure 6. LDI mass spectra in negative ion mode of fresh IL5 with methyl sulphate moiety at m/z 111 (top), IL5 sample from last artificial alteration step with copper as catalyst at $175\text{ }^{\circ}\text{C}$ (middle) and spectrum of IL5 from last artificial alteration step without copper at $190\text{ }^{\circ}\text{C}$ (bottom) showing the increase of hydrogen sulphate at m/z 97 in the artificial alteration steps. LDI: laser desorption ionization; IL: ionic liquid.

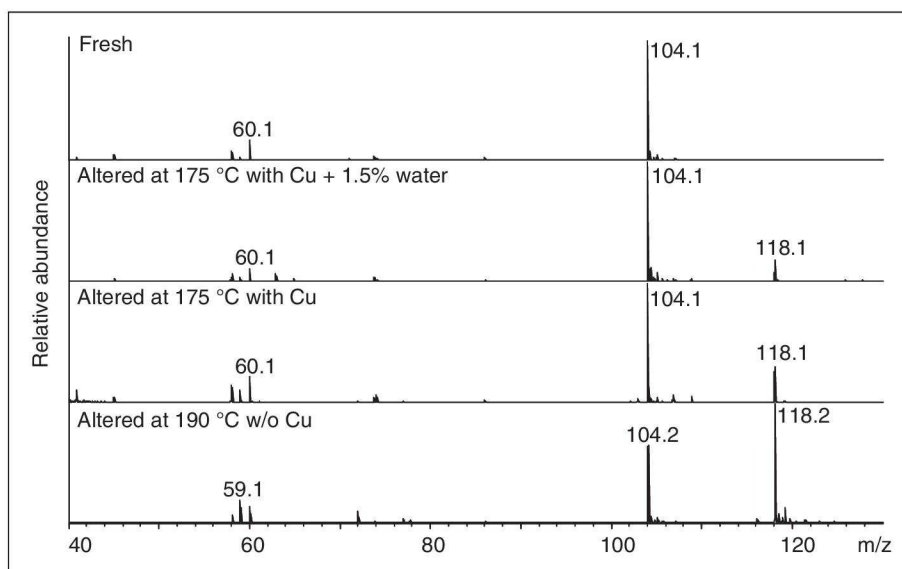


Figure 7. LDI mass spectra in positive ion mode of fresh IL3 compiled with IL3 samples from last artificial alteration steps under each experimental set up, sampled after seventh day. As the degradation product at m/z 118 increases over time in comparison to the fresh IL cation moiety at m/z 104, also the fragment ion at m/z 59 increases.

LDI: laser desorption ionization; IL: ionic liquid.

IL3 altered product identification by UHPLC-ESI-LTQ-orbitrap-MS

In order to confirm the identity of the degraded product at m/z 118, the IL3 sample from the last step of artificial alteration experiment without copper at $190\text{ }^{\circ}\text{C}$ has been measured by UHPLC-ESI-LTQ-orbitrap-MS as described in 'UHPLC-ESI-LTQ-orbitrap-MS approach' using UHPLC method 1. From the full

scan mass spectrum, following ion chromatograms were extracted based on the monoisotopic values: m/z 104.10754 corresponding to authentic IL3 (2-hydroxyethyl)-trimethyl-ammonium cation, m/z 118.08679 corresponding to (carboxymethyl)-trimethyl-ammonium as one possible degradation product and m/z 118.12319 corresponding to (2-methoxyethyl)-trimethyl-ammonium moiety as another possible degradation product. The extracted ion chromatograms

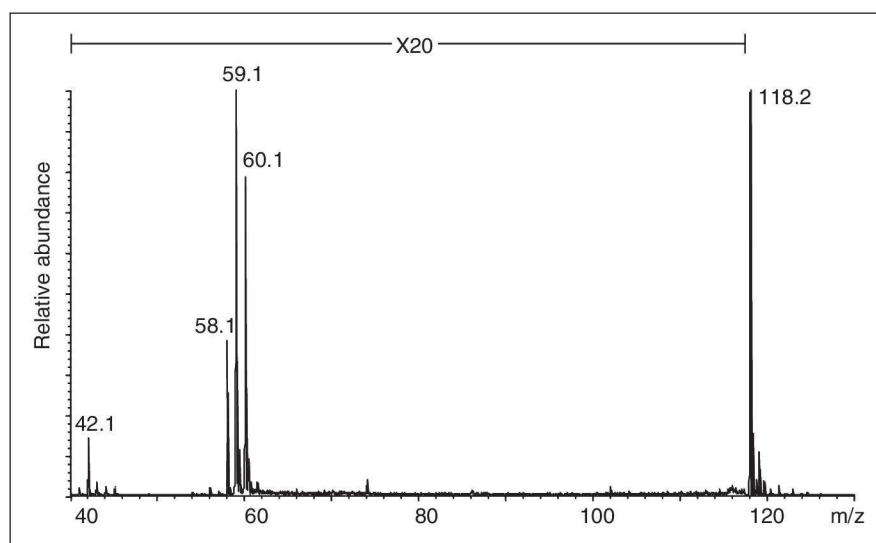


Figure 8. HE-CID spectrum in positive ion mode of 1000 profiles of detected altered product at m/z 118 as precursor ion, in the IL3 sample from artificial alteration without copper presence at 190°C , sampled after seventh day with the obtained product ions for further structural elucidation.

HE-CID: high energy collision induced dissociation; IL: ionic liquid.

obtained are shown in Figure 10. While applying Gaussian smoothing (seven points) and a mass accuracy of 5 ppm, (2-hydroxyethyl)-trimethyl-ammonium cation of IL3 at m/z 104.10754 was detected at a retention time of 0.74 min and only the (2-methoxyethyl)-trimethyl-ammonium at m/z 118.12319 as degradation product was found at a retention time of 0.83 min. These findings clearly exclude the presence of (carboxymethyl)-trimethyl-ammonium.

IL3 altered product quantification by UHPLC-ESI-LTQ-orbitrap-MS

The obtained calibration line (2) enabled quantification of IL3 degradation product from samples subjected to artificial alteration experiments at the second step at 175°C , sampled at the seventh day. The corresponding results are presented in Table 4. As can be seen, the amount of altered product in IL3 is in very similar range regardless of the type of metal or alloy used as potential catalyst or without a metal presence at all. However, lower amount of altered product was quantified in the case of artificial alteration performed under 'closed' condition in sealed glass tube with the addition of 1.5% (w/w) water. This is an important finding since usually a negative influence of water on the stability of ILs is anticipated as reported by Minami, e.g. by Hofmann elimination.^{4,34}

For gaining information on IL3 kinetics of artificial alteration, the IL3 samples from subsequent as well as from discontinuous artificial alterations as described in

'Experiments for degradation mechanism elucidation', were quantified using calibration line (1) and the results were compared as presented in Table 5. The discontinuous artificial alteration at both 175°C and 190°C , respectively, leads to altered product quantities in similar range in comparison with subsequent artificial alteration at second step at 175°C . It could be concluded that the altered product build-up is slow and the highest increase is observed at the subsequent alteration in the third step at 190°C , suggesting that the reaction takes place mostly at higher temperatures over a longer period of time. On the other hand, the amount of reaction product from the experiment using the supposed intermediate product based on methyl methanesulphonate added at 20% (w/w) suggests that once the intermediate product is formed, the reaction takes place at high reaction rate even at low temperature, as can be seen from the quantity of altered product at first day at 150°C . The amount almost doubles at 150°C at the seventh day, probably due to some autocatalytic effect taking place.

IL degradation mechanisms elucidation

The addition of methyl methanesulphonate as alkylation agent to artificial alteration experiments of IL3 gave evidence for the degradation mechanism of IL3 based on transmethylation where methyl methanesulphonate is supposed as intermediate product. In parallel, further experiments with addition of ethyl methanesulphonate at 20% (w/w) were carried out to

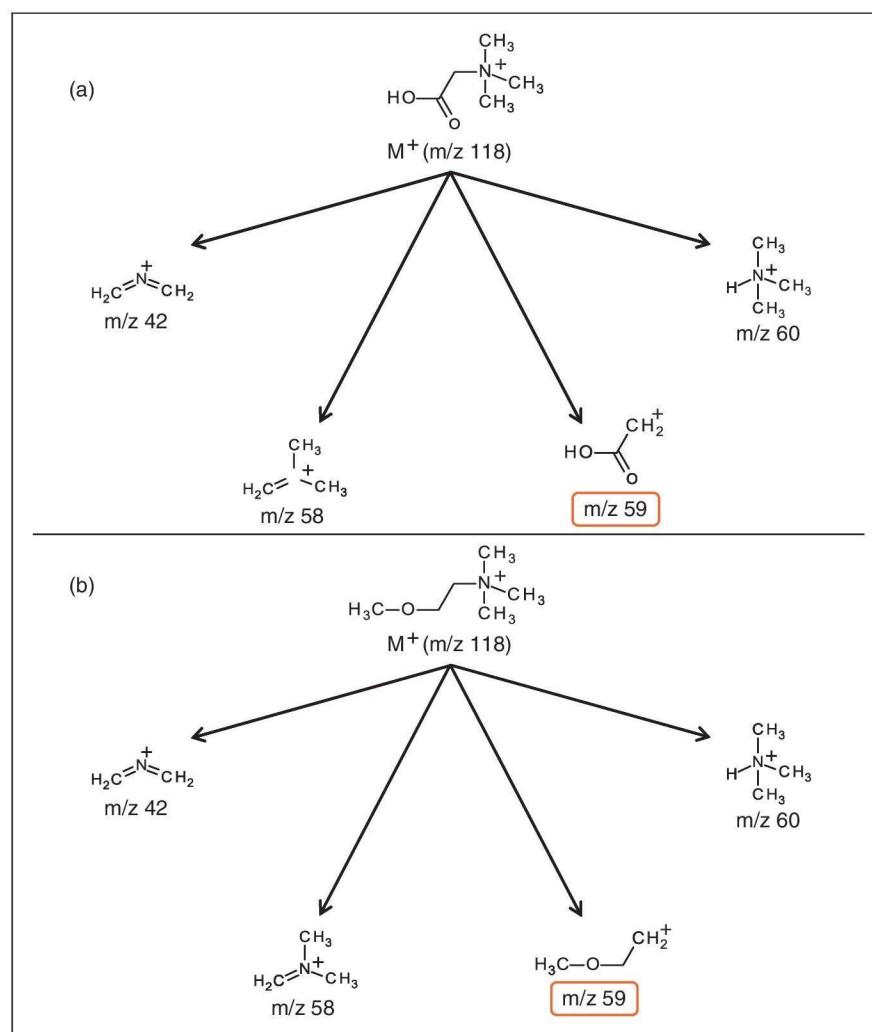


Figure 9. Two possible ambiguous interpretations of the fragmentation of the altered product at m/z 118 based on HE-CID spectra obtained, leading to structural elucidation of either (carboxymethyl)-trimethylammonium (a) or (2-methoxyethyl)-trimethyl-ammonium (b) moiety as the degradation product.

HE-CID: high energy collision induced dissociation.

study the reactivity of an alkylation agent with longer alkyl chain. LDI spectra of both IL3 samples from first sampling day are shown in Figure 11. The high signal intensity of IL3 altered product at m/z 118 is present already at the first sampling day at 150°C , suggesting high reaction rate and high yield of the altered product as confirmed by quantification in Table 5. Additionally, high intensity altered product at m/z 132 is present from artificial alteration with ethyl methanesulphonate corresponding to the expected difference of $\Delta m = 14$ Da from the altered product at m/z 118. Fragment ions in the lower m/z range are also distinguishable: in the case of altered product at m/z 118 (A) the ion at m/z 59 is present at higher abundance. This could be an indication that m/z 59 rather corresponds to $\text{CH}_3\text{OCH}_2\text{CH}_2^+$ than to ion-radical of trimethylamine. In the case of altered

product at m/z 132 (B) a high intensity fragment ion at m/z 45 is characteristic to the artificial alteration in presence of ethyl methanesulphonate.

For the structural elucidation of the altered products at m/z 118 and 132, HE-CID experiments by means of LDI-TOF/RTOF-MS have been performed. As the product ions of precursor ion at m/z 118 were identical (data not shown) to the ones of authentic (2-methoxyethyl)-trimethyl-ammonium moiety as shown in Figure 8, the possible degradation mechanism based on transmethylation with methyl methanesulphonate as intermediate product proved to be feasible. HE-CID spectra of the altered product at m/z 132 yielded product ions at m/z 73, 60, 59, 58, 45 and 42 as shown in Figure 12. They were assigned to the corresponding structural fragments as summarized in Figure 13, confirming the transfer of the ethyl group

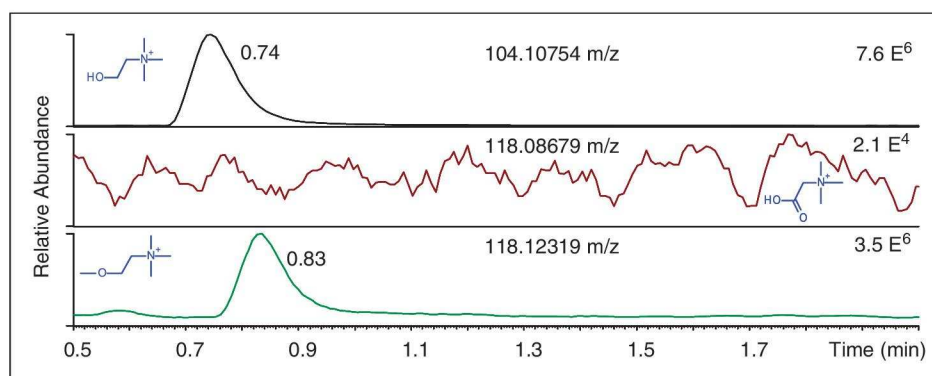


Figure 10. Extracted ion chromatograms of 5 ppm mass accuracy with Gaussian smoothing (seven points) applied to IL3 sample from artificial alteration without copper presence at 190 °C showing the presence of intact (fresh) IL3 (2-hydroxyethyl)-trimethyl-ammonium at m/z 104.10754 eluting at 0.74 min and confirming the identity of (2-methoxyethyl)-trimethyl-ammonium moiety as degradation product at m/z 118.12319 eluting at 0.83 min. There is no evidence for (carboxymethyl)-trimethyl-ammonium at m/z 118.08679. The full scan chromatogram has been measured with method 1. IL: ionic liquid.

Table 4. Amounts of (2-methoxyethyl)-trimethyl-ammonium as altered product in IL3 samples from artificial alteration at second subsequent step at 175 °C, sampled after seventh day.

General condition	Artificial alteration parameter	Added water % (w/w)	Altered product % (w/w)
Without catalyst	Air	–	3.4
Cu	Air	–	3.9
Cu + water	Closed	1.5	1.7
CuSn8P	Air	–	3.3
CuSn8P + water	Closed	1.5	0.6
I00Cr6	Air	–	3.8
I00Cr6 + water	Closed	1.5	NA

IL: ionic liquid.

The quantities are obtained from the calibration (2) and recalculated to weight percentage based on the IL3 sample aliquots used for quantification. 'NA' states that the amount cannot be quantified as it falls below the limit of quantification.

from ethyl methanesulphonate to (2-hydroxyethyl)-trimethyl-ammonium.

As the degradation products formed during IL3 artificial alterations were confirmed unambiguously, it enabled the suggestion of the degradation mechanisms taking place under IL3 long-term thermo-oxidative stress as described in Figure 14. In the first reaction step, an equilibrium between protonated/deprotonated (2-hydroxyethyl)-trimethyl-ammonium and deprotonated/protonated methanesulphonate could be established (1.a). As tetraalkyl ammonium compounds are possible to release an alkyl group to give a tertiary amine, demethylation of (2-hydroxyethyl)-trimethyl-ammonium could occur to form methyl methanesulphonate from methanesulphonate anion (1.b). The intermediate products of deprotonated choline from 1.a and methyl methanesulphonate from 1.b are then able to react with each other to result in (2-methoxyethyl)-

trimethyl-ammonium and methanesulphonate (2). As proposed by the reaction mechanism, methanesulphonate is restored after reaction (2) has taken place and hence seems to act as catalyst. The formation of N,N-dimethyl-ethanolamine as degradation by-product (1.b) has to be unambiguously detected by another suitable technique. By analogy with methyl methanesulphonate, intermediate reaction product 'A' can be replaced by ethyl methanesulphonate.

Toxicity of selected IL

Toxicity studies were carried out using different biological systems of varying complexity. The results expressed as IC_{50} or EC_{50} values in mg/L are listed in Table 6. For IL2–IL6 this results were already published elsewhere⁴⁶ and were added here for the complete overview and comparison.

Table 5. Amounts of (2-methoxyethyl)-trimethyl-ammonium as altered product in IL3 samples expressed as weight percentage.

Artificial alteration						
Parameter	Setup	Temperature	Sampling day	Alkylation agent % (w/w)	Altered product % (w/w)	Calibration curve
Air	Continuous	150 °C	7th	–	1.2	2
		175 °C	14th		3.4	
		190 °C	21st		11	
Closed	Discontinuous	175 °C	1st	–	NA	1
			2nd		NA	
			5th		2.5	
			7th		3.1	
Closed	Discontinuous	190 °C	1st	–	1.9	
			2nd		2.2	
			5th		2.2	
			7th		4.5	
Closed	Discontinuous	150 °C	1st	20	22	2
			7th		42	

IL: ionic liquid.

Methyl methanesulphonate was used as alkylation agent. 'NA' states that the amount cannot be quantified as it falls below the limit of quantification.

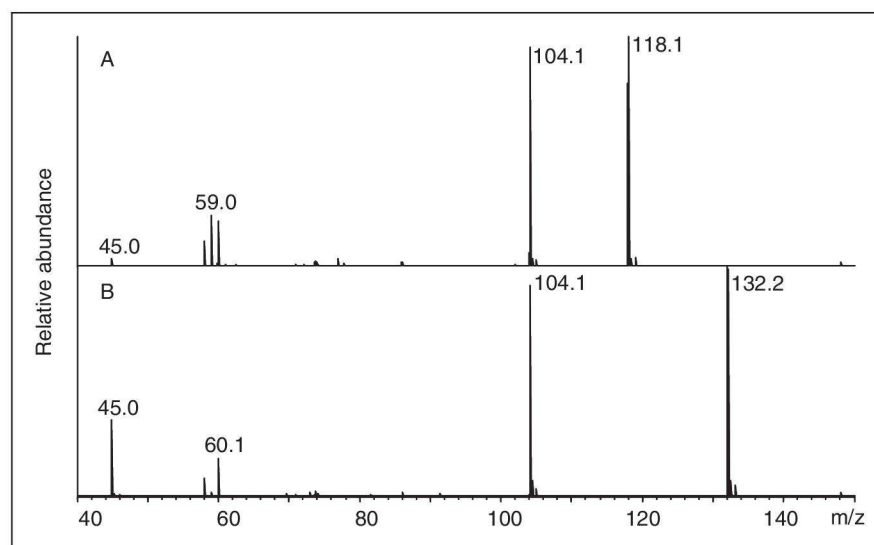


Figure 11. LDI spectra in positive ion mode of IL3 artificial alteration experiments performed with 20% (w/w) addition of methyl methanesulphonate at 150 °C (A), sampled after first day, with the altered product present at m/z 118. Correspondingly, IL3 subjected to artificial alteration with 20% (w/w) of ethyl methanesulphonate at 150 °C (B), sampled after first day, formed altered product at m/z 132.

LDI: laser desorption ionization; IL: ionic liquid.

Using high throughput screening tests with the isolated enzyme AChE, an important biomarker for the central nervous system, all tested IL showed no inhibition effect up to the maximal tested concentration of 100 mg/L. The same results in terms of the luminescence inhibition were obtained for the marine bacterium *V. fischeri*. This is in good agreement to previously reported results, where cations with short alkyl side

chain (such as ethyl) or chains containing functional groups showed significant lower toxicity in several test systems compared to more hydrophobic cations.^{9,10,12,15,17,47}

Additionally, the cytotoxicity tested with the leukemia rat cell line IPC-81 support these results, showing that IL2–IL6 with relatively short side chains and (partly) functional groups gave EC_{50} values of above

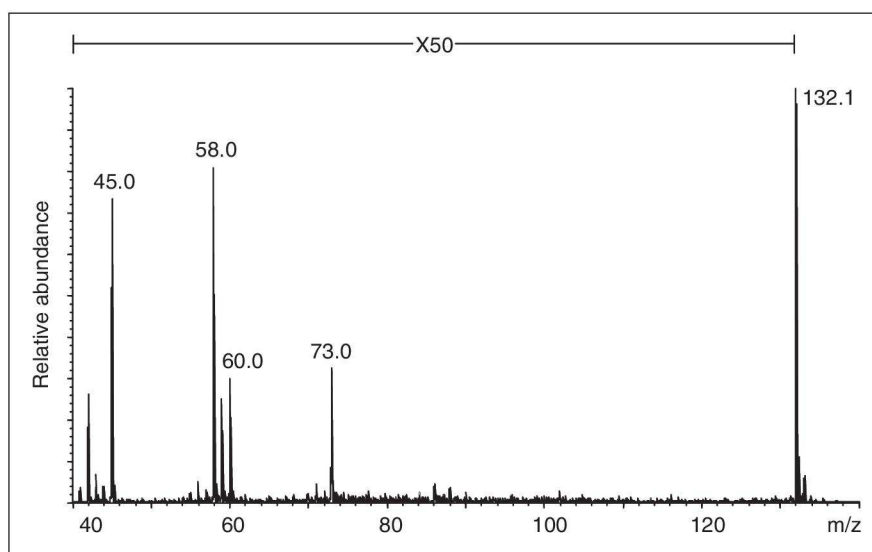


Figure 12. HE-CID spectrum in positive ion mode of the IL3 altered product at m/z 132 found after artificial alteration in the presence of 20% (w/w) ethyl methanesulphonate.

HE-CID: high energy collision induced dissociation; IL: ionic liquid.

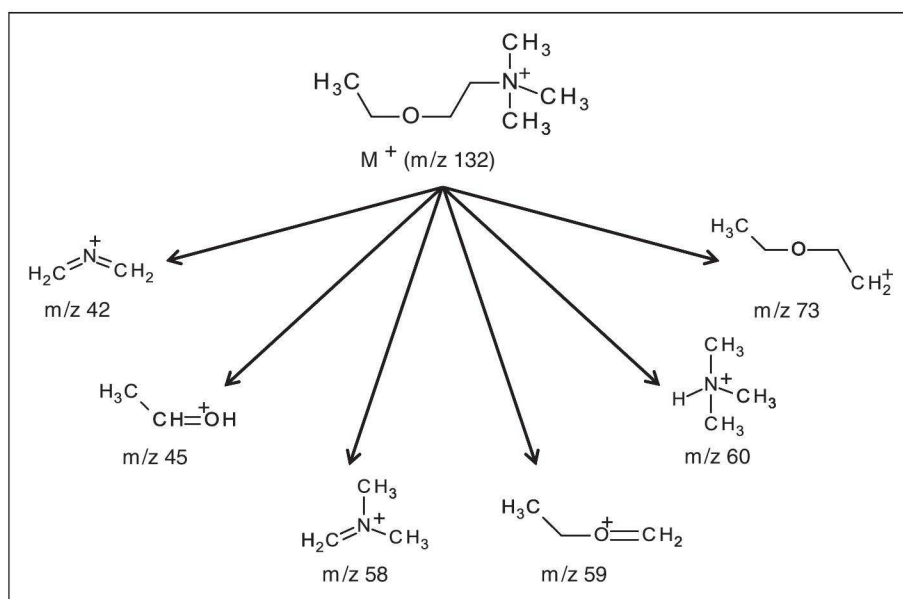


Figure 13. Suggested product ions from fragmentation of IL3 altered product at m/z 132 formed in the presence of 20% (w/w) ethyl methanesulphonate based on HE-CID product ions acquired.

IL: ionic liquid; HE-CID: high energy collision induced dissociation.

1000 mg/L, whereas IL1 with three butyl chains has a lower EC_{50} value of 370 mg/L equivalent to a higher cytotoxicity.

The classification of the studied compounds regarding their toxicity towards an aquatic environment with the crustacean *D. magna* showed for IL3 an LC_{50} value above 100 mg/L which is considered to be 'not harmful to aquatic organisms'. However, all other IL except IL4

revealed values between 10 and 100 mg/L leading to the classification as 'harmful to aquatic organisms'. For IL4, the LC_{50} value was lower than 10 mg/L but greater than 1 mg/L. Thus, IL4 is classified to be 'toxic to aquatic organisms'.⁴⁸

The results obtained and summarized in Table 6 are contrary to the above mentioned rule of thumb regarding side chain length and functionalization. Here, IL1

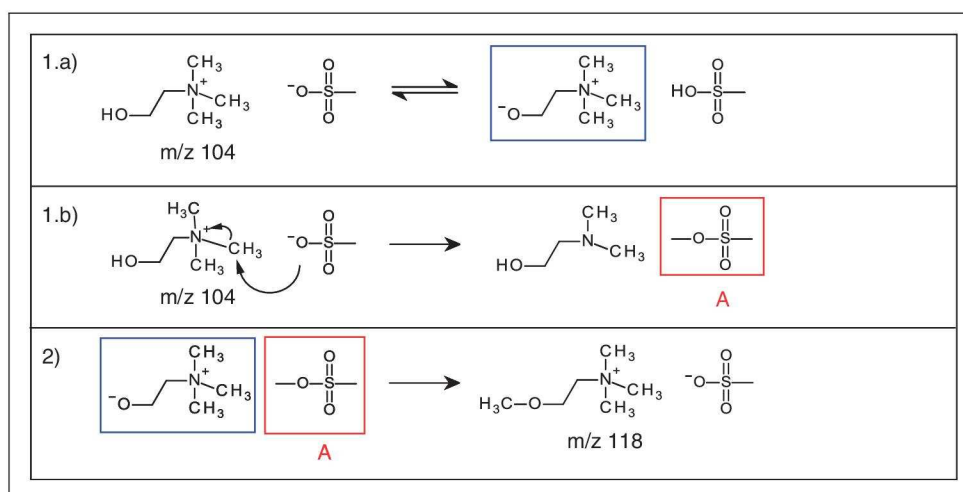


Figure 14. Anticipated degradation mechanism of IL3 is based on the identified degradation products by MS experiments. Possible reaction pathway is supported by the recovery of the IL3 anion as no other degradation species have been found. IL: ionic liquid; MS: mass spectrometry.

Table 6. Toxicity results of investigated ILs in different test systems.

IL	Acetylcholinesterase inhibition	Cytotoxicity IPC-81	Luminescence inhibition (<i>Vibrio fischeri</i>)	Reproduction inhibition (<i>Daphnia magna</i>)
	IC ₅₀ (mg/L) (95% confidence interval)	EC ₅₀ (mg/L) (95% confidence interval)		LC ₅₀ (mg/L) (95% confidence interval)
IL1	> 250	370(±30)	> 100 ¹	40–50
IL2	180(±25) ¹	> 1000 ¹	> 100 ¹	14 ¹
IL3	> 100 ¹	> 1000 ¹	> 100 ¹	> 100 ¹
IL4	> 100 ¹	> 1000 ¹	> 100 ¹	8 ¹
IL5	> 100 ¹	> 1000 ¹	> 100 ¹	15(±2) ¹
IL6	> 100 ¹	> 1000 ¹	> 100 ¹	19(±3) ¹

IL: ionic liquid.

Data from Stolte et al.⁴⁶

containing tributyl-methyl-ammonium cation showed a moderate effect and is less toxic than IL2 and IL4–IL6 which are all characterized by shorter and functionalized side chains. IL4 turned out as the most toxic compound of the investigated matrix showing an LC₅₀ value of only 8 mg/L. Only IL3 passes the above criteria in a positive sense. However, stability studies of this IL showed the formation of (2-methoxyethyl)-trimethyl-ammonium moiety during long-term thermo-oxidative stress. The identified structure corresponds to the cation in fresh IL4 which emerged to be ‘toxic to aquatic organisms’.

Biodegradation of selected IL

The biodegradation experiments were carried out only for IL containing the methanesulphonate anion since (CF₃SO₂)₂N[−] (IL6) is known to be not readily

biodegradable.⁴⁹ Based on the guideline that a substance is considered ‘readily biodegradable’ when biodegradation reaches a minimum of 60% within 28 days, IL4 did not pass this criterion as shown in our recent study⁴⁶ and hence IL5 containing the same cation was not investigated in detail in this study. The biodegradation results of IL1–IL3 based on manometric respirometry test according to OECD guideline 301F are presented in Table 7. Under the applied conditions, only IL3 is readily biodegradable (74%). This result is consistent to previous findings where a biodegradation rate of 89%⁴⁶ was found. However, the application of this IL in industrial processes and its specific degradation mechanism can lead to the formation of (2-methoxyethyl)-trimethyl-ammonium moiety (see IL4) which was shown to be ‘not readily biodegradable’. IL1 and IL2 showed almost no biodegradation

Table 7. Biodegradation results and classification of investigated IL according to OECD 301F (manometric respirometry).

IL	Biodegradation (%)	Classification
IL1	7	Not readily biodegradable
IL2	4	Not readily biodegradable
IL3	74	Readily biodegradable

IL: ionic liquid; OECD: Organization for Economic Co-operation and Development.

(7% and 4%, respectively). Therefore, they are classified as 'not readily biodegradable'. Contrary to these findings, an excellent biodegradation rate of 88% for IL2 has been previously published.⁴⁶ As the inoculum's cell density was the same (10^6 cells/mL), this difference maybe explained by the different origin of the waste water. This may result in a different composition of organisms and thus possibly explaining different abilities to degrade the selected compounds.

Joint interdisciplinary conclusion

Non-functionalized IL1 and IL2 ammonium cations with methanesulphonate anion perform stable under all selected artificial alteration conditions. Hence, they can be recommended for future IL lubricant designs from stability point of view. However, as demonstrated, they do not comply with environmental regulations as both are evaluated as harmful to aquatic organisms and not readily biodegradable. Nevertheless, in case of IL2 it was observed that under specific conditions of suitable waste water composition and specific environmental conditions it was readily biodegradable.

IL4–IL6 based on (2-methoxyethyl)-trimethyl-ammonium cation with three different counter anions were all prone to a low degree of degradation by the formation of (2-hydroxyethyl)-trimethyl-ammonium under all artificial alteration conditions. From the toxicity and biodegradability point of view, these IL are classified as harmful or even toxic to aquatic organisms and are not readily biodegradable. Hence, the IL structural approach based on methoxy group functionalization cannot be recommended in general for IL-based lubricants.

IL3 composed of (2-hydroxyethyl)-trimethyl-ammonium methanesulphonate has been evaluated as instable under the applied experimental conditions. Applying high resolution accurate MS, the altered product has been unambiguously identified as (2-methoxyethyl)-trimethyl-ammonium. Based on the degradation product quantification it can be concluded that the degradation mechanism takes place especially at higher temperatures over a longer period of time. No catalytic effect of copper has been observed. Water seems to suppress the

formation of this degradation product. However, as specially designed experiments revealed, once the intermediate product based on methyl methanesulphonate is formed the reaction takes place rapidly. The suggested degradation mechanism is based on transmethylation and requires the presence of nucleophilic species, as this is the case for the methanesulphonate anion. The occurrence of volatile degradation species as by-products, as proposed in IL3 degradation mechanism, and their detection will be the scope of future research. Contrary to the low stability of IL3, its assessment based on toxicity and biodegradability evaluation recommends this IL as non-toxic and readily biodegradable. Hence, the joint conclusion leads to recommendation of the (2-hydroxyethyl)-trimethyl-ammonium moiety for further structural IL lubricant design in particular in view of tribological performance.

This research study clearly showed that special care has to be taken with the selection of both cation and anion to maintain high thermo-oxidative stability as well as low toxicity and high biodegradability.

Funding

This study was funded within the FP7 program – Marie Curie Initial Training Network MINILUBES [216011-2] – by the European Commission. The LDI/MALDI-tandem MS was made available by a grant of the Vienna University of Technology (to G.A.). This study was also funded by the Austrian COMET-program [824187], ERDF and by the province of Lower Austria (Onlab project) and has been partly carried out within the 'Excellence Centre of Tribology'. This research was also supported by the Polish Ministry of Research and Higher Education under grants (NN204 527139) and (DS 8200-4-0085-1).

Acknowledgements

The author acknowledge Dr Andjelka Ristic from Austrian Centre of Competence for Tribology (Wiener Neustadt, Austria) for providing technical support with operation of UHPLC-ESI-LTQ-orbitrap-MS instrument and Professor Ichiro Minami from Iwate University, Department of Chemistry and Bioengineering (Iwate, Japan), for constructive discussions of IL chemistry.

References

1. Endres F and Zein El Abedin S. Air and water stable ionic liquids in physical chemistry. *Phys Chem Chem Phys* 2006; 8: 2101–2116.
2. Zhou F, Liang Y and Liu W. Ionic liquid lubricants: designed chemistry for engineering applications. *Chem Soc Rev* 2009; 38: 2590–2599.
3. Zhang Z, Yang L, Luo S, et al. Ionic liquids based on aliphatic tetraalkylammonium dications and TFSI anion as potential electrolytes. *J Power Sources* 2007; 167: 217–222.

- Minami I. Ionic liquids in tribology. *Molecules* 2009; 14: 2286–2305.
- Bermudez MD, Jimenez AE, Sanes J, et al. Ionic liquids as advanced lubricant fluids. *Molecules* 2009; 14: 2888–2908.
- Predel T, Pohrer B and Schlücker E. Ionic liquids as alternative lubricants for special applications. *Chem Eng Technol* 2010; 33: 132–136.
- European Commission. REACH homepage of the European Commission, http://ec.europa.eu/environment/chemicals/reach/reach_intro.htm (2011, accessed October 2011).
- Stock F, Hoffmann J, Ranke J, et al. Effects of ionic liquids on the acetylcholinesterase: a structure-activity relationship consideration. *Green Chem* 2004; 6: 286–290.
- Ranke J, Molter K, Stock F, et al. Biological effects of imidazolium ionic liquids with varying chain lengths in acute *Vibrio fischeri* and WST-1 cell viability assays. *Ecotoxicol Environ Saf* 2004; 58: 396–404.
- Stepnowski P, Skladanowski AC, Ludwiczak A, et al. Evaluating the cytotoxicity of ionic liquids using human cell line HeLa. *Hum Exp Toxicol* 2004; 23: 513–517.
- Wang X, Ohlin CA, Lu Q, et al. Cytotoxicity of ionic liquids and precursor compounds towards human cell line HeLa. *Green Chem* 2007; 9: 1191–1197.
- Docherty KM and Kulpa Jr CF. Toxicity and antimicrobial activity of imidazolium and pyridinium ionic liquids. *Green Chem* 2005; 7: 185–189.
- Pernak J, Sobaszekiewicz K and Mirska I. Anti-microbial activities of ionic liquids. *Green Chem* 2003; 5: 52–56.
- Petkovic M, Ferguson J, Bohn A, et al. Exploring fungal activity in the presence of ionic liquids. *Green Chem* 2009; 11: 889–894.
- Latała A, Stepnowski P, Nedzi M, et al. Marine toxicity assessment of imidazolium ionic liquids: acute effects on the Baltic algae *Oocystis submarina* and *Cyclotella meneghiniana*. *Aquat Toxicol* 2005; 73: 91–98.
- Latała A, Nedzi M and Stepnowski P. Toxicity of imidazolium and pyridinium based ionic liquids towards algae. *Bacillaria paxillifer* (a microphytobenthic diatom) and *Geitlerinema amphibium* (a microphytobenthic blue green alga). *Green Chem* 2009; 11: 1371–1376.
- Matzke M, Stolte S, Thiele K, et al. The influence of anion species on the toxicity of 1-alkyl-3-methylimidazolium ionic liquids observed in an (eco)toxicological test battery. *Green Chem* 2007; 9: 1198–1207.
- Stolte S, Matzke M, Arning J, et al. Effects of different head groups and functionalised side chains on the aquatic toxicity of ionic liquids. *Green Chem* 2007; 9: 1170–1179.
- Bernot RJ, Brueske MA, Evans-White MA, et al. Acute and chronic toxicity of imidazolium-based ionic liquids on *Daphnia magna*. *Environ Toxicol Chem* 2005; 24: 87–92.
- Stolte S, Arning J, Bottin-Weber U, et al. Effects of different head groups and functionalised side chains on the cytotoxicity of ionic liquids. *Green Chem* 2007; 9: 760–767.
- Stolte S, Arning J, Bottin-Weber U, et al. Anion effects on the cytotoxicity of ionic liquids. *Green Chem* 2006; 8: 621–629.
- Hao W, Sanjay VM and Arokiasamy JF. Toxicity of various anions associated with methoxyethyl methyl imidazolium-based ionic liquids on *Clostridium* sp. *Chemosphere* 2011; 82: 1597–1603.
- Docherty KM, Joyce MV, Kulacki KJ, et al. Microbial biodegradation and metabolite toxicity of three pyridinium-based cation ionic liquids. *Green Chem* 2010; 12: 701–712.
- Pham TPT, Cho CW, Jeon CO, et al. Identification of metabolites involved in the biodegradation of the ionic liquid 1-butyl-3-methylpyridinium bromide by activated sludge microorganisms. *Environ Sci Technol* 2009; 43: 516–521.
- Stolte S, Abdulkarim S, Arning J, et al. Primary biodegradation of ionic liquid cations, identification of degradation products of 1-methyl-3-octylimidazolium chloride and electrochemical wastewater treatment of poorly biodegradable compounds. *Green Chem* 2008; 10: 214–224.
- Petkovic M, Ferguson JL, Gunaratne HQN, et al. Novel biocompatible cholinium-based ionic liquids: toxicity and biodegradability. *Green Chem* 2010; 12: 643–649.
- Pisarova L, Gabler C, Dörr N, et al. Thermo-oxidative stability and corrosion properties of ammonium based ionic liquids. *Tribol Int* 2012; 46: 73–83.
- Sowniah S, Srinivasadesikan V, Tseng MC, et al. On the chemical stabilities of ionic liquids. *Molecules* 2009; 14: 3780–3813.
- Muhammad N, Man ZB, Bustam MA, et al. Synthesis and thermophysical properties of low viscosity amino acid-based ionic liquids. *J Chem Eng Data* 2011; 56: 3157–3162.
- Heym F, Etzold BJM, Kern C, et al. Analysis of evaporation and thermal decomposition of ionic liquids by thermogravimetric analysis at ambient pressure and high vacuum. *Green Chem* 2011; 13: 1453–1466.
- Seeberger A, Andresen AK and Jess A. Prediction of long-term stability of ionic liquids at elevated temperatures by means of non-isothermal thermogravimetric analysis. *Phys Chem Chem Phys* 2009; 11: 9375–9381.
- Arellano IHJ, Guarino JG, Paredes FU, et al. Thermal stability and moisture uptake of 1-alkyl-3-methylimidazolium bromide. *J Therm Anal Calorim* 2010; 2: 725–730.
- Wooster TJ, Johanson KM, Fraser KJ, et al. Thermal degradation of cyano containing ionic liquids. *Green Chem* 2006; 8: 691–696.
- Minami I, Kamimura H and Mori S. Thermo-oxidative stability of ionic liquids as lubricating fluids. *J Synth Lubr* 2007; 24: 135–147.
- Ohtani H, Ishimura S and Kumai M. Thermal decomposition behaviors of imidazolium-type ionic liquids studied by pyrolysis-gas chromatography. *Anal Sci* 2008; 24: 1335–1340.
- Hao Y, Peng J, Hu S, et al. Thermal decomposition of allyl-imidazolium based ionic liquid studied by TGA-MS analysis and DFT calculations. *Thermochim Acta* 2010; 501: 78–83.
- Bösmann A, Schulz PS and Wassercheid P. Enhancing task specific ionic liquid's thermal stability by structural modification. *Monatsh Chem* 2007; 138: 1159–1161.

38. Meine N, Benedito F and Rinaldi R. Thermal stability of ionic liquids assessed by potentiometric titration. *Green Chem* 2010; 12: 1711–1714.
39. Lacaze N, Gombaudo-Saintonge G and Lanotte M. Conditions controlling long-term proliferation of Brown Norway rat promyelocytic leukemia in vitro: primary growth stimulation by microenvironment and establishment of an autonomous Brown Norway 'leukemic stem cell line. *Leuk Res* 1983; 7: 145–154.
40. DIN 38412-L34:1991. Luminescence inhibition assay with *Vibrio fischeri*. Bestimmung der Hemmwirkung von Flüssigkeitsproben auf die Lichtemission von *Vibrio fischeri*.
41. Organisation for Economic Cooperation and Development OECD. *OECD guideline for testing chemicals: 202 Daphnia sp. acute immobilisation test*. Paris, France: OECD, 2004, pp.1–14.
42. Daphtoxkit F magna – MicroBioTest Inc. *Crustacean toxicity screening test for freshwater*. Standard operational procedure, 1996, pp.1–27. Gent, Belgium: Daphtoxkit F magna – MicroBioTest Inc.
43. R Development Core Team. *R: a language and environment for statistical computing*. Vienna, Austria: R Foundation for Statistical Computing, 2011. <http://www.R-project.org/>.
44. OECD. *OECD 301F*. Adopted by the Council on 17th July 1992; Ready, 2006. Paris, France: OECD.
45. Wasserscheid P, van Hal R and Bösmann A. 1-n-Butyl-3-methylimidazolium (bmim) octylsulfate—an even 'greener' ionic liquid. *Green Chem* 2002; 4: 400–404.
46. Stolte S, Steudte S, Areitioaurtena O, et al. Development of ionic liquids used as lubricants or lubrication additives-ecotoxicity and biodegradability assessment. *Green Chem*. Submitted 26th October 2011.
47. Garcia MT, Gathergood N and Scammells PJ. Biodegradable ionic liquids part II: effect of the anion and toxicology. *Green Chem* 2005; 7: 9–14.
48. European Commission. *COMMISSION DECISION of 24 June 2011 on establishing the ecological criteria for the award of the EU Ecolabel to lubricants*. 2011. Brussels, Belgium: European Commission.
49. Wells AS and Coombe VT. On the freshwater ecotoxicity and biodegradation properties of some common ionic liquids. *Org Process Res Dev* 2006; 10: 794–798.

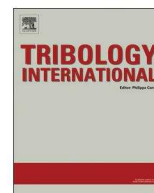
6.3. Insight into degradation of ammonium-based ionic liquids and comparison of tribological performance between selected intact and altered ionic liquid

Tribology International 2013; <http://dx.doi.org/10.1016/j.triboint.2013.02.020> (In Press)



Contents lists available at SciVerse ScienceDirect

Tribology International

journal homepage: www.elsevier.com/locate/triboint

Insight into degradation of ammonium-based ionic liquids and comparison of tribological performance between selected intact and altered ionic liquid

Lucia Pizarova^{a,b,*}, Vladimir Totolin^a, Christoph Gabler^{a,b}, Nicole Dörr^a, Ernst Pittenauer^b, Günter Allmaier^b, Ichiro Minami^c

^a Austrian Centre of Competence for Tribology – AC²T research GmbH, Wiener Neustadt, Austria

^b Institute of Chemical Technologies and Analytics, Vienna University of Technology, Vienna, Austria

^c Department of Chemical Engineering, Iwate University, Iwate, Japan

ARTICLE INFO

Article history:

Received 15 August 2012

Received in revised form

7 February 2013

Accepted 15 February 2013

Keywords:

Ionic liquids

Degradation

Mass spectrometry

Tribological properties

ABSTRACT

Due to lack of experimental work clearly describing ionic liquids (ILs) degradation which could take place under application conditions, specially designed artificial alteration experiments were performed to derive degradation mechanisms most probably taking place under long-term thermo-oxidative stress. The use of mass spectrometry enabled identification of IL degradation products both in liquid and gas phases. The mechanisms of intermolecular transmethylation in ammonium ILs proceeding via anion-derived intermediates have been identified. Hence, care has to be taken for applying ILs in processes, e.g. in lubrication applications, as it is shown that IL altered products can negatively influence friction and wear performance as well as can lead to build-up of vapour pressure in otherwise non-volatile ILs.

© 2013 Elsevier Ltd. All rights reserved.

1. Introduction

Ionic liquids (ILs) have become recognized as promising novel lubricants often outperforming conventional lubricants especially due to their tunable properties, ability to significantly lower friction as well as wear and to effectively dissipate heat under tribological contact [1–9]. They are under consideration and in several cases already in use for applications varying from operating fluids in pumps, compressors, as lubricants in aerospace applications and in nanotechnology, etc. [10–13].

As we just start to understand the structure–property relationships in ILs, these are being deliberately structurally modified with the aim to improve their properties. Lately, an extensive review has been published solely dedicated to the ether and alcohol functionalized ILs discussing their properties and attractive applications [14]. Thus, vinyl and polar functional groups were recently being implemented into IL side chains and investigated for their use as lubricants [15–17]. The above mentioned structural designs, implementing polar functional groups, are in line with IL structural recommendations from research groups studying IL (eco)toxicity and biodegradability [18–20]. Furthermore, non-aromatic IL cation moieties are recommended over the aromatic ones and also the need to replace halogenated IL anions has been disclosed [21–25].

High temperature stability is often reported for ILs, however in the most cases it is assessed by means of thermogravimetric analysis (TGA) applying high heating rates in short time [26–28]. As previously reported, such approach can only serve for relative ILs comparison and cannot be related to IL long-term stability [29,30]. By comparing obtained decomposition temperatures from TGA experiments and also from the vessel scale degradation experiments, such as RPVOT (rotating pressure vessel oxidation test), it was observed that IL stability strongly depends on its anion moiety [26,31–33]. However, IL degradation was in the most cases assessed visually by stating the IL coloration. Just in rare cases where TGA was coupled to detection techniques such as mass spectrometry (MS) or by approach of pyrolysis followed by gas chromatography coupled to electron impact (EI) mass spectrometry (GC–MS), it was possible to detect IL decomposition products [34–36]. Based on the identified products mainly from ILs with halides or halogenated anions, reactions mostly occurring as dealkylation of the cation side chains were proposed. Some studies already described the non-inertness of ILs in which elimination reactions can occur leading to volatile degradation products [37–39]. In our recent experimental study we have concluded that also non-halogenated anion can induce such reactions and can initiate another degradation mechanism depending on the cation moiety [40]. The importance of IL long-term degradation studies due to slow degradation rates has been also highlighted with the emphasis that some reactions do not lead to mass loss and hence are not detected by TGA technique [40,41].

In previous studies we have focused on elucidating the ammonium-based IL degradation products present in the liquid

* Correspondence to: AC²T research GmbH, Austrian Centre of Competence for Tribology, Viktor Kaplan Strasse 2, 2700 Wiener Neustadt, Austria.
Tel.: +43 2622 81600 352.

E-mail address: pizarova@ac2t.at (L. Pizarova).

phase after long-term thermo-oxidative stress [40,42]. In order to complete the evaluation of these ILs stabilities, an approach by means of stable isotopic tracers to track any chemical changes on the molecular level in order to bring unambiguous evidence of the degradation mechanism was selected. After small-scale artificial alteration experiments the presence of degraded species has been investigated by direct infusion of diluted sample aliquots into an electrospray ionization linear quadrupole ion trap orbitrap mass spectrometer (ESI-LTQ-orbitrap-MS).

Furthermore, we focus not just on identification of primary volatile degradation products described in the literature [43–45], but our aim was to elucidate all further major compounds present in the gas phase after long-term thermo-oxidative stress. Such information is essential in order to apply ILs in industrial applications as generated degradation products can alter their (i.e. intact ILs) physico-chemical properties and even cause a build-up of pressure in otherwise non-volatile ILs [46,47]. The volatile degradation species evolved during long-term thermo-oxidative stress were analysed by means of a headspace-cold trap GC-MS approach.

Tribological investigations of selected intact IL and the IL representing its main degradation product, have been performed in order to understand how the performance will be affected when used as lubricants. Therefore, the neat ILs have been evaluated at two different temperatures on steel–steel contacts using an Schwing–Reib–Verschleiss (SRV) tribometer. Friction and wear have been determined and the surfaces were analysed by white light confocal microscopy and X-ray photoelectron spectroscopy (XPS).

2. Experimental

2.1. Investigated compounds

Ionic liquids IL1 to IL6 used in this research work are all based on quaternary ammonium cations, with and without side chain

functionalization, and are combined either with hydrophilic methanesulphonate or hydrophobic bis(trifluoromethylsulfonyl)imide anions. Studied ILs were obtained from IoLiTec (Ionic Liquids Technologies, Heilbronn, Germany). Furthermore, chloride based compound with deuterated (2-hydroxyethyl)-(trimethyl- D_9) ammonium cation, equivalent to non-deuterated IL1 and IL2 cation moiety, was obtained from CIL (Cambridge Isotope Laboratories, Andover, Massachusetts, USA). All compounds together with their cation and anion monoisotopic masses as well as purities as obtained by the suppliers are summarized in Table 1.

2.2. Artificial alteration experiments

In order to gain knowledge about ILs long-term stability, small-scale artificial alteration experiments were performed under thermo-oxidative stress. In order to detect chemical changes on the molecular level during IL degradation, a mixture of methanesulphonate based IL1 and its deuterated cation analogue based on chloride anion was prepared as 4:1 ratio (w/w) mixture. A mixture of 1 g in total was prepared in a 6 mL headspace glass vial sealed by crimping with silicone-PTFE septa, both from Chromacol (Herts, UK) and subjected to 190 °C in a laboratory oven for the duration of 7 days. Analogously, in order to maintain volatile species evolved during IL alteration, temperature of 150 °C was applied for the duration of 7 days. Headspace volume in this experimental set up was increased by use of 10 mL headspace glass vials which were sealed containing 200 mg of IL in presence of air and closed by crimping with ultraclean and high temperature stable silicone-PTFE septa, both from Chromacol (Herts, UK). Under these conditions, the total average mass loss of 10 parallel experiments with IL5 was 5 mg after 7 days at 150 °C, which proved the tightness of the used experimental set-up.

Table 1
Summary of the investigated compounds together with their monoisotopic masses and purity as obtained from the suppliers.

IL Name	Cation	Monoisotopic mass (Da)	Anion	Monoisotopic mass (Da)	Purity
– (2-Hydroxyethyl)-(trimethyl- D_9)-ammonium chloride		113.16403	Cl^-	34.96885	98%
IL1 (2-Hydroxyethyl)-trimethyl-ammonium methanesulphonate		104.10754		94.98029	98% < 100 ppm halides
IL2 (2-Hydroxyethyl)-trimethyl-ammonium bis(trifluoromethylsulphonyl)imide		104.10754		279.91730	99% < 100 ppm halides
IL3 (2-Methoxyethyl)-trimethyl-ammonium methanesulphonate		118.12319		94.98029	98% < 100 ppm halides
IL4 (2-Methoxyethyl)-trimethyl-ammonium bis(trifluoromethylsulphonyl)imide		118.12319		279.91730	99% < 1000 ppm halides
IL5 Tributyl-methyl-ammonium methanesulphonate		200.23728		94.98029	98% < 500 ppm halides
IL6 Tributyl-methyl-ammonium bis(trifluoromethylsulphonyl)imide		200.23728		279.91730	99% < 100 ppm halides

2.3. Applied analytical techniques for IL alteration studies

2.3.1. Elucidation of IL1 degradation mechanisms

Aliquot of IL1 mixture with its chloride analogue after thermo-oxidative stress has been diluted in methanol ($\geq 99.9\%$, Chromasolv grade), supplied from Sigma-Aldrich (Vienna, Austria), to a final concentration at 100 ppm level. The obtained diluted sample was analyzed by direct infusion electrospray ionisation (ESI) in an IonMax API ion source with the ESI probe coupled to LTQ orbitrap XL hybrid tandem MS (ThermoScientific, Bremen, Germany). Measurements were carried out solely in positive ion mode with the experimental conditions applied as follows: spray voltage of 4 kV, capillary voltage of 38 V, all other voltages optimized for maximum molecular ion transmission, nitrogen sheath gas with a flow rate of 10 units (no conversion in SI units is provided by the manufacturer) and the transfer capillary temperature at 275 °C. Full scan high resolution mass spectra ($R=30,000$ FWHM at m/z 400) were collected at a selected m/z range of 50 to 500 with a maximum injection time of 200 ms. For further structural elucidation, low energy-CID (MS/MS) experiments were performed on selected precursor ions with parameters as follows: isolation and activation width of 2 Da, activation time of 30 ms, normalized collision energy optimized from 30 to 50% (100% equals approximately 5 eV according to the manufacturer) and helium (He) as collision gas. For data acquisition and data processing, Xcalibur v2.0 software was used.

2.3.2. Analysis of volatile degradation species

The qualitative information of the present gaseous degradation products after thermo-oxidative treatment was obtained by instrumental set up of the TriPlus headspace (HS) autosampler followed by internal Cold Trap 915 (CT) and Trace GC Ultra capillary gas chromatograph coupled to TSQ Quantum XLS mass spectrometer (GC-MS), all from ThermoScientific (Austin, Texas, USA). After the artificial alteration experiments, each headspace vial was transferred to the HS oven and incubated for additional 30 min at 150 °C while agitated each 20 s in 5 s intervals to enhance the equilibrium state between liquid and gas phase. Afterwards, 100 μ L of the headspace volume was sampled by a gas tight HS syringe heated to 130 °C and injected into a programmable temperature vaporization injector (PTV) operated in constant temperature mode at 200 °C and in splitless mode for 2 min. Sample carry over was avoided by flushing of the HS syringe after each injection with He gas for 30 s. The sample was subsequently cryo-focused with liquid nitrogen at -150 °C with 2 min hold time and transferred to the column by thermal desorption at 30 °C/s rate until 200 °C with 1 min hold time. Chromatographic separation was performed with He as carrier gas at 2 mL/min constant flow using ZB-5 Phenomenex (5%-phenyl-95%-dimethylpolysiloxane phase) capillary column of 60 m length, 0.32 mm I.D. and 0.25 μ m film thickness. The GC temperature program was set to 40 °C initial temperature for 4 min hold time followed by 10 °C/min temperature ramp until 250 °C with 10 min hold time. The transfer line was kept at 250 °C and the effluent was ionized by EI (70 eV) with source temperature at 200 °C while the mass analyzer operated in the scan mode between m/z 10 to 300. For data acquisition and data processing, Xcalibur v2.0 software was used.

2.4. Tribological investigation

Tribological properties of selected intact IL1 and IL3 related to the main degradation product of IL1, as elucidated by our previous research work [40], were compared in 100Cr6 (AISI52100) steel-steel contacts at 100 and 150 °C under

Table 2

Overview of the tribometrical conditions applied under oscillating reciprocating motion on steel-steel contact for selected ILs performance comparison.

Parameters	Applied load (N)	100	
	Hertz contact stress (GPa)	1.46	
	Hertz deformation indentation (μ m)	4.37	
	Frequency (Hz)	50	
	Stroke (mm)	1	
	Temperature (°C)	100 and 150	
	Duration (min)	60	
Specimens	Fluid quantity (mL)	~ 0.05 (1 drop)	
	Ball	Material	100Cr6
		Diameter (mm)	10
		Hardness (HRC)	60
		Surface roughness R_a (μ m)	0.025
	Disc	Material	100Cr6
		Size (mm)	$\varnothing 24 \times 7.9$
Surface roughness R_z (μ m)		0.45–0.65	

atmospheric conditions. An SRV tribometer (Optimol Instruments Prüftechnik, Munich, Germany) with ball-on-disc configuration in oscillating reciprocating motion was employed these ILs. The details of the tribometrical conditions are listed in Table 2. Fresh metal specimens were used for each lubricant and experiment. The specimens were washed in three different solvents (toluene, isopropanol and petroleum ether) for ten minutes each, using an ultrasonic bath, before and after the experiment. Friction coefficients were continuously recorded over time and each experiment was performed twice. Average friction coefficients were calculated for each experiment after a run-in period of 10 min. Exceptions from this general procedure are discussed in Section 3.4.

2.5. Surface analyses

White light confocal microscope μ ^{SURF} (NanoFocus, Oberhausen, Germany) was used to evaluate surface topographies. The obtained topographic data were used for calculation of average ball wear scar diameters (length and width) and average ball and disc wear volumes, using a wear volume calculation tool developed at AC²T research GmbH [48].

XPS analyses were conducted using a Thermo Fisher Scientific Theta Probe (East Grinstead, UK) with a monochromatic Al K_{α} X-ray source ($h\nu=1486.6$ eV) and a hemispherical analyzer. The measurements were performed at a base pressure of 2×10^{-9} mbar. The elemental and chemical composition of the wear track surfaces was obtained by spot analysis with an X-ray beam with a diameter of 400 μ m at a pass energy of 200 eV for the survey spectra and 50 eV for the detail spectra.

Depth profiles were acquired from each tribolayer by sputtering an area of 2×2 mm² of the wear tracks with Ar⁺ ions at an acceleration voltage of 3 kV and a sputter current of 1 μ A. From these parameters, an approximate sputter yield of 0.05 nm/s was calculated. After each sputter level, snap shot spectra at a pass energy of 150 eV of the elements C, Fe, S, and O were obtained. The spectra were analyzed with the Advantage Data System software version 4.75 (Thermo Fisher Scientific, East Grinstead, UK), using Gaussian-Lorentzian peak fitting.

3. Results and discussion

3.1. IL1 degradation mechanism elucidation

Investigating the degradation mechanism of IL1 suggested to be based on transmethylation via methyl methanesulphonate as

intermediate product [40], the aim is now to unambiguously detect that a former step of demethylation is taking place in the IL cation by using deuterated IL1 cation analogue. This is now possible by use of accurate mass spectrometry at high resolution due to difference in m/z corresponding to methyl-chain versus deuterated methyl- D_3 chain enabling disclosure of elemental composition.

Hence, diluted sample aliquots of the mixture consisting of IL1 and its deuterated chloride based analogue (as described in Section 2.2.), sampled on the 1st and 7th day from artificial alteration process at 190 °C, were analysed by ESI-LTQ-orbitrap-MS as described in Section 2.3.1 and their corresponding mass spectra are shown in Fig. 1.

In the positive ion ESI mass spectra obtained, not only the intact cations of (2-hydroxyethyl)-trimethyl-ammonium (IL1) at m/z 104.10653, but m/z 104 throughout the paper, and (2-hydroxyethyl)-(trimethyl- D_3)-ammonium at m/z 113 of its deuterated analogue were present, but unexpectedly also high signal intensity of m/z 107 and 110 were detected. Based on the obtained accurate m/z values ($\Delta m=0.001$) enabling elucidation of their elemental composition and on the analysed MS/MS data presented in Fig. 2, these structures were elucidated as singly (m/z 107) and doubly (m/z 110) D_3 -methylated species of the former IL1 cation (m/z 104). This gives clear evidence for a cross-methylation taking place between the cation moieties present and it is suggested that it is initiated via anion-derived intermediates.

Furthermore, clear signal intensities at m/z 118, 121, 124, 127, 130 were detected. As the IL1 degradation proceeds through methylation of its cation functionalized hydroxyl chain, the ion at m/z 118 is assigned to (2-methoxyethyl)trimethyl ammonium moiety. In analogy, the ion at m/z 130 shall correspond to fully D_3 -methylated moiety of the former deuterated cation of m/z 113 and this is supported by its elemental composition. The structures of ions at m/z 121, 124 and 127 – which could represent either methylated or D_3 -methylated cations with the same elemental composition – were elucidated by fragmentation together with

ions at m/z 118 and 130, in order to obtain their product ions which are shown in Fig. 3.

By studying the obtained product ions, it was possible to confirm that they originate from both feasible structural variations of ions at m/z 121, 124, 127 and their elucidated fragmentation pathways are summarized in Fig. 4.

These findings are another evidence of further methyl group rearrangements suggested to be based on the reaction of the anion-derived intermediates with the cation hydroxyl group. As the methyl chloride is highly volatile, hence lost, it can be concluded that methyl methanesulphonate plays a more significant role as intermediate in the formation of (2-methoxyethyl)-trimethyl-ammonium moieties.

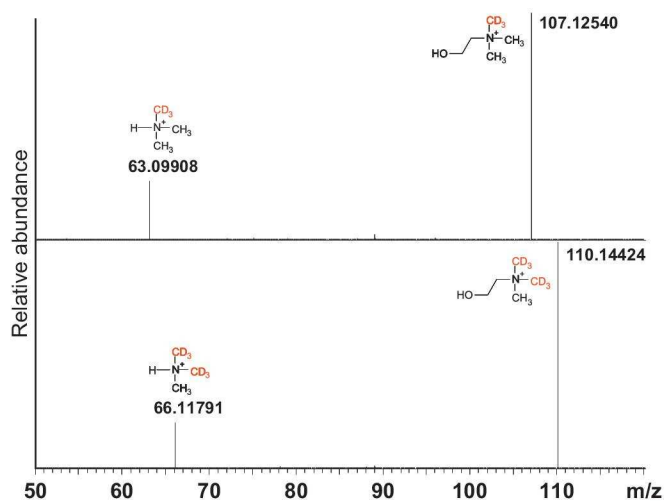


Fig. 2. Low energy CID (MS/MS) spectra of degradation products detected at m/z 107 and 110, leading to structural elucidation of retro-alkylated IL1 cation with one or two methyl- D_3 groups.

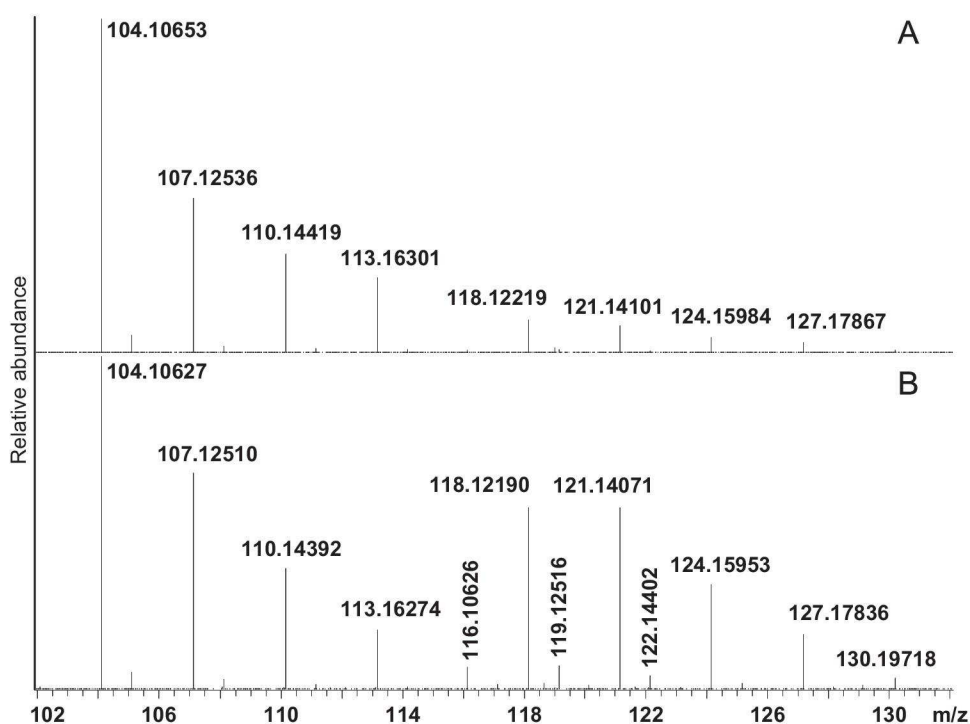


Fig. 1. ESI-LTQ-orbitrap-mass spectra of 4:1 (w/w) mixture consisting of IL1 and its chloride based deuterated analogue, measured after 1st day (A) and 7th day (B) at 190 °C.

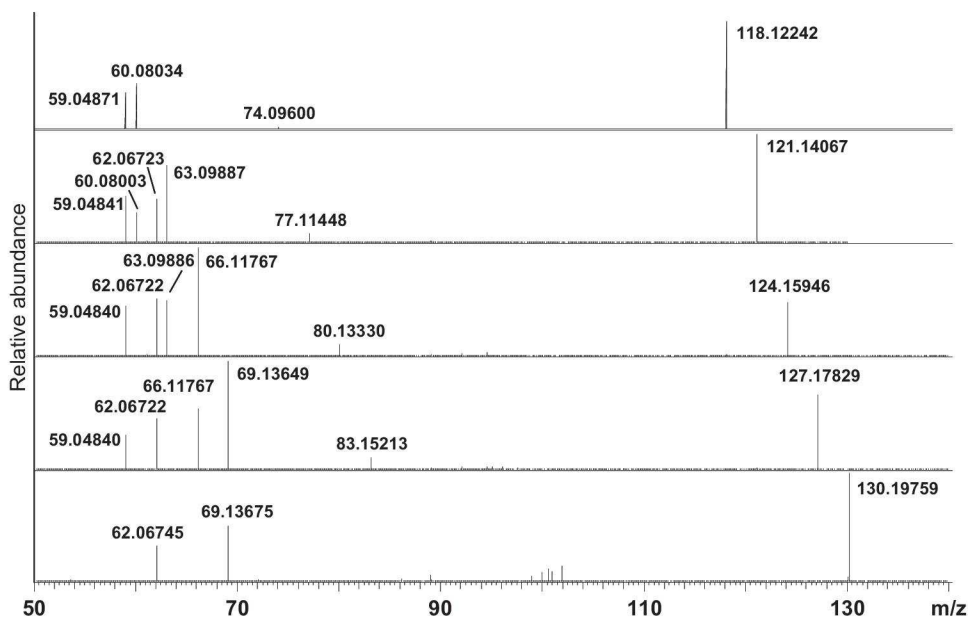


Fig. 3. Low energy CID (MS/MS) spectra of degradation products detected at m/z 118, 121, 124, 127 and 130 with their corresponding product ions as obtained by ESI-LTQ-orbitrap-MS analysis.

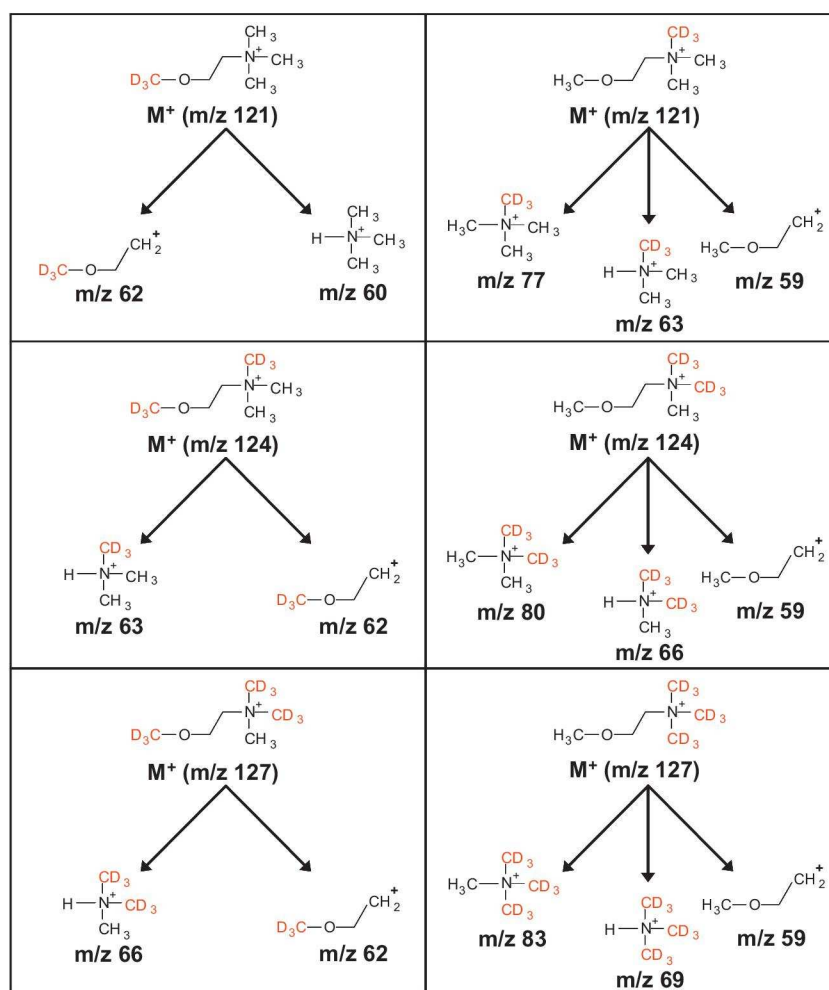


Fig. 4. Elucidated fragmentation pathways of degradation products detected at m/z 121, 124 and 127, confirming the presence of both feasible degradation product species for each selected mass. The ions at m/z 118 and 130 shown in Fig. 3 refer to purely non-deuterated and fully D_3 -methylated species, respectively, hence have unambiguous chemical structures.

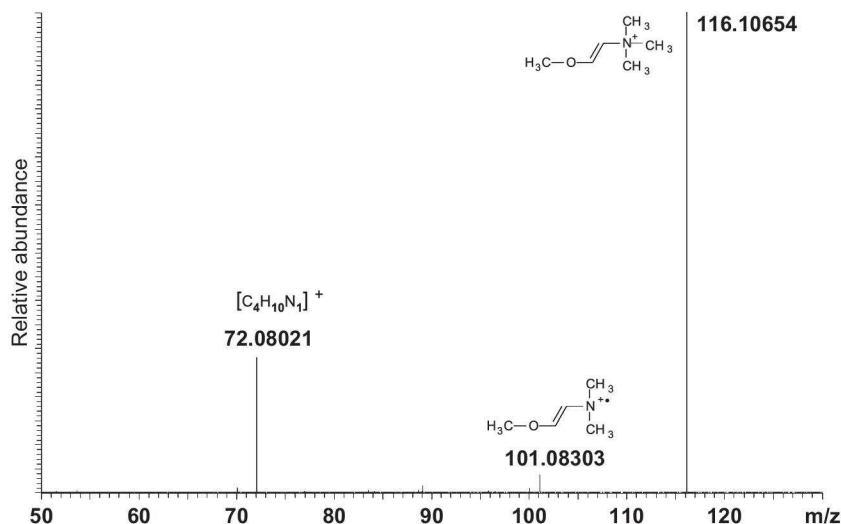


Fig. 5. Low energy CID (MS/MS) spectrum of degradation product at m/z 116 suggested to be a secondary degradation product of primary degradation product of (2-methoxyethyl)-trimethyl-ammonium moiety, as based on the elucidated product ions.

Table 3
Summary of degradation species formed in the mixture of IL1 and its deuterated chloride based analogue after 7 days of thermo-oxidative stress at 190 °C as identified by ESI-LTQ-orbitrap-MS. The further D_3 -methylated analogues of 122 m/z have not been detected.

Monoisotopic mass (Da)	Elemental composition	Structure	Monoisotopic mass (Da)	Elemental composition	Structure	Monoisotopic mass (Da)	Elemental composition	Structure
104.10754	$C_5H_{14}NO$		118.12319	$C_6H_{16}NO$		121.14201	$C_6D_3H_{13}NO$	
107.12636	$C_5D_3H_{11}NO$		121.14201	$C_6D_3H_{13}NO$		124.16084	$C_6D_6H_{10}NO$	
110.14519	$C_5D_6H_8NO$		124.16084	$C_6D_6H_{10}NO$		127.17968	$C_6D_9H_7NO$	
113.16403	$C_5D_9H_5NO$		127.17968	$C_6D_9H_7NO$		130.19850	$C_6D_{12}H_4NO$	
116.10753	$C_6H_{14}NO$		119.12636	$C_6D_3H_{11}NO$		122.14519	$C_6D_6H_8NO$	

Additionally to the above described degradation species, ions of low signal intensities corresponding to ions at m/z 116, 119 and 122 were detected only after the 7th day at 190 °C. Based on performed MS/MS analyses and with the knowledge of the ion elemental composition, the suggested structure of the detected m/z 116 ion can represent a secondary degradation product of (2-methoxyethyl)-trimethyl-ammonium cation as shown in Fig. 5.

Correspondingly, ions at m/z 119 and 122, can represent degradation products of species with m/z 121 and 124, all produced by hydrogen elimination. No degradation species of m/z 127 and 130 have been detected. All elucidated degradation species present after artificial alteration after 7 days at 190 °C are summarized in Table 3.

3.1.1. Degradation products of IL1 impurities

In the obtained IL1 used for artificial alteration experiments, the presence of two impurities with longer hydroxyl

functionalized chains was detected. These impurities represent $[HO-CH_2-O-C_2H_4-N(CH_3)_3]^+$ and $[HO-C_2H_4-O-C_2H_4-N(CH_3)_3]^+$ as elucidated from the obtained product ions and presented in Fig. 6. This additional species with longer hydroxyl functionalized chains were investigated in order to verify if they follow the same degradation mechanisms as the IL1 cation.

After artificial alteration at 190 °C of the above described mixture of IL1 and its chloride based deuterated analogue, species with common mass difference of 3 Da, corresponding to replacement of CH_3 by CD_3 group, were detected in the mass spectrum obtained after 1 day as shown in Fig. 7.

This resembles the degradation products of IL1 cation. Due to low signal intensities of newly found ions at m/z 137, 140 and 151, 154, 157 and 162, 165, 168 series, their low energy CID (MS/MS) fragmentations could not be successfully carried out. Hence, the nature of this species is based solely on their high accurate m/z values and hence their derived elemental composition, while taking into account the possible analogy with IL1 cation reactions

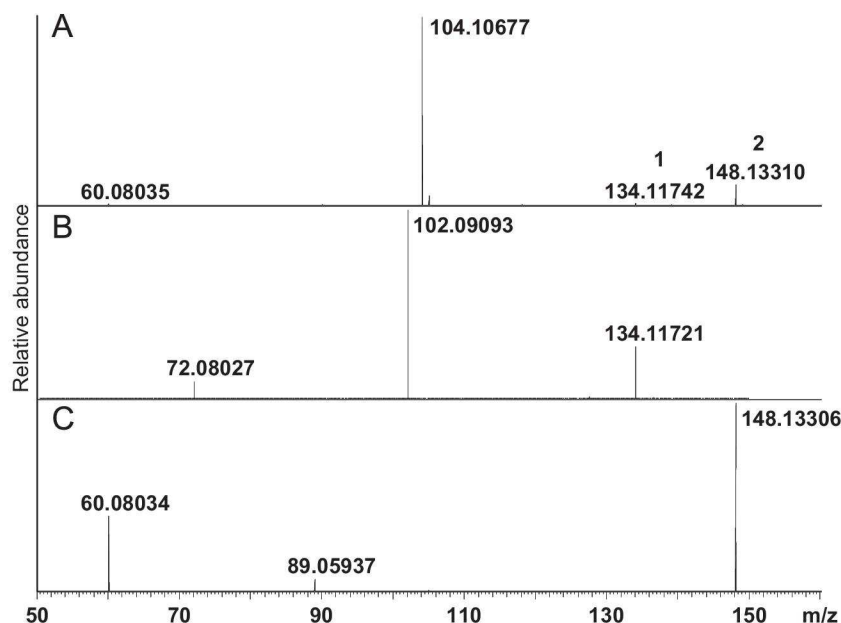


Fig. 6. Full scan mass spectra of IL1 (A) containing two impurities in the obtained batch, followed by low energy CID (MS/MS) spectra of impurity 1 with m/z 134 (B) and of impurity 2 with m/z 148 (C).

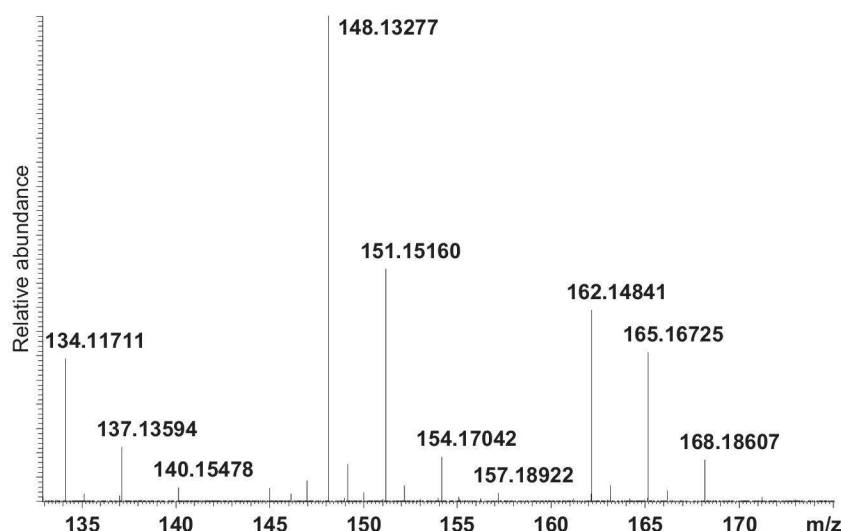


Fig. 7. Full scan mass spectrum of two impurities in IL1 together with their detected degradation species which evolved after artificial alteration carried out for 1 day at 190 °C.

and their proposed assigned structures are summarized in Table 4. Based on the mass spectra obtained after 7 days at 190 °C, it was observed that the above described impurities and their associated degradation species were not stable under applied conditions as they almost utterly vanished (data not shown).

3.2. IL degradation under tribometrical conditions

After the tribometrical experiments discussed further below, the IL samples were collected and analysed with ESI-LTQ-orbitrap-MS by direct infusion. In the obtained mass spectra from IL1 used as lubricant during SRV experiments at 100 and 150 °C, traces of ion at m/z 118 have been detected. This could be due to slow reaction kinetics, as the SRV experiments have been performed at significantly lower temperatures and only for 1 h compared to artificial alteration experiments. Nevertheless,

detection of the ion at m/z 118 and its MS/MS product ions being identical to those of (2-methoxyethyl)trimethyl ammonium moiety, unambiguously confirmed that the chosen tribometrical conditions lead to the same degradation product as the artificial alteration experiment.

In the case of IL3, the obtained mass spectra have not revealed presence of any degradation product after the performed tribometrical experiments at both 100 and 150 °C.

3.3. Ionic liquids volatile degradation products

As suggested by the degradation species detected during artificial alteration of IL1 and its chloride based deuterated analogue, the reactions taking place under the applied conditions require the presence of anion-originating intermediates, such as methyl chloride and/or methyl methanesulphonate. Thus, the detection of both was the aim of these investigations in order to

Table 4
Summary of degradation species originating from two IL1 impurities, namely $[\text{HO}-\text{CH}_2-\text{O}-\text{C}_2\text{H}_4-\text{N}(\text{CH}_3)_3]^+$ and $[\text{HO}-\text{C}_2\text{H}_4-\text{O}-\text{C}_2\text{H}_4-\text{N}(\text{CH}_3)_3]^+$, formed after 1 day of thermo-oxidative stress at 190 °C and identified by ESI-LTQ-orbitrap-MS.

Impurity	Monoisotopic mass (Da)	Elemental composition	Structure	Monoisotopic mass (Da)	Elemental composition	Structure	Monoisotopic mass (Da)	Elemental composition	Structure
1	134.11809	$\text{C}_6\text{H}_{16}\text{NO}_2$		148.13374	$\text{C}_7\text{H}_{18}\text{NO}_2$		151.15258	$\text{C}_7\text{D}_3\text{H}_{15}\text{NO}_2$	
	137.13693	$\text{C}_6\text{D}_3\text{H}_{13}\text{NO}_2$		151.15258	$\text{C}_7\text{D}_3\text{H}_{15}\text{NO}_2$		154.17140	$\text{C}_7\text{D}_6\text{H}_{12}\text{NO}_2$	
	140.15575	$\text{C}_6\text{D}_6\text{H}_{10}\text{NO}_2$		154.17140	$\text{C}_7\text{D}_6\text{H}_{12}\text{NO}_2$		157.19024	$\text{C}_7\text{D}_9\text{H}_9\text{NO}_2$	
	143.17459 ^a	$\text{C}_6\text{D}_9\text{H}_7\text{NO}_2$		157.19024	$\text{C}_7\text{D}_9\text{H}_9\text{NO}_2$		160.20906 ^a	$\text{C}_7\text{D}_{12}\text{H}_6\text{NO}_2$	
	148.13374	$\text{C}_7\text{H}_{18}\text{NO}_2$		162.14939	$\text{C}_8\text{H}_{20}\text{NO}_2$		165.16823	$\text{C}_8\text{D}_3\text{H}_{17}\text{NO}_2$	
	151.15258	$\text{C}_7\text{D}_3\text{H}_{15}\text{NO}_2$		165.16823	$\text{C}_8\text{D}_3\text{H}_{17}\text{NO}_2$		168.18705	$\text{C}_8\text{D}_6\text{H}_{14}\text{NO}_2$	
	154.17140	$\text{C}_7\text{D}_6\text{H}_{12}\text{NO}_2$		168.18705	$\text{C}_8\text{D}_6\text{H}_{14}\text{NO}_2$		171.20589 ^a	$\text{C}_8\text{D}_9\text{H}_{11}\text{NO}_2$	
	157.19024	$\text{C}_7\text{D}_9\text{H}_9\text{NO}_2$		171.20589 ^a	$\text{C}_8\text{D}_9\text{H}_{11}\text{NO}_2$		174.22471 ^a	$\text{C}_8\text{D}_{12}\text{H}_8\text{NO}_2$	
2									

^a Indicates that these species were not detected and are listed only as they contribute to the degradation series detected.

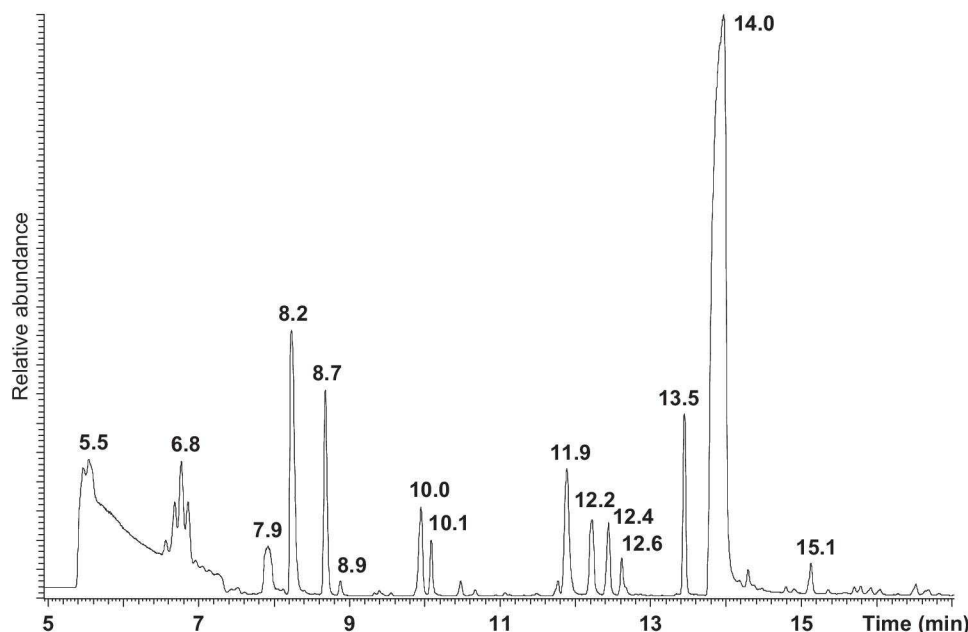


Fig. 8. Total ion chromatogram of headspace phase obtained by HS-CT-GC-EI-MS analysis of mixture consisting from IL1 and its chloride based deuterated analogue subjected to artificial alteration at 190 °C for 1 day.

Table 5

Summary of volatile species present in the mixture of IL1 and its deuterated chloride based analogue after 1 day at 190 °C, as identified by HS-CT-GC-EI-MS.

Retention time (min)	5.5	6.8	7.9	8.2	8.2
Structure	<chem>O=C-O</chem>	<chem>H3C-Cl</chem>	<chem>H-O-H</chem>	<chem>H3C-OH</chem>	<chem>C=C</chem>
Molecular ion (<i>m/z</i>)	44	50 (53) ^a	18	32 (35) ^a	44
Match/reverse match/probability (%)	928/929/33	821/946/99	676/686/66	859/872/89	806/810/46
Retention time (min)	8.7	8.9	10.0	10.1	11.9
Structure	<chem>CN(C)C</chem>	<chem>HO-C</chem>	<chem>C(=O)O</chem>	<chem>Cl-CH2-Cl</chem>	<chem>CN(C)CO</chem>
Molecular ion (<i>m/z</i>)	59 (62,65,68) ^a	46	74 (77) ^a	84	76 (79) ^a
Match/reverse match/probability (%)	884/884/78	792/898/86	834/911/91	914/915/96	913/915/97
Retention time (min)	12.2	12.4	13.5	14.0	15.1
Structure	<chem>CN(C)CO</chem>	<chem>Cl-CH2-CH2-O</chem>	<chem>C1COCCO1</chem>	<chem>CN(C)CO</chem>	<chem>C1COCCO1</chem>
Molecular ion (<i>m/z</i>)	90 (93) ^a	94 (97) ^a	88	89	101 (104) ^a
Match/reverse match/probability (%)	832/840/90	893/894/95	909/909/80	891/906/62	874/875/96

unambiguously confirm a degradation mechanism based on cation demethylation followed by methylation of hydroxyl functionalized cation side chain.

Hence, the gaseous phase obtained after 1 day at 190 °C was analysed by a HS-CT-GC-EI-MS in order to detect the primary produced volatile degradation species. The obtained total ion chromatogram (TIC) is presented in Fig. 8 with major volatile compounds labelled by their corresponding retention times. A summary of the identified volatile species is presented in Table 5 together with their corresponding *m/z* values of the molecular ions and the obtained indicators of the library match serving for qualitative identification.

Each of the detected peaks was identified by comparison of its measured mass spectrum with NIST mass spectral library (National Institute of Standards and Technology, Gaithersburg, Maryland, USA, 2008 edition). The most abundant volatile detected is (2-hydroxyethyl)-dimethyl-amine with a retention

time (t_R) of 14.0 min confirming the demethylation of the IL1 cation and representing the volatile by-product of IL1 degradation. The anion-intermediate product based on methyl chloride ($t_R=6.8$ min) is detected as well, as it represents a low boiling compound. However, the methyl methanesulphonate is not detected in the presented separation/detection system. This could be due to its less nucleophilic nature in comparison to chloride anion which could lead to slow reaction kinetics and the fact that after methylation of the hydroxyl group of cation side chains it is restored as initial anion methanesulphonate, whereas methyl chloride is lost. Some of the detected volatiles at t_R 8.2, 8.7, 8.9 and 12.4 min, give evidence of dealkylation taking place on the hydroxy- and methoxy-functionalized ammonium side chain as well. Most of the other identified volatiles can be contributed to the further thermo-oxidative degradation of the amine itself, as it leads to carboxylic acids, aldehydes and to species with ring annulation [49,50].

Not just primary volatile degradation species of ionic liquids IL1 to IL6, but also those evolved after long-term thermo-oxidative stress after 7 days at 150 °C were identified by method described in Section 2.3.2 using HS–CT–GC–EI–MS set up. The summary of the detected volatile compounds present after the 7 days artificial alteration experiments is shown in Table 6.

In general, it can be stated that bis(trifluoromethylsulfonyl)imide based ILs (IL2, IL4 and IL6) produce considerably less type of volatile degradation products in comparison to methanesulphonate based ILs. In the case of bis(trifluoromethylsulfonyl)imide based ILs for all cation variations, the methylated anion has been detected, however in considerable lower amounts in the case of tributyl-methyl-ammonium cation, hence not listed in Table 6. This can probably be because of steric hindrance of longer butyl chains as the cation methyl group is not readily accessible. However, it is concluded that even anions of low nucleophilicity can play a substantial role in IL degradation mechanism.

On the contrary, methyl methanesulphonate as suggested intermediate product in methanesulphonate based ILs degradation mechanism was detected only in the case of (2-methoxyethyl)-trimethyl-ammonium (IL3). In this case, the methylated anion does not have the option to be fully regenerated back to initial anion as it is in the case of (2-hydroxyethyl)-trimethyl-ammonium (IL1). Regarding IL5, both feasible amine types of tributyl-methyl-ammonium cation – dibutyl methylamine and tributylamine – are detected at t_R 18.3 and 22.3 min. This is the one and only case where the supposed amines as by-products of quaternary ammonium dealkylation are detected and it allows to deduce that these non-functionalized amines are more stable as the functionalized amine analogues of IL1 to IL4. In summary, IL5 provided the largest variety of types of major volatiles degradation products with many species originating from cation butyl chain and further oxidation reactions. Most of the other identified volatiles of IL1 to IL6 can be contributed to the continuously ongoing thermo-oxidative degradation of the amines itself [49,50].

3.4. Tribological investigation of IL1 and its degradation product related to IL3

As concluded from IL1 degradation behaviour discussed above, the (2-methoxyethyl)trimethyl-ammonium moiety is present in the liquid phase as the primary degradation product. Hence, its formation can possibly influence the tribological properties of IL1, once applied as fresh neat lubricant. The (2-methoxyethyl)trimethyl-ammonium moiety together with the methanesulphonate anion – thus identical to IL3 – was used for comparison of its tribological performance to intact IL1 in order to investigate how friction and wear could be affected by the degradation product build-up.

Therefore, the tribological investigations were carried out on steel–steel contacts at two elevated temperatures at 100 and 150 °C, respectively, to take account for the alteration conditions chosen. The representative friction curves obtained over the time under boundary lubrication conditions and the corresponding average friction coefficients together with standard deviations for each experiment performed are based on data points obtained as presented in Fig. 9.

For each of the experiments, no pronounced running-in period took place under the selected conditions. Friction coefficient of IL1 at both 100 and 150 °C was around a value of 0.1 with slight decrease at the end of experiment at 100 °C as opposite to mild increase at 150 °C. Furthermore, in case of IL1, between 20 and 30 min, some high friction spikes (partial seizures) are observed during the experiments at both temperatures, as can be seen in Fig. 9. Such spikes were not considered for the calculation of the

average friction coefficients as they do not represent the stable friction regime.

The IL3 shows at 100 °C a constant friction in the range of IL1 friction coefficient until about 30 min, however afterwards has increasing trend in contrast to decreasing friction of IL1. Even more different performance of IL3 can be observed at 150 °C, where after an initial low friction, a sharp increase in friction coefficient is observed for about 30 min, followed by a recovery to a lower friction region. This same behaviour was also observed in the duplicate experiment under the same conditions. The high friction regime was stable only for about 5 min in each run at friction coefficients of 0.20 and 0.21, respectively, after which friction started to descent into the lower friction area. Thus, the average friction coefficients were calculated in the case of IL3 experiments at 150 °C after the high friction regime. It can be observed that IL3 leads at both temperatures, but especially at 150 °C to higher average friction values than IL1. Similar friction behaviour as for IL3 at 150 °C was described for $[\text{BF}_4]^-$ and $[\text{PF}_6]^-$ based ILs and was related to tribo-chemical reactions at the interface [2,8]. Hence, we could suspect that the high friction regime represents some kind of “induction period” within which tribo-chemical interactions lead to tribolayer formation eventually resulting in lower friction.

The wear-preventing properties were studied by comparing the topography of rubbed surfaces, as shown in Figs. 10 and 11. While the ball and disc wear at 100 °C for both ILs shows several abrasion grooves, smoother wear scars were obtained at 150 °C.

In general, the obtained wear volumes on the disc (range of $10^6 \mu\text{m}^3$) were higher than those on the ball (range of $10^5 \mu\text{m}^3$) as depicted in Fig. 12. The average wear volumes were calculated based on two subsequent experiments with error bars representing the minimum and maximum values within two experiments performed. However, the ball wear volume for IL3 at 150 °C represents single value due to observed corrosion which prevented measurement of the correct ball wear volume in the second run.

From Fig. 12 it can be seen, that the ball wear volumes for both ILs are in similar range at 100 °C, while the disc wear volume of IL3 is already notably higher. More apparent difference between the IL performances can be seen at 150 °C, where both ball and disc wear volumes of IL3 are significantly higher than that of IL1, indicating decline of IL3 wear preventing properties. Furthermore, average of the ball wear scar diameters (length and width) of both runs for particular IL and temperature were calculated based on values measured with an optical microscope. The average values of the ball wear scar diameters were at 100 °C as follows: 677 and 713 μm for IL1, 769 and 719 μm for IL3. The same trend was found at 150 °C: 768 and 682 μm for IL1, 822 and 848 μm for IL3. Thus, these results mirror the similar trend of increasing average wear volumes with temperature, while IL3 causing more pronounced wear than IL1.

3.5. Elemental and chemical surface analyses by XPS

The IL3 special friction characteristics at 150 °C were examined in detail by stopping the tribometrical experiment at 150 °C after 10 min in the higher friction regime to be able to compare the elemental and chemical surface composition with the surface after completed experiment exhibiting low friction.

The XPS surface analysis after the interrupted and completed tribological experiments with IL3 did not reveal significant difference in neither the elemental composition nor the chemical binding state of the studied elements. Interestingly, no nitrogen from the (2-hydroxyethyl)-trimethyl-ammonium cation of IL3 was observed on both surfaces by XPS approach.

Table 6
Summary of major volatile compounds of IL1 to IL6 present in the gas phase after 7 days at 150 °C, as identified by HS-CT-CC-MS. In the case of IL6 it was not possible to differentiate between butene isomers.

	7.9	8.2	8.3	8.6	8.7	9.3	10.0	10.7	11.9	12.2	13.5
IL 1											
	666/666/ 94	941/942/95	927/930/86	906/908/93	911/919/ 81	907/907/ 96	930/935/95	809/901/59	928/952/96	870/918/83	954/954/ 84
	Match/reverse match/ probability (%)										
	Reten- tion time (min)										
	14.9	15.8	16.1	17.8							
	Match/reverse match/ probability (%)										
	Reten- tion time (min)										
IL 2											
	604/604/ 98	954/958/86	901/920/93	895/895/95	934/939/ 94	953/957/ 77	929/929/93	946/947/84	922/922/77	921/922/97	794/819/ 73
	Match/reverse match/ probability (%)										
	Reten- tion time (min)										
	7.9	8.3	8.2	8.6	10.0	10.7	12.3	13.2	13.5	14.4	14.5
	Match/reverse match/ probability (%)										
	Reten- tion time (min)										
IL 3											
	578/581/ 99	887/921/97	901/920/93	895/895/95	934/939/ 94	953/957/ 77	929/929/93	946/947/84	922/922/77	921/922/97	794/819/ 73
	Match/reverse match/ probability (%)										
	Reten- tion time (min)										
	16.4										
	Match/reverse match/ probability (%)										
	Reten- tion time (min)										
IL 4											
	627/630/ 75	920/920/93	913/930/87	893/893/96	876/878/ 95	907/916/ 92	912/916/78	926/927/94	900/901/98		
	Match/reverse match/ probability (%)										
	Reten- tion time (min)										
	7.8	8.2	8.3	9.4	9.9	10.0	11.0	11.5	14.2		
	Match/reverse match/ probability (%)										
	Reten- tion time (min)										
IL 5											
	754/754/ 96	918/918/92	929/939/30	911/927/82	927/930/ 92	919/920/ 83	908/908/96	908/912/89	935/936/86	946/947/89	951/951/ 65
	Match/reverse match/ probability (%)										
	Reten- tion time (min)										
	15.4	16.8	17.2	18.3	18.8	22.3					
	Match/reverse match/ probability (%)										
	Reten- tion time (min)										
IL 6											
	821/845/ 93	948/955/30	943/953/27	955/962/30	952/958/ 85	920/924/ 93	915/919/90				
	Match/reverse match/ probability (%)										
	Reten- tion time (min)										
	7.8	8.3	8.5	8.6	9.4	11.0	11.1				
	Match/reverse match/ probability (%)										
	Reten- tion time (min)										

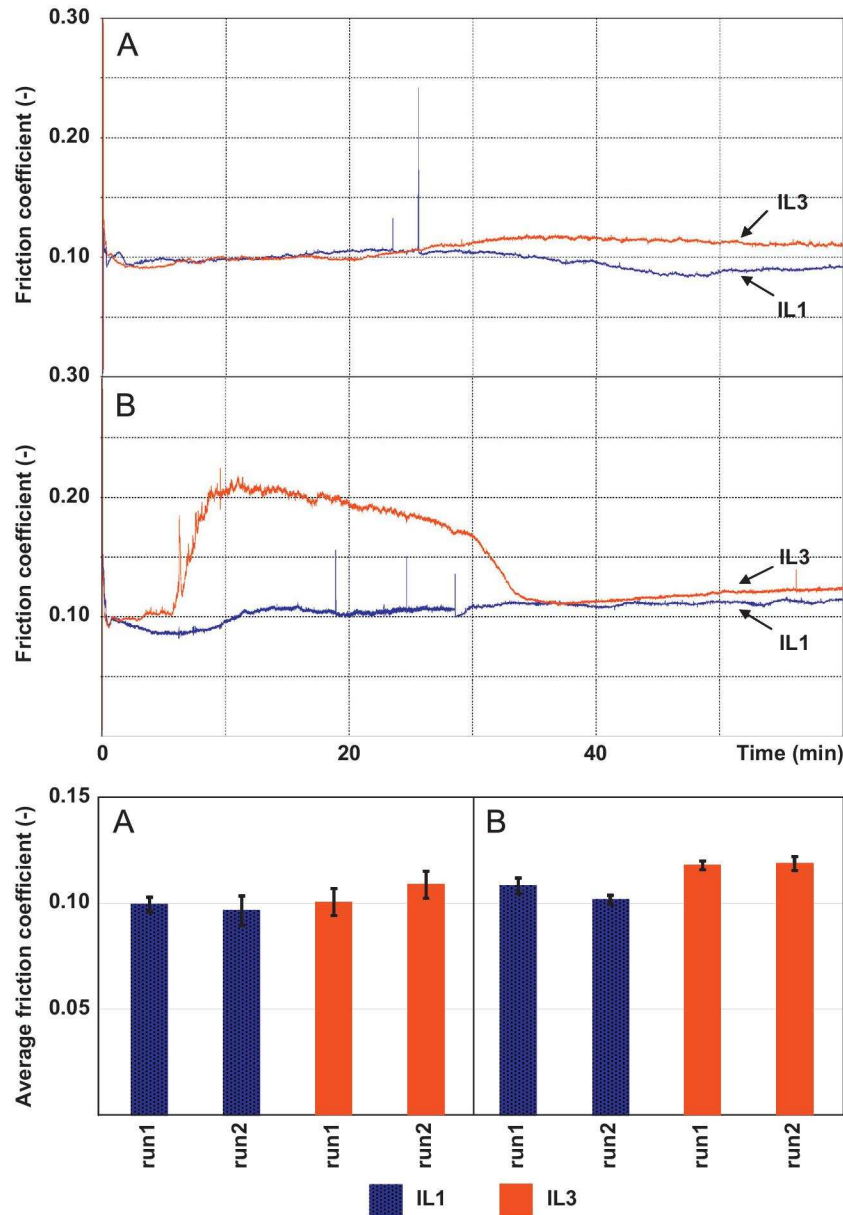


Fig. 9. Plot of friction coefficients of IL1 and IL3 versus time as observed at 100 °C (A) and at 150 °C (B) under tribometrical conditions summarized in Table 2. The average friction coefficients across each experiment performed twice (run 1 and 2) with error bars indicating standard deviation, are taken after the run-in period (10 min) apart from IL3 at 150 °C where the friction coefficient is averaged after the friction stabilized again at lower level (after 35 min).

Prior to the XPS analyses, it was hypothetically assumed that the surface of the interrupted experiment exhibiting high friction is lacking sulphides, which are known to be generated through tribo-chemical reactions in the tribocontact. Since these sulphides have superior tribological properties, lack of these compounds could explain the observed higher friction coefficient. The binding energies measured for sulphur were located at 168.3 (± 0.1) eV, assignable to the sulphur of the IL3 anionic moiety (sulphonate), and at several sulphidic binding states in the range of 161.1 to 161.7 eV which are shown in Fig. 13. The overall sulphur content on both surfaces was about 5 atomic % and the ratio between sulphonate and the sulphide was around 1.

Since the surface analysis of the observed layers from interrupted and completed tribological experiments did not result in significant difference to explain the different tribological

behaviour, the depth profiles of the wear tracks were acquired to analyse their approximate thickness and composition.

Both surfaces were cleaned by soft sputtering with Ar⁺ ions using 1 kV acceleration voltage and 1 μ A sputter current for a period of 20 s before measurements, hence about 50% of the carbon contamination on the surface was removed.

The depth profiles of the two tribolayers revealed that the sulphur content within the layer of the interrupted experiment was significantly lower than in the case of the completed experiment as presented in Fig. 14.

Although the chemical information especially for sulphur is lost through the sputtering process, it can be assumed that sulphides are the dominant sulphuric compounds in the layer and therefore are considered being responsible for the tribological properties of the respective surfaces, which would explain the different friction behaviour according to the stated hypothesis.

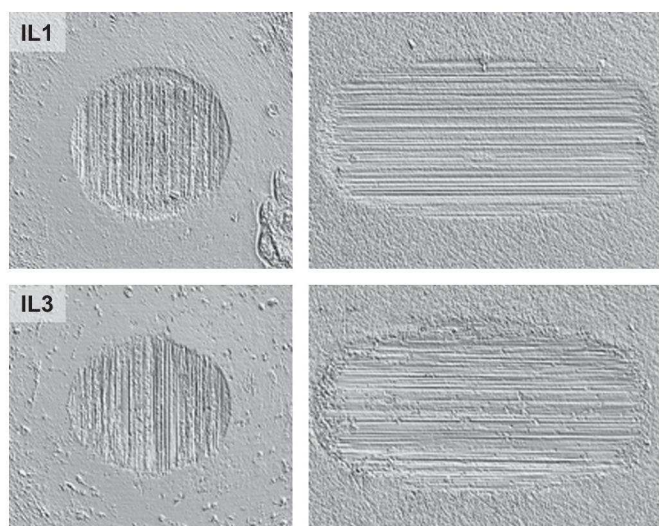


Fig. 10. Surface topographies of 100Cr6 ball and disc after tribological experiments at 100 °C using IL1 (upper row) and IL3 (bottom row) as neat lubricants.

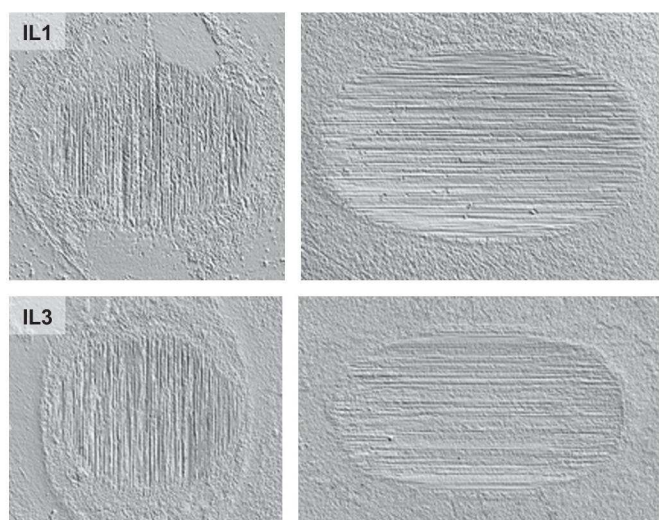


Fig. 11. Surface topographies of 100Cr6 ball and disc after tribological experiments at 150 °C using IL1 (upper row) and IL3 (bottom row) as neat lubricants.

Both layers have a thickness of about 250 nm as based on the estimated sputter yield of 0.05 nm/s.

4. Conclusions

Our aim was to find out how ILs can be altered during their use as lubricants by performing artificial alteration experiments to simulate long-term thermo-oxidative stress. By use of mass spectrometry, it was possible to show, that cross-methylation on IL cation takes place via an inter-molecular mechanism based on a nucleophilic attack of anions to the ammonium methyl group which leads to the generation of volatile amines. Additionally, anion-originating intermediate products are involved in the subsequent methylation of hydroxyl functionalized cation side chains leading to new IL moieties and hence altering the properties of the former IL. Due to the observed initial higher signal intensities of newly formed cross-methylated cations, it can be concluded that the demethylation of the cation takes place faster than the hydroxyl-group methylation. In summary, these processes in fact

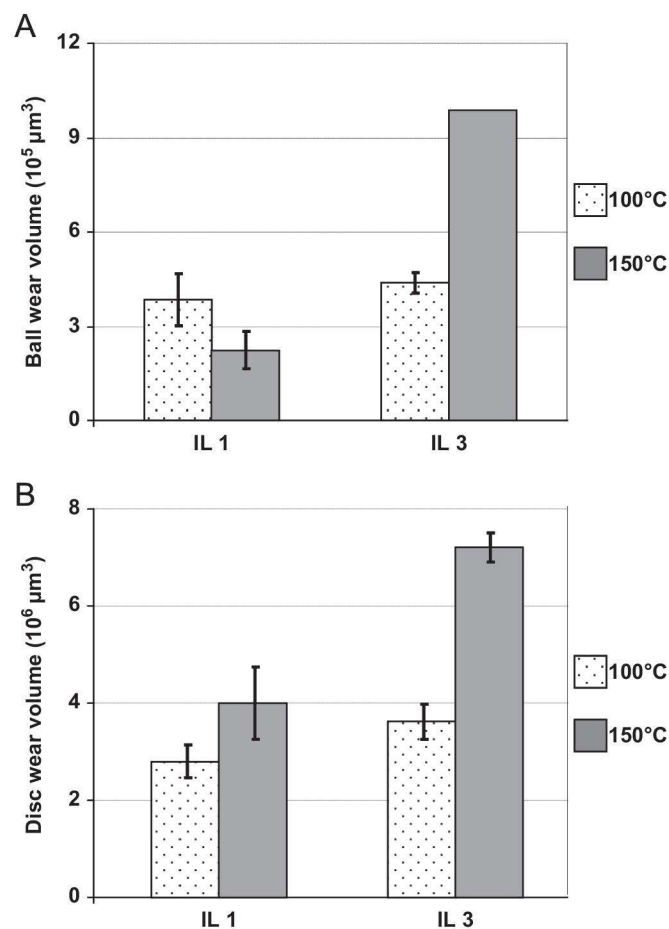


Fig. 12. Calculated average wear volumes of ball (A) and disc (B) after tribometrical experiments with IL1 and IL3 as neat lubricants. The error bars indicate the maximum and minimum values obtained within 2 runs. In the case of IL3 at 150 °C, the ball wear volume represents only single value due to corrosion in the second experiment.

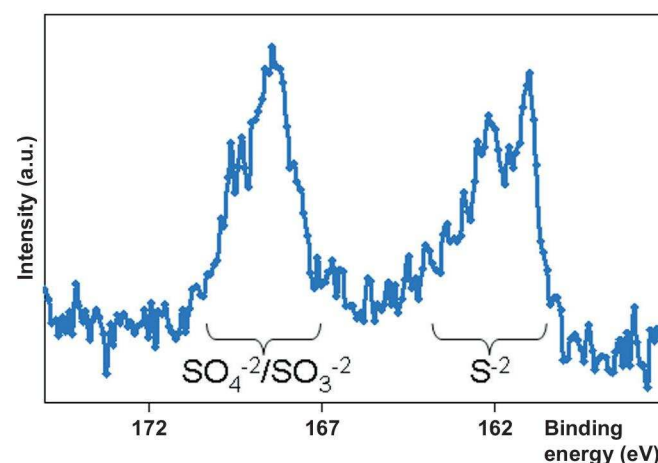


Fig. 13. Sulphur binding energies obtained from S2p spectrum measured in the middle of the wear track after completed tribometrical experiment with IL3.

hinder the total degradation of the ammonium ILs, however they give a rise to mixture of species with divergent properties, supposedly causing problems once used in long-term real-world applications. The complex mixture of volatile species evolved during the IL deterioration can also cause significant build-up of

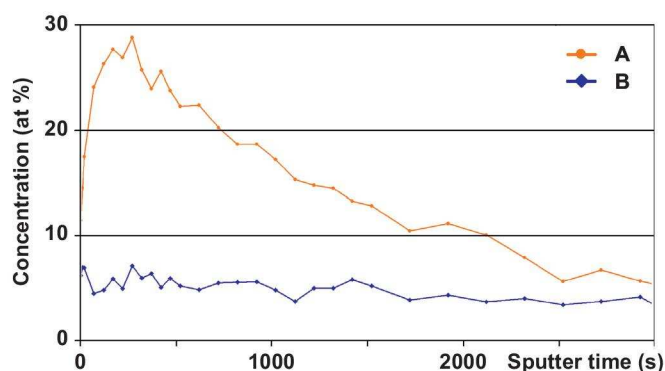


Fig. 14. Obtained depth profiles showing distribution of sulphur in the tribolayers after completed (A) and interrupted (B) tribological test with IL3.

pressure in the lubricant containing objects in contrast to otherwise unaltered, hence non-volatile ILs.

It is also important to note, that stability of IL used as oil additive together with conventional additives in base oils can be distinctively different from the findings gained in this work. Hence, this research topic will be the scope of our further investigations. By considering the tribological performance of selected ILs representing potential intact lubricant (IL1) and its main degradation product (IL3), it was observed that the presence of the degradation product could in principle have a negative impact on the wear formation, especially at higher temperature as observed in the obtained wear data.

Acknowledgments

This study was funded within the FP7 program – Marie Curie Initial Training Network MINILUBES [216011-2] – by the European Commission and by the “Austrian COMET-program” in the frame of K2 XTribology and carried out within the “Excellence Centre of Tribology” – AC²T research GmbH. The surface analytical work with XPS was also supported with EFRE funding and with support of the country of Lower Austria within the project “Onlab”. This work was also partly supported by KAKENHI [23246030].

References

- Minami I. Ionic liquids in tribology. *Molecules* 2009;14:2286–305.
- Bermudez MD, Jimenez AE, Sanes J, Carrion FJ. Ionic liquids as advanced lubricant fluids. *Molecules* 2009;14:2888–908.
- Zhou F, Liang Y, Liu W. Ionic liquid lubricants: designed chemistry for engineering applications. *Chemical Society Reviews* 2009;38:2590–9.
- Predel T, Pohrer B, Schluucker E. Ionic liquids as alternative lubricants for special applications. *Chemical Engineering and Technology* 2010;33:132–6.
- Minami I, Inada T, Sasaki R, Namao H. Tribo-chemistry of phosphonium-derived ionic liquids. *Tribology Letters* 2010;40:225–35.
- Jimenez AE, Bermudez MD. Ionic liquids as lubricants of titanium–steel contact. Part 2: Friction, wear and surface interactions at high temperature. *Tribology Letters* 2010;37:431–43.
- Schluucker E, Wasserscheid P. Ionische Flüssigkeiten in der Maschinentechnik. *Chemie Ingenieur Technik* 2011;83:1476–84.
- Jimenez AE, Bermudez MD. Ionic liquids as lubricants for steel–aluminium contacts at low and elevated temperatures. *Tribology Letters* 2007;26:53–60.
- Bermudez MD, Jimenez AE. Surface interactions in lubrication of titanium, aluminium and titanium–aluminium alloys with the ionic liquid [C₂mim]Tf₂N under increasing temperature. *Journal of Engineering Tribology* 2011. <http://dx.doi.org/10.1177/1350650111416406>.
- Predel T, Schluucker E, Wasserscheid P, Gerhard D, Arlt W. Ionic liquids as operating fluids in high pressure applications. *Chemical Engineering and Technology* 2007;30:1475–80.
- Palacio M, Bhushan B. A review of ionic liquids for green molecular lubrication in nanotechnology. *Tribology Letters* 2010;40:247–68.
- Mo Y, Huang F, Zhao F. Functionalized imidazolium wear-resistant ionic liquid ultrathin films for MEMS/NEMS applications. *Surface and Interface Analysis* 2011;43:1006–14.
- Street Jr KW, Morales W, Koch VR, Valco DJ, Richard RM, Hanks N. Evaluation of vapor pressure and ultra-high vacuum tribological properties of ionic liquids. *Tribology Transactions* 2011;54:911–9.
- Tang S, Baker GA, Zhao H. Ether- and alcohol-functionalized task-specific ionic liquids: attractive properties and applications. *Chemical Society Reviews* 2012;41:4030–66.
- Jimenez AE, Bermudez MD. Ionic liquids as lubricants of titanium–steel contact. *Tribology Letters* 2009;33:111–26.
- Li D, Cai M, Feng D, Zhou F, Liu W. Excellent lubrication performance and superior corrosion resistance of vinyl functionalized ionic liquid lubricants at elevated temperature. *Tribology International* 2011;44:1111–7.
- Zhu LY, Chen LG, Yang X, Song HB. Functionalized ionic liquids as lubricants for steel–steel contact. *Applied Mechanics and Materials* 2012;138–139: 630–4.
- Stolte S, Arning J, Bottin-Weber U, Mueller A, Pitner WR, Welz-Biermann U, et al. Effects of different head groups and functionalized side chains on the cytotoxicity of ionic liquids. *Green Chemistry* 2007;9:760–7.
- Coleman D, Gathergood N. Biodegradation studies of ionic liquids. *Chemical Society Reviews* 2010;39:600–37.
- Pham TPT, Cho C-W, Yun Y-S. Environmental fate and toxicity of ionic liquids: a review. *Water Research* 2010;44:352–72.
- Matzke M, Stolte S, Thiele K, Jufferholz T, Arning J, Ranke J, et al. The influence of anion species on the toxicity of 1-alkyl-3-methylimidazolium ionic liquids observed in an (eco)toxicological test battery. *Green Chemistry* 2007;9:1198–207.
- Nockemann P, Thijs B, Driesen K, Janssen CR, Van Hecke K, Van Meervelt L, et al. Choline saccharinate and choline acesulfamate: ionic liquids with low toxicities. *Journal of Physical Chemistry B* 2007;111:5254–63.
- Petkovic M, Ferguson JL, Gunaratne HQN, Ferreira R, Leitao MC, Seddon KR, et al. Novel biocompatible cholinium-based ionic liquids–toxicity and biodegradability. *Green Chemistry* 2010;12:643–9.
- Stolte S, Steudte S, Igartua A, Stepnowski P. The biodegradability of ionic liquids—the view from a chemical structure perspective. *Current Organic Chemistry* 2011;15:1946–73.
- Stolte S, Steudte S, Areitioaurtena O, Pagano F, Thoeming J, Stepnowski P, et al. Ionic liquids as lubricants or lubrication additives: an ecotoxicity and biodegradability assessment. *Chemosphere* 2012. dx.doi.org/10.1016/j.chemosphere.2012.05.102.
- Domanska U. Thermophysical properties and thermodynamic phase behavior of ionic liquids. *Thermochimica Acta* 2006;448:19–30.
- Muhammad N, Man ZB, Bustam MA, Mutalib MIA, Wilfred CD, Rafiq S. Synthesis and thermophysical properties of low viscosity amino acid-based ionic liquids. *Journal of Chemical and Engineering Data* 2011;56:3157–62.
- Heym F, Etzold BJM, Ch Kern, Jess A. Analysis of evaporation and thermal decomposition of ionic liquids by thermogravimetric analysis at ambient pressure and high vacuum. *Green Chemistry* 2011;13:1453–66.
- Seeberger A, Andresen AK, Jess A. Prediction of long-term stability of ionic liquids at elevated temperatures by means of non-isothermal thermogravimetric analysis. *Physical Chemistry Chemical Physics* 2009;11:9375–81.
- Ferreira AF, Simoes PN, Ferreira AGM. Quaternary phosphonium-based ionic liquids: thermal stability and heat capacity of the liquid phase. *Journal of Chemical Thermodynamics* 2012;45:16–27.
- Minami I, Kamimura H, Mori S. Thermo-oxidative stability of ionic liquids as lubricating fluids. *Journal of Synthetic Lubrication* 2007;24:135–47.
- Luo H, Huang JF, Dai S. Studies on thermal properties of selected aprotic and protic ionic liquids. *Separation Science and Technology* 2008;43:2473–88.
- Green MD, Schreiner Ch, Long TE. Thermal rheological, and ion-transport properties of phosphonium-based ionic liquids. *Journal of Physical Chemistry A* 2011;115:13829–35.
- Ohtani H, Ishimura S, Kumai M. Thermal decomposition behaviors of imidazolium-type ionic liquids studied by pyrolysis–gas chromatography. *Analytical Sciences* 2008;24:1335–40.
- Del Sesto RE, McCleskey TM, Macomber C, Ott KC, Koppisch AT, Baker GA, et al. Limited thermal stability of imidazolium and pyrrolidinium ionic liquids. *Thermochimica Acta* 2009;491:118–20.
- Hao Y, Peng J, Hu S, Li J, Zhai M. Thermal decomposition of allyl-imidazolium-based ionic liquid studied by TGA-MS analysis and DFT calculations. *Thermochimica Acta* 2010;501:78–83.
- Chowdhury S, Mohan RS, Scott JL. Reactivity of ionic liquids. *Tetrahedron* 2007;63:2363–89.
- Siedlecka EM, Czerwicka M, Stolte S, Stepnowski P. Stability of ionic liquids in application conditions. *Current Organic Chemistry* 2011;15:1974–91.
- Sowmiah S, Srinivasadesikan V, Mch Tseng, Chu YH. On the chemical stabilities of ionic liquids. *Molecules* 2009;14:3780–813.
- Pisarova L, Steudte S, Doerr N, Pittenauer E, Allmaier G, Stepnowski P, et al. Ionic liquid long-term stability assessment and its contribution to toxicity and biodegradation study of untreated and altered ionic liquids. *Journal of Engineering Tribology* 2012;226:903–22.
- Meine N, Benedetto F, Rinaldi R. Thermal stability of ionic liquids assessed by potentiometric titration. *Green Chemistry* 2010;12:1711–4.
- Pisarova L, Ch Gabler, Doerr N, Pittenauer E, Allmaier G. Thermo-oxidative stability and corrosion properties of ammonium based ionic liquids. *Tribology International* 2012;46:73–83.

- [43] Baranyai KJ, Deacon GB, MacFarlane DR, Pringle JM, Scott JL. Thermal degradation of ionic liquids at elevated temperatures. *Australian Journal of Chemistry* 2004;57:145–7.
- [44] Wooster TJ, Johanson KM, Fraser KJ, MacFarlane DR, Scott JL. Thermal degradation of cyano containing ionic liquids. *Green Chemistry* 2006;8: 691–6.
- [45] Kroon MC, Buijs W, Peters CJ, Witkamp GJ. Quantum chemical aided prediction of the thermal decomposition mechanisms and temperatures of ionic liquids. *Thermochemica Acta* 2007;465:40–7.
- [46] Liebner F, Patel I, Ebner G, Becker E, Horix M, Potthast A, et al. Thermal aging of 1-alkyl-3-methylimidazolium ionic liquids and its effect on dissolved cellulose. *Holzforschung* 2010;64:161–6.
- [47] Wendler F, Todi LN, Meister F. Thermostability of imidazolium ionic liquids as direct solvents for cellulose. *Thermochemica Acta* 2012;528:76–84.
- [48] Hunger H, Litzow U, Genze S, Doerr N, Karner D, Eisenmenger-Sittner C. Tribological characterisation and surface analysis of diesel lubricated sliding contacts. *Tribologie und Schmierungstechnik* 2010;57:6–13.
- [49] Bello A, Idem RO. Pathways for the formation of products of the oxidative degradation of CO₂-loaded concentrated aqueous monoethanolamine solutions during CO₂ absorption from flue gases. *Industrial and Engineering Chemistry Research* 2005;44:945–69.
- [50] Lepaumier H, Picq D, Carrette PL. New amines for CO₂ capture. II. Oxidative degradation mechanisms. *Industrial and Engineering Chemistry Research* 2009;48:9068–75.

Curriculum vitae



Lucia Pisarova

Personal Data

Telephone + 421 911600054
e-mail senesiova.lucia@gmail.com
Date of birth 26.12.1984
Nationality Slovak

Education

2007-2009 **M.Sc. degree in Analytical Chemistry**,
Slovak University of Technology, Slovakia.
2004-2007 **B.Sc. degree in Chemistry**,
Slovak University of Technology, Slovakia.

Work Experience

07.2012-Present **Scientist**, Advanced chemical analysis department,
AC²T research GmbH, Austria.
07.2009-06.2012 **“Early Stage Researcher“ within Marie Curie Initial Training
Network MINILUBES (No. 216011-2) in FP7 programme**,
AC²T research GmbH, Austria.
10.2010-12.2010 **PhD exchange program**, Department of Environmental Analysis,
University of Gdańsk, Poland.
07.2008-09.2008 **Internship**, Chemistry department,
National University of Ireland, Galway, Ireland.
07.2007-09.2007 **Internship**, Chemistry department,
National University of Ireland, Galway, Ireland.

Trainings

2013 **Management seminar at AC²T research GmbH**, A. Reisenbauer
(SYSCOMM), Wiener Neustadt, Austria.
2012 **Entrepreneurship at AC²T research GmbH**, Prof. R.D. Hisrich
(Thunderbird school), Wiener Neustadt, Austria.
2012 **Seminar on polymer lubrication at Petru Poni Institute**, Prof. B.C.
Simionescu and Prof. V. Habaragiu, Iasi, Romania.
2012 **Seminar on ionic liquids at University of Gdańsk**, Prof. P. Stepnowski,
Gdansk, Poland.

- 2011 **Tribology course at University of Ljubljana**, Prof. M. Kalin, Ljubljana, Slovenia.
- 2011 **Project management training Level D**, The International Project Management Association (IPMA), Austria
- 2011 **Contact mechanics seminar at Cardiff University**, Prof. F.M. Borodich and Prof. H.P. Evans, Cardiff, UK.
- 2010 **Industry training at ESK Ceramics GmbH & Co. KG and GKN Sinter Metals SA**, Kempton, Germany and Bruneck, Italy.
- 2010 **Nanotribology and Nanomechanics at Vienna University of Technology**, Prof. B. Bhushan (Ohio State University), Vienna, Austria.
- 2010 **Tribology seminar at Fundacion Tekniker**, Dr. A. Igartua, Eibar, Spain.

Skills

Language

Slovak	Mother tongue
English	Fluent
German	Lower intermediate

Computer skills

OS	MS Windows
Applications	MS Office, LIMS, Symyx Draw, OPUS, Xcalibur, ChemStation

Additional skills

Experience in working in multinational environment
 Writing and presentation skills, good time management

Publications, conference proceedings and oral presentations

1. Pisarova L, Totolin V, Gabler Ch, Doerr N, Pittenauer E, Allmaier G, Minami I. *Insight into degradation of ammonium-based ionic liquids and comparison of tribological performance between selected intact and altered ionic liquid*. Tribology International (2012), <http://dx.doi.org/10.1016/j.triboint.2013.02.020> (In press)
2. Pisarova L, Steudte S, Doerr N, Pittenauer E, Allmaier G, Stepnowski P, Stolte S. *Ionic liquid long-term stability assessment and its contribution to toxicity and biodegradation study of untreated and altered ionic liquids*. Proceedings of the Institution of Mechanical Engineers, Part J: Journal of Engineering Tribology 226 (2012), 903-922.
3. Pisarova L, Gabler Ch, Doerr N, Pittenauer E, Allmaier G. *Thermo-oxidative stability and corrosion properties of ammonium based ionic liquids*. Tribology International 46 (2012), 73-83.
4. Gabler Ch, Tomastik Ch, Brenner J, Pisarova L, Doerr N, Allmaier G. *Corrosion properties of ammonium based ionic liquids evaluated by SEM-EDX, XPS and ICP-OES*. Green Chem 13 (2011), 2869-2877.
5. Pisarova L. *Detection of ionic liquid's volatile degradation products by headspace GC-MS*. GC & GC-MS user seminar, 19.02.2013, Vienna, Austria.

6. Pisarova L, Totolin V, Gabler Ch, Doerr N, Allmaier G. *Comparison of tribological performance between intact and altered ionic liquid*. X-Tribology Partner Day, 14.11.2012, Wiener Neustadt, Austria.
7. Pisarova L. *Are Ionic liquids as stable as assumed?* Minilubes Symposium, 18-19.09.2012, Wiener Neustadt, Austria.
8. Pisarova L, Doerr N, Allmaier G. *Ionic liquid degradation and its influence on tribological performance*. 39th Leeds-Lyon Symposium on Tribology, 04-07.09.2012, Leeds, UK.
9. Pisarova L, Doerr N, Allmaier G. *Orbitrap mass spectrometry in lubrication science illustrated by the degradation studies of lubricants*. X-Tribology Partner Day, 23.11.2011, Wiener Neustadt, Austria.
10. Pisarova L, Gabler C, Doerr N, Pittenauer E, Allmaier G. *Evaluation of the long-term stability of ammonium based ionic liquids by mass spectrometry*. COIL-4, 15-18.06.2011, Washington DC, USA.
11. Pisarova L, Gabler Ch, Doerr N, Pittenauer E, Allmaier G. *Long-term stability evaluation of ammonium based ionic liquids by mass spectrometry*. Ecotrib & Viennano 2011, 07-09.06.2011, Vienna, Austria.
12. Pisarova L, Steudte S, Doerr N, Stepnowski P, Pittenauer E, Allmaier G. *Stability assessment of ammonium based ionic liquids as potential lubricants*. Minilubes Scientific Fellow's Congress, 01-03.06.2011, Vigo, Spain.
13. Senesiova L, Gabler Ch, Doerr N. *Design and evaluation of sustainable ionic liquid based lubricants*. 37th Leeds-Lyon Symposium on Tribology, 07-10.09.2010, Leeds, UK.